

This is to certify that the

thesis entitled
The Sources, Pathways, and Sinks of Cr, Mn,
Fe, Co, Ni, and Cu in Near Surface
Sabkha Sediments: Laguna Madre Flats, Texas

presented by

James Tolbert

has been accepted towards fulfillment of the requirements for

Master's degree in Geology

Navna L. King Major professor

Date 6/3/85

MSU is an Affirmative Action/Equal Opportunity Institution

O-7639



RETURNING MATERIALS:
Place in book drop to remove this checkout from your record. FINES will be charged if book is returned after the date stamped below.

11:7674802

THE SOURCES, PATHWAYS, AND SINKS OF

Cr, Mn, Fe, Co, Ni, AND Cu IN NEAR

SURFACE SABKHA SEDIMENTS: LAGUNA MADRE FLATS, TEXAS

by

James Tolbert

# A THESIS

Submitted to

Michigan State University

in partial fulfillment of the requirements

for the degree of

MASTER OF SCIENCE

Department of Geological Sciences
1985

\_\_

#### **ABSTRACT**

THE SOURCES, PATHWAYS, AND SINKS OF

Cr, Mn, Fe, Co, Ni, AND Cu IN NEAR

SURFACE SABKHA SEDIMENTS: LAGUNA MADRE FLATS, TEXAS

by

# James N. Tolbert

From data on the partitioning of Cr, Mn, Fe, Co, Ni, and Cu in sediment from the sabkha, Laguna Madre Flats, Texas, the hydrology of the sabkha, and previous works on trace metals, the following constraints are placed on the sources, pathways, and sinks of Cr, Mn, Fe, Co, Ni, and Cu in the near surface sabkha sediments. The dominant source of metal is from the sediment transported to the sabkha; significant amounts of Cu, and Ni, may be supplied by flood waters. The bacterial decay of algal mats effects the partitioning of metals in the sabkha. Sulfides are an important sink for Fe and Cu, and possibly for Co and Ni. Organics are a sink for Cr, Fe, Co, Ni, and Cu. Carbonates may be the dominant sink for Mn, as Mn is not totally removed from the sediment in the reducing conditions below the surface of the sabkha.

#### **ACKNOWLEGEMENTS**

#### I extend thanks to:

- my adviser, Dr. David Long, for his help and patience,
- the members of my committee, Dr. Duncan Sibley and Dr. Grahame Larson, and the faculty of the Department of Geological Sciences for their guidance and teachings,
- the occupants of Room 236, Mike, Rico, Tim, Dale, Steve, Jim, Omar, and John, for their friendship: without with this Master's would not have been worth it, and
- my wife, Sheila, for more reasons than I can list.

This research was funded partially by the Geological Society of America and the United States Geological Survey. Dr. David Long and John Marsh assisted as invaluble field assistants, and Dr. Chuck Holmes helped make the field work possible by coordinating our efforts with the U.S.G.S. and by suplying a free room in South Texas.

# TABLE OF CONTENTS

			page
1	Intr	oduction	
	1.1	Statement of the Problem	. 1
	1.2	Development of the Problem	1
	1.3	Metals in Sediments	2
	1.4	Related Research	6
		1.4.1 Hydrology	8
		1.4.2 Major Florest of	8
		1.4.2 Major Element Chemistry	13
2	Area	1.4.3 Heavy Metals	17
	2.1	of Study	. 21
		Regional Geology	21
	2.3	Climate	21
	2.4	Geologic History	27
	2 5	Sedimentology	28
	2 6	Groundwater	29
3	Metho	ode droundwater	
	3 1	ods	40
	~	5.4010 Sembles	40
4	Discu	Sediment Samples	
•	4 1	ssion I: Hydrology	58
	A + T	Incloduction	58
	4.2	Flood Recharge Area	59
	A A	Area Influenced by Padre Island	66
5	Dicon	The Basin and Marginal Slope	
J	ביו	ssion II: Transition Metals	70
	J. I	Metal Partitioning	70
	5.2	The Hydromorphic Fraction	74
	5.3	Partitioning Within the Hydromorphic Fraction	83
		5.3.1 Partitioning in Sediments	
		Transported to the Sabkha	83
		5.3.2 Manganese	92
		5.3.3 Iron	97
		5.3.4 Cobalt and Nickel	100
		5.3.5 Copper	102
٤	Con - 1.	5.3.6 Chromium	104
) \ <b>~~</b>	Conclu		106
bī	pendix	A: Description of the Sediments	110
b	endix	B: Sediment Data	129
h	pendix	C: Water Chemistry	133
bt	pendix	D: Coefficients of Determination for	
		Metal Partitioning Data	136
pp	endix	E: Piezometric Potentials	137
pp	endix	F: Location of Sites	139
16	liogra	phy	140

# LIST OF TABLES

Tab]	le	Page
1.	Metal concentrations in sediments and waters.	75
2.	An estimate of the fraction of metal in the hydromorphic fraction supplied by flood water.	78
3.	Mixed manganese-calcium carbonates reported in the literature.	96

# LIST OF FIGURES

Figure		Page
1.	Inputs and outputs of water to a sabkha	10
2.	Chemical changes during the evaporation	-
	of seawater.	14
3.	Map of the South Texas Coast.	22
4.	Map of the Laguna Madre Flats.	26
5.	Bromide concentrations across the	20
•	sabkha: August, 1979	. 38
6.	Hypothetical well for calculating	. 50
0.	piezometric potentials.	46
7.	Flow chart for sediment analyses.	51
8.		21
٥.	Bromide concentrations across the	<b>C</b> 0
_	sabkha: August, 1982.	<b>6</b> 0
9.	Groundwater Na/Br, Cl/Br, and K/Br ratios	
	across the sabkha.	61
10.	Piezometric potentials across the sabkha	62
11.	Groundwater Mn/Br and Fe/Br ratios	
	across the sabkha.	80
12.	Metal partitioning in the sediments at	
		37-90
13.	Model of the sources, pathways and sinks	
	of metals in the sabkha sediments.	108
14.	The sediment core from site 16.	111
15.	The sediment core from site 6	113
16.	The trench at site 24.	115
17.	Sediment from 100 cm depth at site 24.	116
18.	The trench at site 10.	118
19.	Plain and side view of the sediment from	
_,	140 cm depth at site 10.	119
20.	The trench at site 19	121
21.	Adjacent clay and sand from 120 cm	
	depth at site 19.	122
22.	Algal mat from 80 cm depth at site 19.	123
23.	The trench at site 22.	125
24.	Colored spots from 72 and 78 cm	
2 T .	denth at cite 22	126
25	depth at site 22. The trench at site 23	
25.	The trench at site 23	120

#### CHAPTER 1

#### INTRODUCTION

# 1.1 STATEMENT OF THE PROBLEM

Many low temperature, stratiform Cu, Pb, Zn, Ag, and U ore deposits are associated with sabkha sediments (Renfro, 1974; Smith, 1976; Long and Angino, 1976; Davis, 1977; Lange and Murray, 1977; Van Edan, 1978; Stein, 1980; Garlick, 1981, 1982; Lange and Ebby, 1981). However, since processes which could cause metal enrichment in active sabkhas are undefined, models for ore formation which invoke sabkha processes remain tenuous.

To better understand (1) the processes that may cause metal enrichment in sabkha sediments, (2) the geological cycling of metals, and (3) the behavior of metals in natural environments, the geochemical behavior of metals in active sabkhas needs to be evaluated. Therefore, the goal of this research is to place constraints on the sources, pathways,

and sinks of Cr, Mn, Fe, Co, Ni, and Cu in the surface sediments of a modern coastal sabkha. To accomplish this goal, five questions are addressed:

- 1. What controls the hydrology of the sabkha?
- 2. How much Cr, Mn, Fe, Co, Ni, and Cu are in the sabkha sediments?
- 3. What are the sources of these metals to the sabkha sediments?
- 4. What are the forms of these metals in the sabkha sediments?
- 5. What reactions do these metals undergo in the sabkha?

By placing constraints on the answers to these questions, we can constrain the sources, pathways, and sinks of Cr, Mn, Fe, Co, Ni, and Cu in the sediments from the Laguna Madre Flats, Texas.

#### 1.2 DEVELOPMENT OF THE PROBLEM

The term "sabkha" is derived from an Arabic word used to describe salt flats or salt marshes; in the literature, the term "sabkha" is used to describe an arid environment where topography is controlled by the water table, and where evaporation exceeds precipitation, causing groundwater salinities to increase beyond that of seawater. In a classical work, Kinsman (1969) describes the formation of a coastal sabkha as the normal end product of regressional offlap in an arid climate.

Sabkha facies are common, both in the rock record (Schenk, 1967 & 1969; Bosellini and Hardie, 1973; Beales and Lozej, 1975; Armstrong, 1975; Handford, 1981), and in present arid and semiarid climates (i.e. Abu Dhabi, U.A.E.; the Pekelmeer, Bonaire, the Netherlands Antilles; Sharks Bay, Southern Australia; Bradwell coastal plain, northern Sinai; northern Gulf of California, Mexico; the Laguna Madre Flats, In the rock record, sabkha facies are South Texas). associated with dolomite (Goldberg, 1967; West, et al., 1968; Nichols, 1974); petroleum reserves (Fuller and Porter, 1969), low temperature copper, lead, zinc, silver, and uranium deposits (Renfro, 1974; Smith, 1976; Long and Angino, 1976; Davis, 1977; Lange and Murray, 1977; Van Edan, 1978; Stein, 1980; Garlick, 1981, 1982; Lange and Ebby, 1981), and silicified evaporites (Folk and Pittman, 1971; Siedlecka 1972 and 1976; Tucker 1976).

Research on the physical and chemical processes active in modern sabkhas has focused primarily on the sedimentation (Thompson, 1968; Kinsman, 1969; Evans, et al., 1969; Logan, et al., 1970; Miller, 1975; Schneider, 1975; Woods and Brown, 1975; Fryberger, et al., 1983), and the hydrology and major element chemistry of the groundwater (i.e. Patterson and Kinsman, 1977, and 1981; Levy, 1977, a and b; McKenzie, et al., 1980; Long and Gudramovics, 1983). Important geologic processes occuring in modern sabkhas include dolomite

formation (Illings, et al., 1965; Deffeyes, et al., 1965; Butler, 1969), evaporite mineral formation (Mason, 1955; Kinsman, 1969), algal mat growth (Kendall and Skipwith, 1968; Kinsman and Park, 1976; Horodyski, et al., 1977), and reduction of sulfate to sulfide by bacterial decay of algal mats (Horodyski, et al., 1977; Jorgensen and Cohen, 1977).

Models for the behavior of heavy metals in sabkha sediments have been developed to explain the observed association of ores with sabkha sediments in terms of processes which may occur in sabkhas (Renfro, 1974; Bush, 1970). These models have focused on four issues: 1) the source of metals, 2) the source of sulfide, 3) the hydrology of the system, and 4) the location and timing of metal deposition.

By examining the relationship of sabkha sediments to stratiform ores and the chemistry of fluid inclusions in Mississippi-valley type lead-zinc deposits, Bush (1970) suggests that the following post burial processes may allow a sabkha to be a source of metal and/or sulfide to an ore deposit. As the sabkha brines are expelled from the sediment during compaction, the chloride rich brines may leach metals from the sediments by forming chloride-metal complexes; if these brines interacted with sulfide bearing water, metal sulfides would precipitate with the potential to form an ore deposit. Alternatively, Bush (1970) suggests that the

reduction of sulfate in gypsum or anhydrite, during interaction with hydrocarbons, can increase the sulfide content in the sabkha pore waters; the expulsion of this water during continued compaction may be a source of sulfide for an ore deposit. Finally, Bush (1970) suggests that both of these processes may occur: first, expelled chloride rich brines may leach metals out of the surrounding sediments; later, hydrocarbons may react with calcium sulfate to form sulfide bearing brines, which when expelled and mixed with the chloride-metal brines would cause the precipitation of metal sulfides.

Renfro (1974) proposed a model for the formation of low temperature, stratiform ore deposits in coastal sabkhas in which processes active in modern sabkhas are used to explain metal sulfides in ancient sabkha emplacement of sediments. In this model, buried algal mats host sulfate reducing bacteria, which increase the dissolved sulfide concentration in the sabkha groundwater. Inland of the sabkha, continental groundwater, which is oxidizing and slightly acidic, leaches metals from the sediments it passes A regional groundwater head causes the continental groundwater to flow into the sabkha, and as the continental groundwater mixes with the sulfide enriched sabkha groundwater, metal sulfides are precipitated in the order of their reduced stabilities. The result would be a zoning of

metal sulfides, from the inland side to the ocean side of a sabkha, of galena, chalcocite, sphalerite, pyrite.

Renfro's (1974) model has been used to explain the distribution of copper sulfides in the San Angelo Copper Trend in the Permian of Texas (Smith, 1976) and the distribution of silver bearing copper sulfides in the Precambrian Belt Supergroup of Montana (Lange and Eby, 1981). Also, sulfur isotopes support a biogenic source of sulfide in the Dunchuan Copper Deposit in China (Fan, 1984), and in Late Proterozoic copper mineralization at Copper Clain, South Australia (Lambert, et al., 1984).

#### 1.3 METALS IN SEDIMENTS

The amount of metal in a sediment is controlled by the amount of metal transported to the site of deposition: this includes the transportation of clastic sediments created by mechanical weathering and dissolved metals from chemical weathering. Metals bound in the sediment are divided between the hydromorhic fraction and the crystalline fraction. The metals in the hydromorphic fraction of a sediment are the metals available for reaction without altering the framework of silicate or other resistant minerals; common forms of metals in the hydromorphic fraction include metal oxides, metals adsorbed on clays, and metals bound with organics. The crystalline or residual fraction of a metal is the metal bound in lattice sites of resistant minerals. In sedimentary

environments, the total amount of metal available for reaction consists of the hydromorphic fraction in the sediment and the dissolved metal in solution.

There are three major pathways between the hydromorphic fraction of a sediment and the dissolved fraction in a fluid:

- 1. precipitation/dissolution reactions involving metal oxides, sulfides carbonates, or other solid phases,
- adsorption/desorption reactions involving surfaces such as metal oxides, clay minerals, or solid organics, and
- 3. reaction with organic molecules via either living organism, or solid organic mater.

In a natural system, whether a metal will be dissolved, bound as an oxide or sulfide, adsorbed, or bound with organics is dependent on (1) the affinity of the metal for the different substrates, (2) the chemistry of the solution, and (3) the nature of the sediment. The chemistry of the solution controls such factors as which solids are stable in precipitation/dissolution reactions, the amount of complexing in solution, and the ionic strength which effects electrostatic interactions.

Previous studies have designed sequential chemical extractions which remove specific forms of metals from a sediment (Chester and Hughes, 1967; Gupta and Chen, 1975; Tessier, et al., 1979). By measuring the amount of metal leached from a sediment by these chemical extractions, constraints can be placed on the forms of metals in the

sediment. Sequential chemical extractions have been used to study trace metal behavior in numerous environments (i.e. Piper, 1971; Addy, et al., 1976; Demina, et al., 1978; Filipek and Owen, 1979; Filipek, et al., 1981; Tessier, et al., 1985).

#### 1.4 RELATED RESEARCH ON SABKHAS

Coastal sabkhas are off lap sediments where potential evapotranspiration exceeds precipitation. This definition does not constrain the sediments which compose the sabkha, and modern sabkhas are found in a variety of sediments: from Um Said, SE Qatar, where a dominant off-shore winds are driving a clean quartz, eolian sand sheet into the Persian Gulf (Shinn, 1973); to Abu Dhabi, U.A.E., where a restricted, shallow coastline hosts a carbonate dominated sabkha (Purser, 1973). Though sediments vary between coastal sabkhas, there are similarities in the major element geochemistry and hydrology of the groundwaters.

# 1.4.1 Hydrology

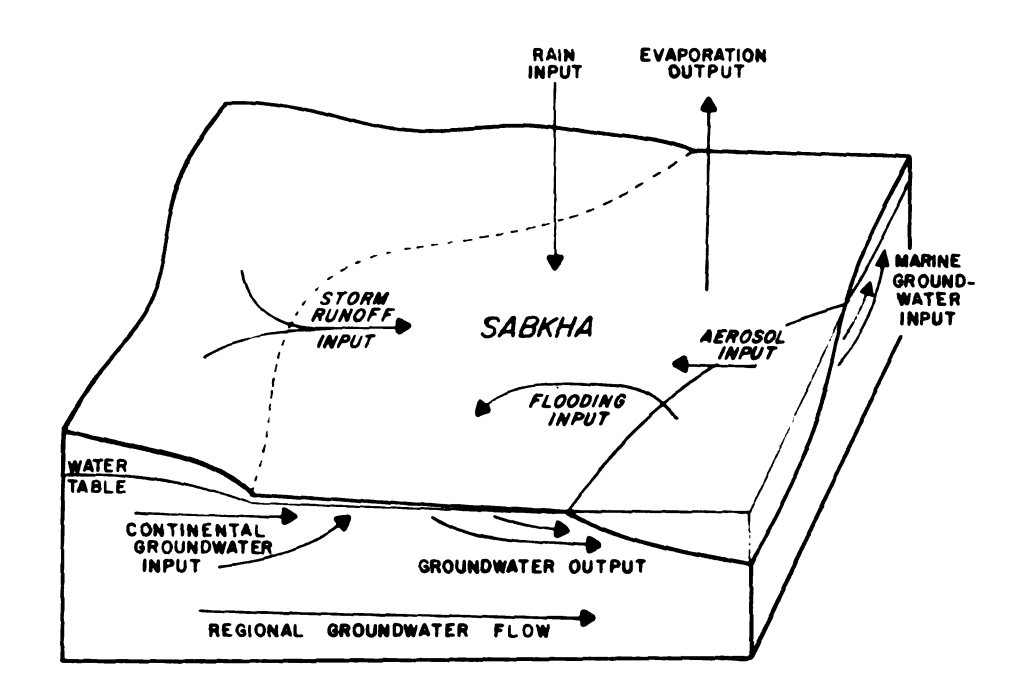
The hydrology of a modern sabkha can be described interms of inflows and outflows of water to the sabkha. The possible inflows of water to a sabkha are (1) continental groundwater, (2) seawater derived groundwater, (3) seawater flooding, (4) storm runoff from surrounding land, (5) rain water, and (6) aerosols from breaking waves. The major outflows of water from a sabkha are (1) evaporation and (2)

groundwater flow into the ocean, an estuary, or a canal. Figure 1 shows the possible inputs and outputs of water in a hypothetical sabkha.

The overall hydrology of a modern sabkha is a combination of these inflows and outflows, with different areas of a sabkha effected by different flows (Patterson and Kinsman, 1977 and 1981; McKenzie, et al., 1980; Butler, 1969). Four models have been proposed for the hydrology of a sabkha which use different forces to move different source of water into and through the sabkha: 1) flood recharge (Mason, 1955; Fisk, 1959; Butler, 1969), 2) seepege reflux (Adams and Rhodes, 1960), 3) capillary action (Friedman and Sanders, 1967), and 4) evaporitive pumping (Hsu and Siegenthaler, 1969).

In flood recharge (Butler, 1969), the input of water sabkha is from marine flooding, with possible contributions from storm runoff. The flood waters overly the water table, creating a hydraulic head which causes the flood waters to move down into the sabkha sediments. The flood waters are concentrated by evaporation during aerial exposure and by evaporation through the unsaturated zone in the Outputs of water from the sabkha are from evaporation and from groundwater flow. Due to the elevation head, piezometric potentials should decrease with depth when flooding has occured; after flood waters penetrate the sabkha

Figure 1. Inputs and outputs of water to a sabkha.



sediments, and the associated elevation head decays, the relationship of piezometric potentials with depth may vary. At Abu Dhabi, U.A.E., a flood guage inserted in a shallow well recorded sharp increases in the groundwater table after flooding, followed by a slow decay (McKenzie, et al., 1980).

Similar to flood recharge, the input of water in seepage reflux (Adams and Rhodes, 1960) is from flooding. In this model, the path of groundwater is similar to that in flood recharge, but the cause for groundwater movement is different. On the surface of the sabkha, flood waters are concentrated by evaporation until they are denser then the underlying groundwater. This causes the flood waters to reflux through the less dense groundwater, and flow toward the ocean. The outputs of water from the system are again evaporation and groundwater movement, and piezometric potentials should decrease with depth.

In capillary action (Friedman and Sanders, 1967) continental groundwater, under a regional head, flows through the sabkha and into the ocean. In the sabkha sediments, evaporation through the capillary fringe concentrates the continental groundwater. Piezometric potentials will decrease toward the ocean, and increase with depth. This is the hydrology which best fits the Renfro (1974) model for the deposition of stratiform ore deposits, and occurs where flooding is infrequent on the landward side of the sabkha at

Abu Dhabi, U.A.E. (Patterson and Kinsman, 1977 and 1981; McKenzie, et al., 1980).

In evaporitive pumping (Hsu and Siegenthaler, 1969), evaporation of the groundwater through the capillary fringe of the unsaturated zone is the only output of water from the sabkha. The evaporation decreases the piezometric potential at the surface, causing an upward inflow of either marine or continental groundwater. Piezometric potentials decrease from the sides of the sabkha toward the center. This is not a major hydrologic process in modern sabkhas (i.e. Abu Dhabi, U.A.E., Patterson and Kinsman, 1977 and 1981; McKenzie, et al., 1980; Umm Said, SE Qatar, DeGroot, 1973; the Laguna Madre Flats, South Texas, Gudramovics, 1981)

These four models (flood recharge, seepage reflux, capillary action, and evaporitive pumping) represent different processes controlling the inflows and outflows of water to a sabkha. These are not the only possible pathways for water through the sabkha. Generally, modern sabkhas have a combination of inflows and outflows of water, controlled by factors such as the frequency of flooding (which controlled by topography, dominant wind direction, distance the source of flooding, and other physical the tidal flat), or the regional characteristic of Also. the sabkha sediments groundwater head. heterogeneous; large differences in permeability can alter

the direction of groundwater flow through the sabkha, and trap continental groundwater in confined aquifers below the sabkha.

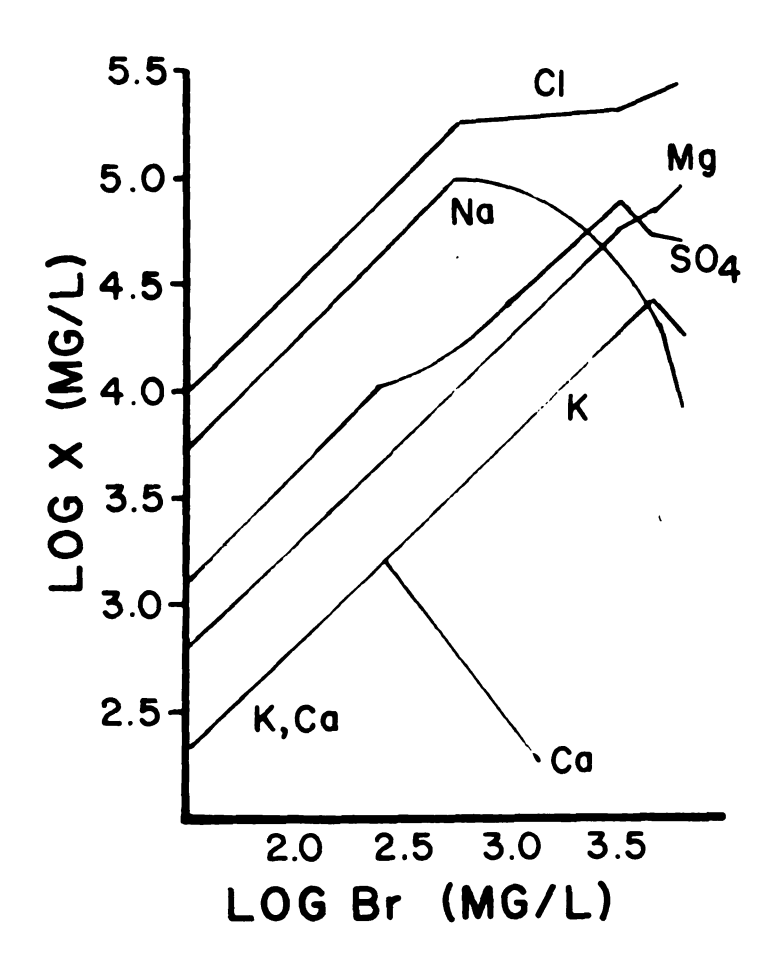
# 1.4.2 Major Element Chemistry

The two major sources of groundwater to modern sabkha are seawater and continental derived groundwater. Though these two waters are modified in the sabkha sediments by evaporation, water rock interactions, and mixing, they often retain characteristic chemical signitures which can distinguish them.

The evaporation of seawater derived groundwater causes residual solution to become more concentrated, and the eventually to become saturated with respect to specific minerals. As evaporation continues, the precipitation of the saturated minerals causes changes in the relative concentrations of the major elements in the residual brine. The changes in concentration of the major elements during the evaporation of seawater has been determined, and is shown in Figure 1 (Carpenter, 1978; Eugster and Jones, 1979).

Upon initial evaporation of seawater, all of the major elements increase in concentration proportional to the amount of evaporation. With continued evaporation, CaCO<sub>3</sub> as calcite or aragonite, and CaSO<sub>4</sub> as gypsum or anhydrite will become saturated in the solution and precipitate out. Since sulfate has a higher molar concentration in sea water then calcium,

Figure 2. Chemical changes during the evaporation of seawater (from Carpenter, 1978).



continued precipitation of CaSO<sub>4</sub>, caused by continued evaporation, will deplete the solution in calcium, but not in sulfate. As calcium is depleted, sulfate concentrations will again increase proportional to the amount of evaporation (see Figure 1).

With continued evaporation, halite saturation will be reached, and halite precipitation will occur. Since chloride has a slightly higher molar concentration in seawater then sodium, further evaporation and halite precipitation causes a decrease in the sodium concentration and a stabilization of the chloride concentration. Continued evaporation can lead to the precipitation of magnesium salts, such as MgSO $_{4}$ .

Water rock interactions may also change the chemistry of seawater derived brines. In addition, the dissolution of soluble salts already in the sediment may alter the brine geochemistry (Carpenter, 1978; Levy, 1977, b).

Bromide and potassium are not involved in the reactions described above, instead, bromide and potassium normally behave conservatively. As seawater evaporates, their concentrations increase proportional to the amount evaporation. The conservative behavior of bromide potassium during the evaporation of seawater can be used as a tool in examining the major element evolution of sabkha groundwaters. First, the ratio of patassium to bromide will remain constant for all seawater derived groundwater:

Patterson and Kinsman (1977 and 1981) use an increase in the K/Br ratio as evidence for the presence of a continental groundwater entering the back of the sabkha at Abu Dhabi, U.A.E.. Second, the ratio of the bromide or potassium concentration in seawater derived groundwater to its concentration in seawater will give a concentration factor due to evaporation. Thus, if a seawater derived brine has a bromide concentration of 268 ppm, and sea water has a bromide concentration of 67 ppm, the brine has been concentrated 4 fold by evaporation. Also, the ratio of any element to bromide or potassium, with varying amounts of evaporation should be constant, unless that element is involved in a reaction other then the removal of water by evaporation.

Bromide is generally used as a conservative indicator, as the concentration of potassium can be affected by reactions with clay minerals or by sylvite precipitation/dissolution after excessive evaporation. Also chloride concentrations are conservative prior to halite precipitation.

In arid climates where sabkhas form, continental groundwater is generally saline, with variable major element chemistry. Depending on the initial chemistry of the groundwater, brines formed by the evaporation of continental groundwater may follow a trend similar to the evaporation of sea water; however, the potassium to bromide ratio is,

usually, characteristically different in continental derived groundwater than in seawater derived groundwater.

The mixture of seawater derived groundwater with continental derived groundwater will form a mixed groundwater. The major element chemistry of the mixed groundwater lies on simple mixing trends between the seawater derived and the continental derived groundwater unless evaporation causes mineral precipitation.

### 1.4.3 Heavy Metals

The distribution and concentration of heavy metals in sabkha sediments is not well defined. In sabkha sediments which have been analyzed, heavy metal concentrations are similar to other sedimentary environments. Algal mat growth and decay are suggested to control the metals in sabkha sediments; however, the importance of algal mat biogeochemistry on the behavior of metals in sabkha sediments has not been rigorously defined.

Ferguson and Burne (1981) examine the fate of metals in groundwater inland of the sabkha at Spencer Gulf, South Australia. The sabkha sediments at Spencer Gulf are fine sands to clays, with reducing conditions existing below the surface in the algal-matted intertidal and supratidal zones. Sediment metal concentrations range from 0.06% to 6.5% for Fe, <1 ppm to 50 ppm for Cu, 4 ppm to 78 ppm for Zn, and <5 ppm for Pb. The continental groundwater is oxidizing,

with a range in pH from 6.0 to 6.8, and a high salinity. Two continental aquifers were identified, one unconfined and one confined. In the unconfined surface aquifer, Fe and Mn concentrations are 1 ppm and 0.5 ppm, respectively, and Co, Ni, Cu, and Pb concentrations are all <0.01 ppm. In the confined aquifer, Fe and Mn concentrations are 60 ppm and 5 ppm, respectively, and the Co, Ni, Cu, and Pb concentrations are again all <0.01 ppm.

The continental groundwater emerges as springs inland of the sabkha, away from the reducing conditions on the tidal flat. In these oxidizing conditions, iron in solution forms iron oxides. During dry periods, some springs dry up as the water table drops below the sediment, and sulfate reducing bacteria decrease the Eh. When this occurs, the iron oxides are converted into iron sulfides; however, when the groundwater table raises, the sulfides are totally oxidized by the continental groundwater, and iron oxides form again.

When the continental groundwater discharges in the springs, Ferguson and Burne (1981) suggest that the Cu, Zn, and Pb in the groundwater will either adsorb onto the iron oxides, or will stay in solution until the continental water reaches the reducing tidal flats. However, Ferguson and Burne (1981) only examined surface samples from behind the sabkha where the continental groundwater emerges from the oxidizing sediments; they did not sample where the

continental groundwater enters the reducing sediments.

Dissanayake (1984) reports the total concentrations of 24 elements in 15 samples from the Tidal Flats of Manar Island, northwest Sri Lanka. The samples are algal laminated, clastic sediments. Chromium, manganese, iron, cobalt, nickel, and copper are included in the 24 elements analyzed, and all show no enrichment in the sediment.

Gaudette and Lyons (1984) report the concentration of Fe, Cr, Cu, Zn, and Pb in sediments from two sabkhas: Solar Lake, east of the Sinai and Goto Meer, Bonaire, Netherlands Antilles. Reported metal concentrations are from an 18 hour leach with 10% nitric acid at 60°C, which leaches "as much as 80-85% of the total sedimentary metal" (Gaudette Lyons, 1984, p. 426). of the metals None are concentrated above average values for sedimentary deposits. Copper, zinc and chromium concentrations correlate positively concentrations, and Pb does not. This is attributed to lead being incorporated in carbonates, while the other metals are not. None of the metals correlate with organic carbon content.

Long, et al. (1985) present the metal data from Gaudette and Lyons (1984), and Pb, Cu, and Zn concentrations in sediments from the Sabkha Gavish, east Sinai; Pekelemeer and Cai, Bonaire, the Netherlands Antilles; and one core from the Laguna Madre Flats, South Texas. Metal concentrations of

the hydromorphic fraction (metal available for reaction without altering the lattice of resistant minerals) are presented. Again, metal concentrations are not above average sedimentary values. In all locations, sediments associated with living or decaying algal mats have higher metal concentrations; the sediments from Laguna Madre, Texas, were sequentially leached to distinguish metals bound with organics or sulfides from the rest of the hydromorphic fraction, and most of the metals were associated with organics or sulfides. Long, et al. (1985) conclude that algal mats are important in the initial concentration of metals. They also suggest that metals can be reconcentrated during diagenesis, as metal concentrations change with depth in one core from the Laguna Madre Flats, Texas.

#### CHAPTER 2

### AREA OF STUDY

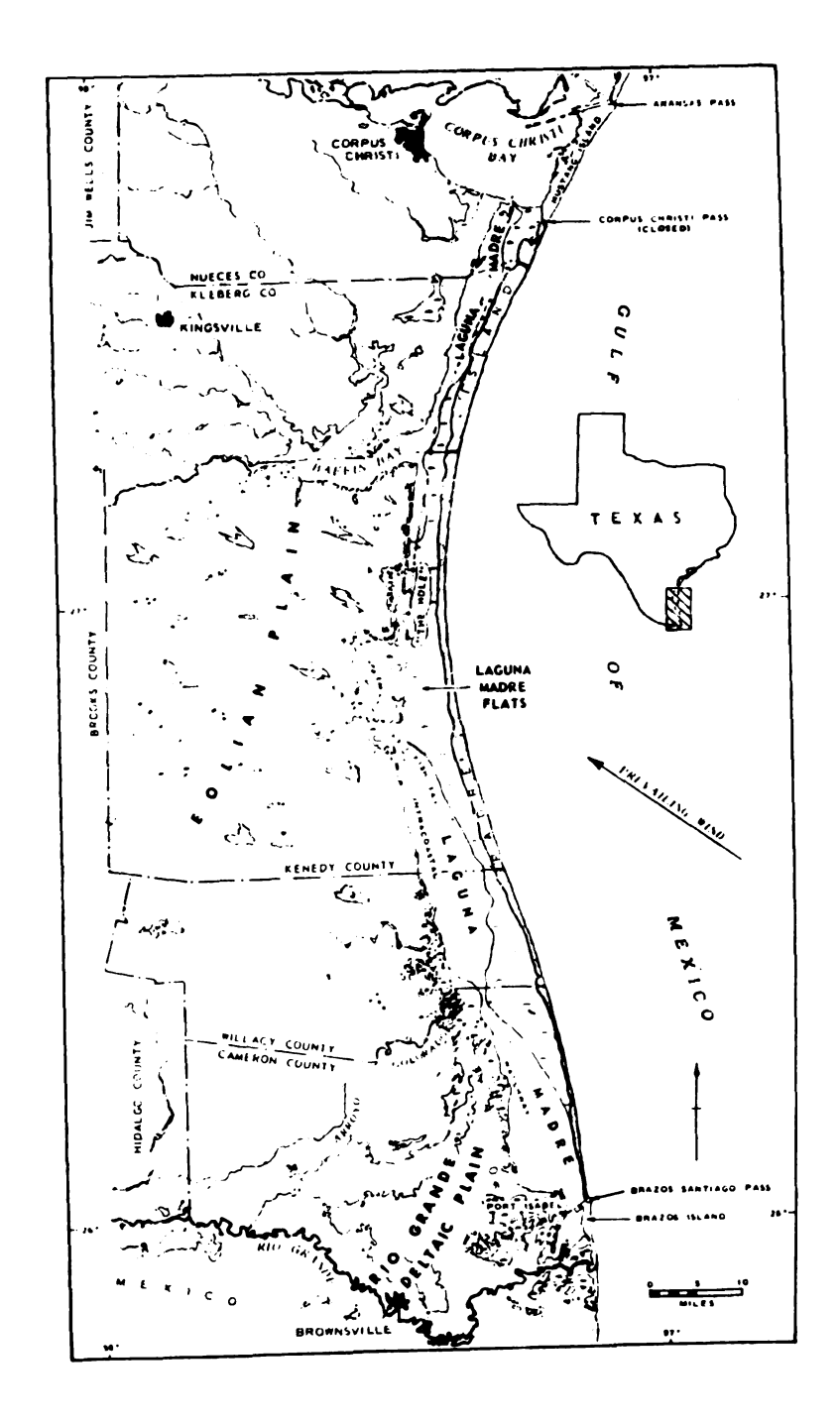
#### 2.1 INTRODUCTION

The sabkha studied is in eastern Kennedy County, Texas, about 90 km north of Brownsville, Texas, and 90 km south of Corpus Christi, Texas. Fisk (1959) initially studied the geology of the sabkha and named it the Laguna Madre Flats. To the east of the sabkha, Padre Island separates the tidal flats from the Gulf of Mexico, and to the west of the sabkha lie extensive private ranches on eolian sediments. The Laguna Madre Flats and the South Texas coast are shown in Figure 3.

# 2.2 REGIONAL GEOLOGY

Pleistocene and Holocene (Recent) sediments cover the South Texas coastal plain. The Pleistocene sediments, deposited during interglacial periods prior to 18,000 years before present, form fluvial, deltaic, and barrier island-strandplain facies. Pleistocene sediments outcrop to the west of the sabkha, where they are partially covered by Holocene eolian sediments. The Pleistocene of South Texas dips toward the gulf at about 1 m/km (Brown, et al., 1977). Holocene sediments unconformably overlie the Pleistocene

Figure 3. Map of the South Texas coast (from Fisk, 1959).



sediments, and form barrier island, lagoon, tidal flat, and eolian plain facies.

Present barrier island sediments form Padre Island, which runs a gently curved, north-south path from Corpus Christi to the Brazos Santiago Pass (see Figure 1). Padre Island is continuous except for one break at Port Mansfield, 40 km north of the Brazos Santiago Pass. The island is 1 to 5 kilometers wide and generally 1.5 to 3 meters above mean sea level. Dunes give local topographic relief of up to 9 meters, and are grass covered except where recently breached by storm tides (Brown, et al., 1977).

Behind the barrier-island facies, South Texas Holocene sediments consist of open lagoon facies in the subsurface, conformably overlain by closed lagoon and tidal flat facies. Present closed lagoon and tidal flat facies form Laguna Madre and the associated wind-tidal flats, respectively (Fisk, 1959).

Laguna Madre, the present closed lagoon facies, extends from Corpus Christi to Brownsville, and is divided into restricted bays by wind-tidal flats. Ninety kilometers south of Corpus Christi, Laguna Madre is divided into two separate lagoons by the Laguna Madre Flats. The two halves of Laguna Madre are connected only by the man made Intercoastal Waterway (ICWW). North of the Laguna Madre Flats, Laguna Madre forms a restricted bay called the Hole. The Hole is

less then 1 m deep, and is connected to the rest of northern Laguna Madre by a narrow, 0.4 m deep channel (Zupan, 1972). South of the Laguna Madre Flats, Laguna Madre forms another restricted bay, called Redfish Bay. Redfish Bay is less then 2.5 m deep and is connected to the rest of southern Laguna Madre by a narrow, 0.5 m deep channel and by the ICWW (Rusnak, 1960; Herber, 1981).

The major element chemistry of the water in Laguna Madre and in the Intercoastal Waterway (ICWW) are equivalent to water in the Gulf of Mexico which has been either concentrated by evaporation or diluted with rain water. Salinities vary from 2 per mil after heavy rains, to 5 times the concentration of the gulf waters. In unrestricted areas, the water in Laguna Madre and the ICWW is usually from 1.1 to 1.5 times the concentration of water in the Gulf of Mexico (Fisk, 1959; Ratzlaff, 1976; Amdurer, 1978; Lind and Ritzlaff, 1979; Gudramovics, 1981).

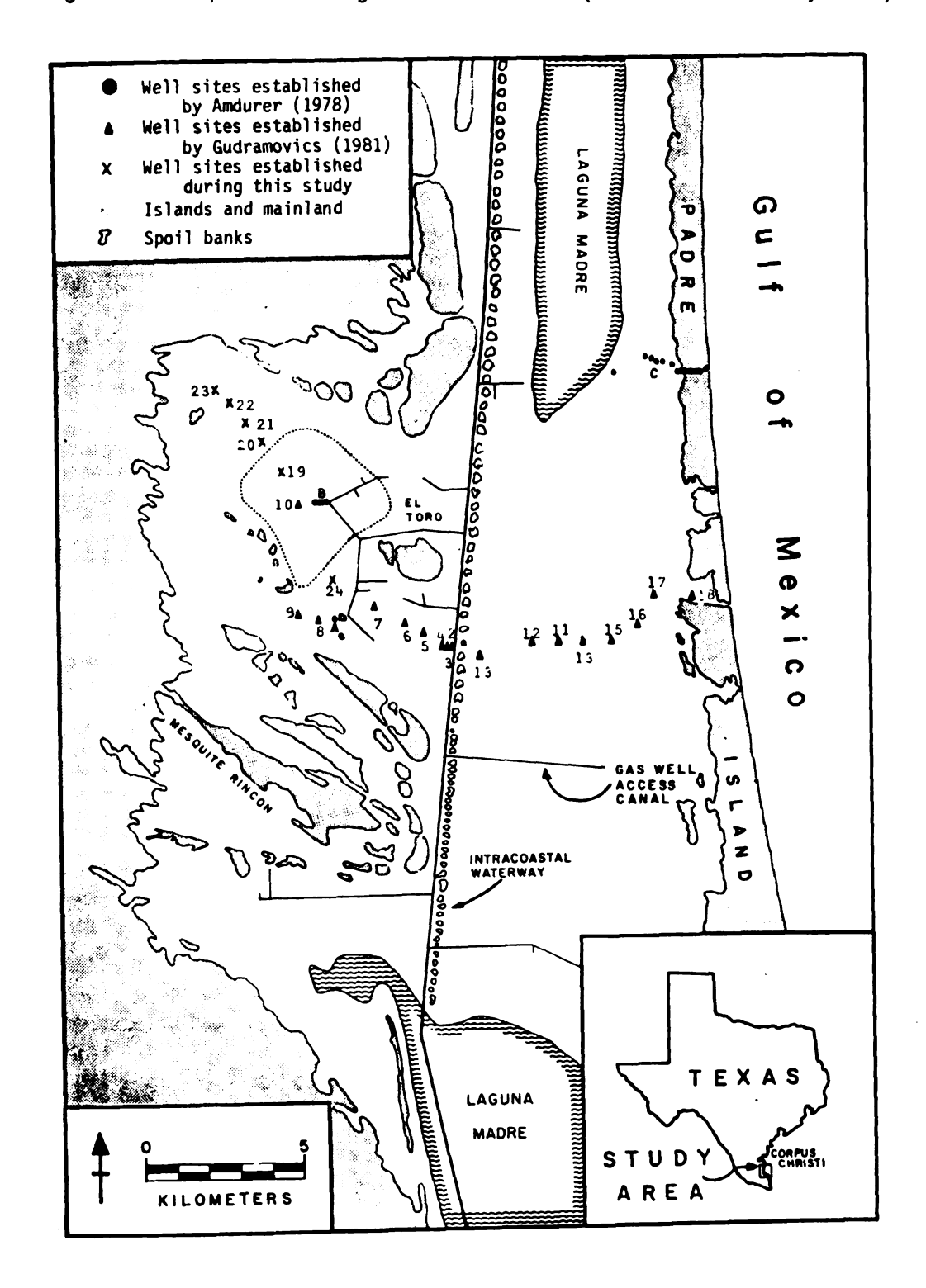
Open circulation of the water from the Gulf of Mexico into Laguna Madre is restricted to Aransas Pass, 70 km to the north of the central flats, and Port Mansfield and Brazos Santiago Passes, 50 and 70 km, respectively, to the south of the flats. Lunar tides in Laguna Madre are at most 5 cm, and cause limited circulation with the Gulf of Mexico. However, wind tides cause considerable circulation between Laguna Madre and the Gulf of Mexico (Fisk, 1959; Rusnak, 1960:

Zupan, 1972). Before the ICWW was constructed in 1949, northern and southern Laguna Madre were isolated, and the average lagoon water was 3 times the concentration of the water in the gulf (Fisk, 1959). The presence of the ICWW allows wind generated tides to flow between northern and southern Laguna Madre, and into the gulf through Aransas, Port Mansfield, or Brazos Santiago Pass. This circulation brings gulf water into Laguna Madre from the south during the prevailing southeasterly winds, and from the north during the winter northerlies (Rusnak, 1960).

The Laguna Madre Flats (shown in Figure 4) form a sabkha 22 km wide and 26 km long. Topographic relief is generally less than 0.2 m per km except on rincons. Rincons are wind deflated relects of old dunes which appear as topographic highs on the sabkha: El Toro and Mesquitte Rincon are two large rincons (Fisk, 1959; Brown, et al., 1977).

On the basis of topography and sediment grain size, Fisk (1959) named different areas of the Laguna Madre Flats. Three of these names will be used in this study: the Sand Bulge, the Basin, and the Marginal Slope. Located east of the ICWW, the Sand Bulge is an area of increased elevation (up to 5 feet above sea level) with dominantly sand size sediments. In contrast, the Basin is an area of decreased elevation (down to sea level) and dominantly clay size sediments; the Basin is outlined with dots in Figure 4.

Figure 4. Map of the Laguna Madre Flats (from Gudramovics, 1981).



Between the Basin and the mainland is an area of increasing grain size and elevation referred to as the Marginal Slope.

#### 2.3 CLIMATE

The Laguna Madre Flats are located in a semiarid climate. Though the average rainfall is about 70 cm per year, the average rainfall minus potential evapotranspiration is -60 cm per year, so there is a net loss of water to the atmosphere in South Texas (Brown, et al., 1977; National Oceanic and Atmospheric Administration, 1982). The average wind speed in Corpus Christi, 90 km north of the sabkha, is 12 mph (National Oceanic and Atmospheric Administration, 1982). The average wind direction across the sabkha is from the southeast, varying from northeast in the late fall and winter to SSE in July (Brown, et al., 1977). This wind regime causes the long shore currents of the western Gulf of Mexico to meet just east of the sabkha, and causes the active dunes on the eolian plain west of the sabkha to align in a southeast direction (Brown, et al., 1977; Fisk, 1959).

Severe tropical storms hit Corpus Christi about once every ten years, and lesser tropical storms about once every 5 years (National Oceanic and Atmospheric Administration, 1982). The occurance over the sabkha should be similar. High flood tides associated with a hurricane breach Padre Island and transport sands onto the Sand Bulge; high flood tides also circulate waters from the Gulf of Mexico into

		~

Laguna Madre (Hayes, 1967; McGowen, et al., 1970). However, the flooding does not alter the geochemistry of the sabkha groundwater, as the flood water can not rapidly penetrate the sabkha sediments (Tolbert, et al., in prep.).

## 2.4 GEOLOGIC HISTORY

The present Texas shoreline has been shaped by the regression and transgression associated with Late Wisconsin glaciation. In South Texas, Early Pleistocene sediments form barrier island, fluvial, and deltaic facies (Brown, et al., 1977). Sediments from an Early Pleistocene barrier beach outcrop just north of Baffin Bay, 10 to 15 feet above present sea level.

Late Wisconsin glaciation caused a global drop in sea level of 90 to 140 meters; this regression shifted the Texas shoreline 80 to 240 km towards the Gulf of Mexico (Russel, 1940; Fisk and McFarlin, 1955; LeBlanc and Hodgson, 1959). During this time of low sea level, river valleys eroded up to 50 meters into the Early Pleistocene sediments (Price, 1933; Fisk, 1959). In the Early Holocene (Early Recent), melting glaciers caused a rise in sea level, which caused a global transgression and formed estuaries in the incised river valleys. Six thousand years before present, with sea level still raising, a barrier island complex began to form on the South Texas coast (Amdurer, et al., 1979). Around 5,000 years before present, mean sea level stabilized near its

present level (Fisk and McFarlin, 1955; Fisk, 1959; LeBlanc and Hodgson, 1959; Beherns and Land, 1972), and by 3,700 years ago, Padre Island had formed (Fisk, 1959).

Since the transgression, estuaries associated with large rivers, such as the Colorado, Brazos, and Rio Grande Rivers, have filled with fluvial sediments, and estuaries associated with rivers having small sediment loads, such as Baffin Bay and Corpus Christi Bay, have partially filled with fluvial, lagoonal, and/or eolian sediments (LeBlanc and Hodgson, 1959; Fisk, 1959). The Laguna Madre Flats lie over an incised river valley which formed an estuary during the Holocene transgression and filled with lagoonal, tidal flat, eolian and barrier island sediments (Fisk, 1959).

## 2.5 SEDIMENTOLOGY

Sediments of the Laguna Madre Flats are predominantly fine clastic sands, silts, and clays. The sand size fraction in Laguna Madre (Rusnak, 1960) and on the wind-tidal flats north of the Hole (Zupan, 1972) is approximately 96% Quartz, 1% to 4% chert and feldspar, with minor heavy minerals and mica. The mineralogy of the clay size fraction on the Laguna Madre Flats is reported to be illite, quartz, and calcite by Fisk (1959), and illite, chlorite/kaolinite, smectite (montmorillonite), quartz, and feldspar by Amdurer (1978).

authigenic calcium carbonate, gypsum, halite, and dolomite are associated with the wind-tidal flats. Calcium carbonate is associated with the algal mats, and is a cement in some buried sediments (Herber, 1981). Amdurer (1978) reported up to 8% calcite in sandy aggregates from the northern Sand Bulge. Gypsum precipitates in the sediments when it is oversaturated in the brines (Gudramovics, 1981). Gypsum commonly forms either white, fine grained layers, 1 mm to 1 cm thick, or clear to gray rossettes (Mason, 1955; Herber, 1981). Halite occurs predominantly as crusts on the surface of the sediments. Dolomite was found by Herber (1981) in sediments from the wind-tidal flats south of Redfish Bay.

By the "tracing of the laminations which cover datable tracks, etc., into closely adjacent undisturbed areas of the flats," Fisk (1959, p. 116) estimated local rates of sedimentation to be from 6.3 to 8.4 mm per year. Fisk (1959) also reports 25 to 30 feet of sediment deposited in the last 5,000 years, which gives a lower average sedimentation rate of 1.3 to 1.8 mm per year. Erosion by wind deflation does occur when the flats are dried, however deflation is not considered an important process (Fisk, 1959).

On the basis of heavy mineral suites, Van Andel and Poole (1960) divided the South Texas shoreline and shelf into three sedimentary provinces: the Western Gulf, Rio Grande,

and Texas Coastal Provinces. The Western Gulf Province includes sediments on Padre Island north of the Laguna Madre Flats and the Gulf of Mexico shelf east of the Laguna Madre Flats. The sediments which form this province are derived from rivers north of the sabkha and from reworked gulf sediments. Sediments from the Rio Grande Province form a Rio Grande delta complex on the shelf of the Gulf of Mexico, to the south of the sabkha. Long shore drift has transported sediments from the Rio Grande Province along the the gulf coast as far north as the Laguna Madre Flats (Lohse, 1956; Van Andel and Poole, 1960). Behind Padre Island, reworked pleistocene sediments form the Texas Coastal Province; Van Andel and Poole (1960) found this province in Baffin Bay, to the north of the Laguna Madre Flats.

Van Andel and Poole (1960) did not sample sediments on the Laguna Madre Flats. However, from the samples analyzed on Padre Island to the east of the sabkha constraints can be placed on the province of the sediments on the flats. As noted before, the prevailing southeast winds cause the north-ward and south-ward long shore currents in the western Gulf of Mexico to meet just east of the Laguna Madre Flats. This is consistant with the results of Van Andel and Poole (1960), as the sediments on Padre Island and the gulf shoreline sampled east of the flats are a mixture of the Western Gulf Province and the Rio Grande Province (which is

transported north by the longshore currents). This mixture of sediments on Padre Island is the source of sediments to the Laguna Madre Flats by eolian transport and storm transport (Hayes, 1967; McGowen, et al., 1970; Brown, et al., 1977). Thus the sand fraction of the sediments on the Laguna Madre Flats should be a combination of Rio Grande and Western Gulf Provinces.

The source of clay size material to the Laguna Madre Flats is variable. Clay size material in Laguna Madre is transported to the sabkha in flood tides from the north during winter northerlies, and in flood tides from the south during the prevailing southeast winds. Clay size material from the Gulf of Mexico is transported to the sabkha in storm tides generated by hurricanes. In addition, clay size material from the eolian plain complex west of the Laguna Madre Flats is transported onto the sabkha by ebb tides after tropical storms and by storm runoff.

## 2.6 GROUNDWATER

Amdurer (1978) and Gudramovics (1981) studied the groundwater in the Laguna Madre Flats. By analyzing the major element chemistry of the groundwater, both studies interpreted the groundwater to be evaporated Gulf of Mexico water, with a possible continental groundwater source in the Basin. Both studies also examined the hydrology of the sabkha.

Amdurer (1978) (see also Amdurer and Land, 1982) established well sites in three areas shown on Figure 4: at A south of the basin, two well sites were established next to an unnamed hummock; at B in the Basin, four well sites were established on a 450 m line; at C on the northeast corner of the sabkha, 16 well sites were established which traverse Padre Island and the northern most portion of the Sand Bulge. At each well site, 1.5 m and 3.0 m long pieces of 2 inch diameter poly vinyl chloride (PVC) pipe were driven into the flats, and the sediments were removed from the interior of the pipes. In June, August, and October of 1975, and April of 1976, water samples were collected and water table heights recorded at the 16 sites labled C in Figure 2. In July of 1975, water samples were collected at the sites labled A and B in Figure 4.

In the northern portion of the Sand Bulge, the major element chemistry of the groundwater is similar to evaporated seawater, with chloride concentrations reaching 6.8 times the concentration of seawater. Amdurer (1978) noted that sulfate concentrations are not drastically depleted, and speculated that gypsum was kept undersaturated in the brines by the uptake of calcium as algal micrite. However, sulfate concentrations are slighty depleted relative chloride; also, calculated activity products show that gypsum is near equilibrium with the groundwater, though calcite is highly

undersaturated. Thus, gypsum precipitation is suggested to occur in the nothern Sand Bulge, and to effect calcium and sulfate concentrations in the groundwater.

Magnesium concentrations deviated from an evaporated seawater trend. In the groundwater with concentrations less than 5 times the concentration depleted relative to chloride. seawater. magnesium is Amdurer (1978) suggests three reasons for magnesium depletion: 1) cation exchange with clay minerals in the sediment, 2) authigenic formation of chlorite, 3) Though no dolomite was found by Amdurer dolomitization. (1981), Herber (1981) did find dolomite on the wind-tidal flats south of Redfish Bay. In groundwater with chloride concentrations higher than 5 times that of magnesium concentrations are higher then those predicted by evaporating seawater. No reason for this enrichment was presented.

The hydrology of the northern Sand Bulge is dominated by flood recharge. The flood recharge model is supported by piezometric potentials which decreased with depth and by the following evidence that flood waters penetrate the sediments. A portion of the Sand Bulge was flooded by water with a salinity of 5 per mil; when the flood water receded, surface groundwater was sampled where the flood water had covered the sabkha and 5 m to 20 m away where the floodwater had not

covered the flats. Groundwater salinities ranged from 171 per mil to 182 per mil in the flooded area, and from 200 per mil to 212 per mil in the adjacent unflooded area. Thus, some of the flood water penetrated the sabkha sediments and recharged the groundwater.

Groundwater from Padre Island (at C on Figure 4) is chemically distinct from evaporated seawater. Piezometric surfaces across Padre Island increased after rain fell, and a tide guage set in a well on Padre Island showed that the water table increases quickly after a rain event, and then decreased slowly. From the hydrology, major element chemistry, and analogy to other studies, Amdurer (1978) suggests that the source of the groundwater on Padre Island is rain water and aerosols from the Gulf of Mexico.

Amdurer (1978) attributes the groundwater in the Basin to two different sources. Trench samples are attributed to evaporated seawater, as their major element chemistries match those predicted by the evaporation of seawater. Samples from 3.0 m deep are presented as different from the surface groundwater due to (1) an increase in dissolved silica, (2) a salinity, (3) а decrease in in concentrations, and (4) an artesian head on some of the 3.0 m deep wells. However, these are not good characteristics to differentiate two waters. Dissolved silica (1) is necessarily a conservative species, but may be controlled by water-rock interactions. A decrease in brine concentration with depth (2) can be caused if the water at depth has undergone less evaporation then the water at the surface. Sulfate concentrations (3) should decrease with depth if the brine salinity decreases with depth. Finally, an artesian head (4) indicates that there is a force acting to raise the water, not that the groundwater from 3.0 m deep is different than the surface groundwater. Though a regional or continental head may be causing the artesian head, it cannot be said that the groundwater sampled from 3.0 m deep is continental groundwater.

Gudramovics (1981) (see also Long and Gudramovics, 1981) established well sites numbered 2 through 18 on figure 2. At each well site, 1.9 m and 3.8 m long pieces of 2 inch diameter PVC pipe were driven into the flats and the sediments removed from within the pipe. Gudramovics (1981) collected water samples and recorded water tables for the two wells and a trench at each of the new well sites in August, 1979 and March, 1980. During the August, 1979 trip, the well sites which Amdurer (1978) established in the basin (labled B in figure 4) were also sampled.

At well sites on the east-west traverse from site 16 to site 7 the major element chemistry of the groundwater is similar to evaporated seawater; the groundwater at well sites 17 and 18 is effected by the fresh water under Padre Island.

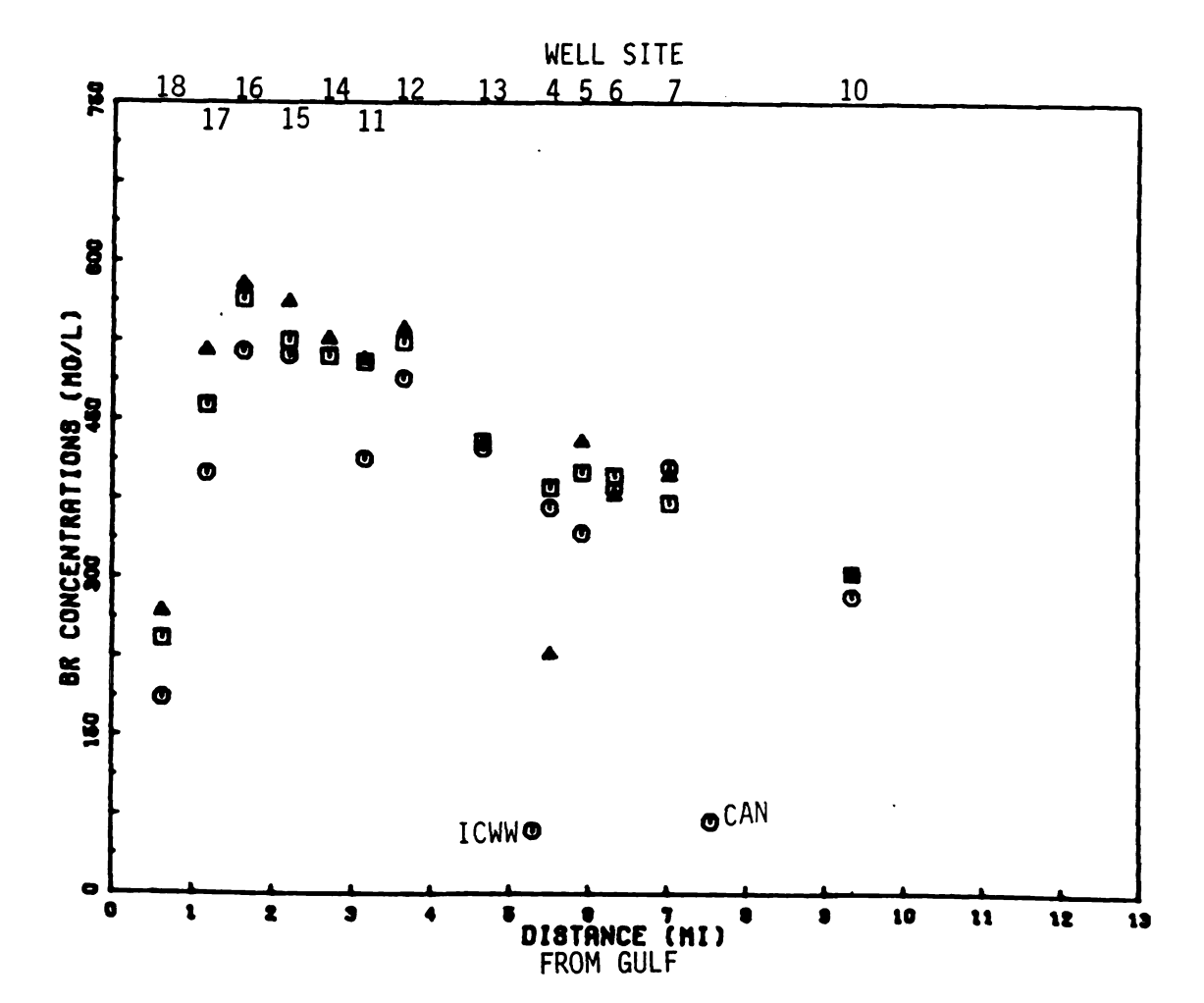
The concentrations of the conservative ion bromide are plotted across this traverse in Figure 5, for the March, 1980, sampling. A maximum bromide concentration 9.7 times the concentration in seawater is reached just west of Padre Island at site 16. West of site 16. the concentrations (relative amount of evaporation) decrease. Consistant with the evaporation of seawater, calcium is depleted in the brines due to removal as carbonates and sulfates. Strontium is also depleted in the groundwater; Gudramovics (1981) attributes strontium depletion to the substitution of strontium for calcium in calcium carbonates and/or sulfates.

On the traverse from site 16 to site 9, the flood recharge model adequately describes the piezometric surfaces and the chemistry of the groundwater. Flooding would decrease from site 9 to site 16, as the dominantly southeast winds drive wind-tides from Redfish Bay toward the western sites, and an increase in elevation from site 12 to site 18 should decrease the amount of flooding in the east.

Similar to Amdurer (1978), Gudramovics (1981) suggests that the groundwater in the basin is from two different sources. The groundwater from the trenches is attributed to the evaporation of seawater. The groundwater from the 3.0 m deep wells (3.8 m at site 10) is distinguished from evaporated seawater by (1) an increase in the chloride to

Figure 5. Bromide concentrations across the sabkha: August, 1979.

- Trench or surface sample Shallow well (1.9 m depth) Deep well (3.8 m depth)



bromide ratio, and (2) a change in the magnesium to calcium ratio. An artesian head is again noted on some of the deeper wells. Gudramovics (1981) attributes the deeper groundwater to a mixture of seawater derived groundwater and either eolian plain groundwater or water from the underlying Goliad Aquifer.

## CHAPTER 3

#### **METHODS**

In this study, the groundwater and surface water, and the sediments of the Laguna Madre Flats were collected and analyzed. The methods used on liquid samples and sediment samples are presented separately.

## 3.1 LIQUID SAMPLES

Samples of the groundwater and surface water of the Laguna Madre Flats were collected in August, 1982. Water samples were collected from 29 of the sites shown on Figure 4: well sites 3 through 24, the four well sites in the basin labled B (Am2, Am3, Am4, and Am5), the Intercoastal Waterway (ICWW), the canal in the basin, and the Gulf of Mexico east of site 18. The locations of these sites are given in Appendix F. Sampling was conducted by J.N. Tolbert, Dr. D.T. Long, and J.N. Marsh.

Well sites 19 through 24 were established during this study. At each site, 1.9 m and 3.8 m lengths of 2 inch diameter, ploy vinyl chloride (PVC) pipe were driven into the sediment with a diver-corer system (Martin and Miller, 1982). The 1.9 m and 3.8 m long PVC pipes are referred to as the shallow and deep wells, respectively. Sediments within the

PVC pipes were removed with an auger, and the water which filled the tubes was purged twice. Caps were placed on the PVC pipes to prevent excess evaporation or contamination by rain water, flood water, or wind blown sediment. Evaporation through the seal of the cap, and condensation inside the PVC tube created possible errors, so all wells were purged within 24 hours of sampling.

Well sites 3 through 18 were established by Gudramovics (1981). Again, each site has 2 wells which are 1.9 m and 3.8 m deep, referred to as the shallow and deep wells, respectively. Well sites Am2, Am3, Am4, and Am5, labled B in Figure 2, were established by Amdurer (1978). At these four sites, the shallow and deep wells are 1.5 m and 3.0 m deep, respectively.

Sampling was conducted during three to four day trips to the sabkha. On the first day at a site (1) water table heights were recorded in the shallow and deep wells, (2) wells were purged of water, and (3) a trench was dug and the surface groundwater was sampled. On the following day, the shallow and deep wells were sampled, and the water level in the trench was recorded. Later measurements indicate that the water level in the trenches did not raise after this initial period, so the water level recorded on the second day at a site represents the groundwater table. Sampling of the water was done with a peristaltic hand pump. Tygon tubing

was the only surface in contact with the water sample, and the tubing was purged with 500 ml of distilled, demineralized water prior to each sampling. Samples were pumped into 500 ml Nalgene polypropylene bottles. Trench, shallow, and deep samples from a well site are labled by placing a T, S, or D, respectively, after the well site identification; thus, sample 22S is the sample from the 1.9 m well at site 22.

Immediatly upon sampling, the temperature and pH were recorded. The pH was measured with a model 399A Orion Research Ionalyzer. Alkalinity was measured within 12 hours of collection by an electrometric titration (U.S.G.S. method I-1030-78; Skougstad, et al., 1979). In this method the sample is titrated with  $\rm H_2SO_4$  to a pH of 4.5, and the alkalinity is reported as mg/l  $\rm CaCO_3$ . Though other anions may have contributed the the alkalinity (i.e. sulfides and phosphates), the carbonate system is suggested to be the dominant control. Amdurer (1978) showed that sulfides did not suply a measurable portion of the alkalinity to the sabkha groundwater.

Within 72 hours of collection, the samples were brought to the United States Geological Survey (U.S.G.S.) laboratory in Corpus Christi, Texas, where they were (1) filtered through a 0.45 micron membrane filter, (2) analyzed for dissolved chloride by a Mohr titration (U.S.G.S. method I-1183-78; Skougstad, et al., 1979), (3) acidified to a

pH < 2 with concentrated nitric acid, and (4) returned to their sampling bottle. The polyethylene bottles were then sealed with teflon tape around the caps, packaged, and sent to the Department of Geological Sciences at Michigan State University (M.S.U.). At M.S.U., the samples were stored at room temperature until analyses were preformed in September, 1983, through July, 1984.

Visible solid precipitates formed during storage in samples 19S, 20S, 24S, Am3T, Am4T, Am4D, Am5T, and Am5D. In subsampling for analysis, the precipitates were brought into suspension, and sampled with the liquid. A 1 ml pipet with the end chipped off was used for sampling to avoid preferentially sampling the liquid. Out of 20 trials, the average delivery of the pipet was 0.97057 ml with a standard deviation of 0.00608. The precipitate was not visible in any of the dilutions, and is assumed to have dissolved.

Potassium, sodium, and calcium were analyzed on a Perkin Elmer 560 Atomic Absorption Spectrophotometer, with an optional furnace attachment (HGA 2200 Controller and AS 40 Autosampler). Potassium was measured on 1/1000 dilutions with 1000 mg/l Na background in all standards and samples to eliminate the effects of sodium variations in the samples and supress potassium ionization in the flame (U.S.G.S. method I-1630-78; Skougstad, et al., 1979). Sodium was measured on 1/1000 dilutions with a 10 g/l La background, as LaCl<sub>3</sub>, in

all standards and samples. Calcium was measured on 1/100 dilutions with a LaCl<sub>3</sub> background (U.S.G.S. method I-1152-78; Skougstad, et al., 1979).

Bromide was analyzed colorimetrically by the change in absorbtion at 595 millimicrons upon oxidation of the bromide with chloramine-T. The method used was originally proposed by Presely (1971), and was modified by Gudramovics (1981) for higher bromide concentrations.

Transition metals were extracted from the brines methyl iso-butyl ketone (MIBK) with ammonium pyrrolidine dithiocarbamate (APDC), by a procedure adapted from Parker (1972).In this procedure, 50 ml of sample, with a pH adjusted to 2.5 with hydrochloric acid or ammonium hydroxide, are combined with 5 ml of 1% APDC, and shaken for 1 minute to allow the APDC to form strong complexes with the metals Next, 20 ml of MIBK are added and the solution is shaken vigorously for 3 minutes. When this mixture is let stand, the MIBK seperates from the sample, and the APDC is highly partitioned into the MIBK, extracting the chelated metals from the brine. The MIBK was analyzed for metals by flame and flameless atomic absorption spectrophotometry. eighteen samples analyzed, cobalt, nickel, and copper were undetected, with a limit of detection of 0.005 ppm, 0.005 ppm, and 0.01 ppm, respectively, in the initial sample. Zinc was contaminated in the MIBK (equivalant to >>0.1 ppm in the initial sample). Manganese and iron data are reported in Appendix C.

Density could not be measured directly due to the precipitation of solids in some of the samples, so density was calculated from the concentration of chloride and sodium in the groundwater. Sodium, chloride and bromide concentrations were regressed against density in 116 from the Laguna Madre Flats analyzed by Gudramovics (1981). The multiple linear regresson of sodium and chloride against density gave the best fit line, and is used to calculate the density of the water samples in this study. The equation used is:

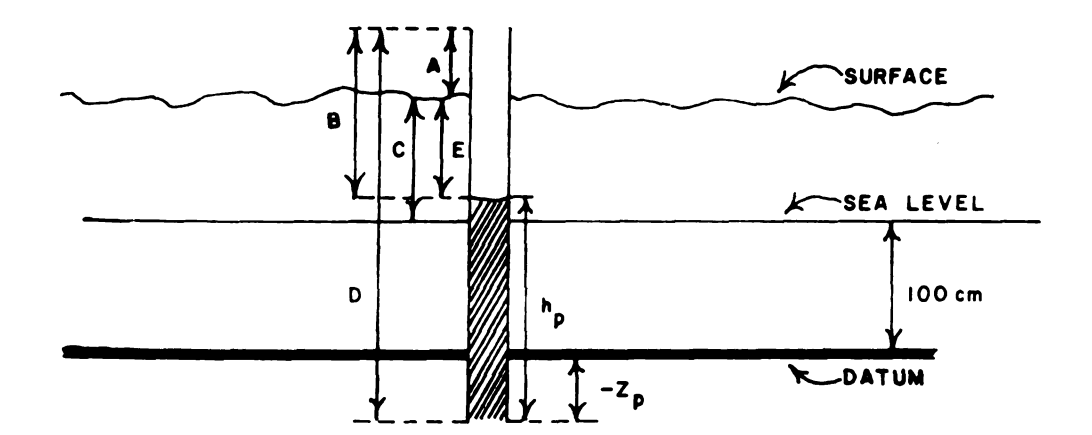
density =  $1.0018 + 1.2993*10^{-6}$  (Na) +  $4.3092*10^{-7}$  (C1), where (Na) and (C1) equal the sodium and chloride concentrations in ppm, and density is in grams per milliliter. For this regression, the standard deviation of density about the regression line is 0.00504 and r-squared equals 0.986, adjusted for 113 degrees of freedom.

The piezometric potentials (phi) for wells and trenches are calculated by the equations used by Gudramovics (1981). Figure 6 shows a hypothetical well, where the distances A and B were measured in the field and the distance C was measured by an alidade. The piezometric potential is defined by:

phi = Density 
$$(h_p + z_p)$$

Where phi is the piezometric potential,  $h_{D}$  is the head

Figure 6. Hypothetical well for calculating piezometric potentials (from Gudramovics, 1981). See text for discussion.



potential, and  $z_p$  is the elevation potential. Calculating  $z_p$  from a datum 100 cm below sea level,  $h_p$  and  $z_p$  can be defined as follows:

$$h_D = D - B$$
,

and

$$z_{D} = A + C + 100cm - D.$$

Thus,

$$phi = density(A - B + C + 100cm).$$

Piezometric potential (phi), density, site elevation (C), and water level (A-B) are given in appendix E.

## 3.2 SEDIMENT SAMPLES

The sabkha sediments were sampled at two times. In March, 1980, sediments were sampled at sites 6, 8, and 16; in August, 1982, sediments were sampled at sites 10, 19, 22, 23, and 24.

In March, 1980, diver cores were taken at sites 6, 8, and 16, using the coring device described in Martin and Miller (1982). The cores were taken in PVC tubing with an interior diameter of two inches. After sampling the cores were immediately sealed on both ends and shipped to Michigan State University, East Lansing, Michigan where the cores were stored at room temperature until September of 1984.

When the cores were opened, the sediments from sites 6 and 16, described in Appendix A, were moist and unlithified. The sediments in the core from site 8 were moist and unlithified over the top two thirds of the core, where the changed from a yellowish brown sand at the top, to a gray

sand with depth; however, the bottom third of the core was dry, orangish brown, and partially lithified. These bottom sands had a fine grained, calcium carbonate matrix which was not totally removed by two washes with sodium acetate buffer (pH=5). Since the groundwater at site 8 is not highly depleted in calcium relative to evaporated seawater, it is suggested that the calcium carbonate cement did not precipitate from the sabkha groundwater prior to sampling of Instead, the dryness, the oxidizing appearence (yellowish brown sediments), and the calcium carbonate cement are attributed to the interaction between the sediments in the core and the atmosphere through the bottom seal in the Also, due to the moist, unlithified sediments in the core. cores from sites 6 and 16, the seals on these cores are assumed to have effectively inhibited interaction between the sediments and their surroundings during storage.

Due to the probable interaction of the sediments from site 8 with their surroundings, these sediments were not analyzed. The sediments in the cores from sites 6 and 16 were sampled at interesting lithologies, identified in Appendix A.

In the sediments from sites 6 and 16, it is assumed that the dominant metal partitioning in the sediments did not change during 4 years of storage. The total metal removed by the two sequential leaches used would only be effected by

storage if there was insitu weathering of silicate minerals during the four years of storage, or the formation of resistant minerals which are not dissolved by the leach. suggested that the redox conditions of the sediments did not change enough to effect metal behavior, though continued decay of organic mater may have changed the redox conditions. This is supported by the similarity of the metal partition in the sediments at these sites to those at other sites, and by The sediments in core 6 the appearence of the sediment. appeared orangish brown (oxidizing) at the top, and changed to gray (reducing) with depth; the sediments in core 16 were orangeish brown (oxidizing). completely However, metal repartitioning is possible at these sites, so the data from sites 6 and 16 should be interpreted with caution.

The sediments at sites 10, 19, 22, 23, and 24 were sampled in August, 1982. At each site, samples were taken from the side of a pit at 20 cm intervals and at interesting lithologies, and photographs were taken of the wall of the pit. The samples were individually placed in polyethylene bags, and shipped to Michigan State University where they were frozen until analyzed.

In the laboratory, two subsamples were taken from each of the core samples and frozen samples. One subsample was used for analysis of grain size and clay mineralogy, and the other subsample was used for the analysis of metal

partitioning and organic carbon content (see Figure 7: flow chart for sediment analysis).

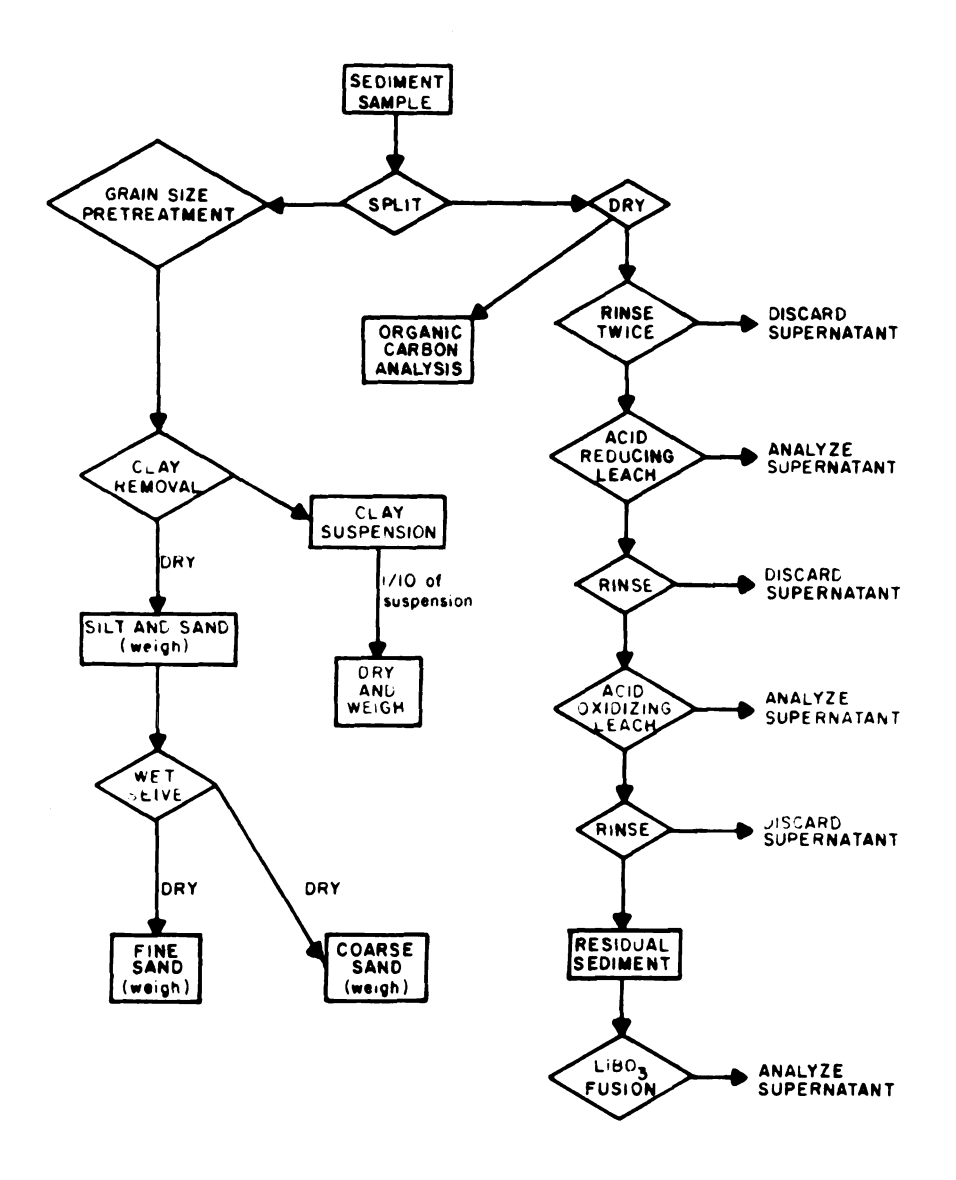
Two to twenty grams of sediment were subsampled for clay mineralogy and grain size analysis, depending on grain size and availability of sediment. A sonic vibrator and a rubber policeman were used to disaggregate and disperse clays. Sample preparation followed advice from Dr. M. Mortland (personnel communication, 1984).

Carbonates and soluble salts were removed by digestion in 1 N NaOAc (pH of 5 with acetic acid) for 2 hours. The mixture was centrifuged at 2000 rpm for 50 minutes, and the supernatant discarded. This step was repeated on samples with large amounts of carbonate.

Organic carbon was removed by digestion with 30% hydrogen peroxide. Twenty milliliters of 30%  $\rm H_2O_2$  were added to the sediment (in 5 ml increments to avoid frothing over). The solution was heated to  $60-80^{\rm O}{\rm C}$  in a water bath, and occasionally stirred for at least two hours. Up to 50 ml of additional  $\rm H_2O_2$  were added to organic rich samples. The solution was centrifuged at 2000 rpm for 50 minutes, and the supernatant discarded. The sediment was then washed a minimum of two times with distilled water.

The clays in many of the samples still flocculated after this treatment, so repeated  $H_2O_2$  washes were preformed. This still did not stop many samples from flocculating. It was

Figure 7. Flow chart for sediment analyses.



suggested by Dr. M. Mortland (personal communication, 1984) that the flocculating clays were calcium saturated smectites. Divailent cations on a smectite can not be removed by rinses with water or hydrogen peroxide, and can cause the collapse of the double layer, allowing the clay to flocculate. remove the calcium, the samples were washed two times with a 300 q/l NaCl solution to displace the calcium with sodium, and then rinsed with distilled water to remove the sodium from the exchange sites. Only the samples from 40 cm and 60 cm depth at site 22 continued to flocculate after this In these samples, a large amount of sand size treatment. gypsum crystals were identified by their large, cleavage faces. After seiving, minor amounts of gypsum were also identified in the sand size fraction of some other samples from sites 22 and 16.

Clay size particles (<2 microns) were separated from silt and sand size particles (>2 microns), by a method which uses the Stoke's settling velocity under centrufigal force (Jackson, 1979). In this method, the sediment is randomly distributed in 10 cm column of water and centrifuged at 750 rpm on an International no. 2 centrifuge for a temperature dependent time. The centrifuge times for temperatures from

20-30°C are:

degrees centigrade
20 21 22 23 24 25 26 27 28 29 30
3:18 3:13 3:08 3:04 2:58 2:54 2:50 2:47 2:43 2:40 2:36
minutes:seconds

This procedure causes particles with a Stoke's diameter greater than 2 microns to settle out. The supernatant, with the suspended clays, was placed in a 500 ml volumetric, and the procedure was repeated until the 500 ml volumetric was full. The last supernatant withdrawn varied from clear for sandy sediments, to slightly cloudy for clay rich sediments. This procedure is assumed to leave only a negligible amount of clay in the sand and silt residual.

Fifty milliliters of the 500 ml clay suspension were placed in a preweighed beaker, dried at 50°C, cooled in a desicator, and equilibrated with room humidity for 12 hours. The beaker and the clay were weighed, and the mass of the clay in the sample was calculated.

The residual silt and sand was rinsed with water into a preweighed beaker, dried, and cooled. The sediment and beaker were weighed to determine the mass of the silt and sand. Next, the silt and sand fraction was wet sieved through two micro sieves with fall diameters of 62.5 and 250 micrometer, which are taken as the silt to fine sand and fine sand to coarse sand cutoffs, respectively. The sediment caught in the sieves was rinsed into preweighed beakers,

dried, cooled, and weighed. Thus, the mass of the fine and coarse sand size fractions were measured directly. The mass of the silt fraction was taken as the masses of the fine sand plus the coarse sand minus the mass of the silt and sand size fraction. From the weight of each size range, the fraction of sediment in that size range was calculated, and is presented in Appendix B.

Clay mineralogy was determined by X-ray diffraction of Cu K-alpha radiation with a Ni filter on a sample after each of four treatments: 1) Mg-glycerol saturated, air dried, 2) potassium saturated air dried, 3) potassium saturated, heated to 350°C and 4) potassium saturated, heated to 550°C. The clay mineralogy is reported in Appendix A.

Twenty grams of sediment were subsampled for the metal and organic carbon analyses. The sediment was placed in an acid washed beaker and dried at 35-55°C. After cooling in a desiccator, the sediment was disaggregated with a mortar and pestal, and stored in a glass vial.

For metal analysis, 5.000 grams of the dried sediment were placed in an acid washed, 200 ml pyrex centrifuge tube. The sediment was washed twice with double distilled water to remove excess soluble salts, and sequentially leached to remove metals bound as (1) acid soluble and reducible species, and (2) oxidizable species.

The acid-reducible metals were leached from the sediment with a hydroxyalamine hydrochloride-acetic acid solution (Chester and Hughes, 1967). The 5.000 gram sample was combined with 50 ml of the leaching solution and shaken on a wrist action shaker for 4 hours. After centrifuging at 2000 rpm for 50 minutes, the supernatant was drawn off and analyzed for Cr, Mn, Fe, Co, Ni, and Cu by atomic absorption spectrophotometry. The metal content of the acid-reducible fraction of the sediment was calculated using 50 ml of leachate per 5 g sediment. The remaining sediment was washed once with double distilled water, centrifuged, and the supernatant discarded.

The amount of oxidizable metal in the sediment was determined by leaching the residual sediment from the acid reducing leach with acidified  $\rm H_2O_2$  (similar to Gupta and Chen, 1975). The sediment reacted with 15 ml of 0.02 N HNO\_3 and 15 ml of 30%  $\rm H_2O_2$  (pH=2 with HNO\_3) at 85°C +/-2°C. After 45 minutes, another 10 ml of acidified 30%  $\rm H_2O_2$  were added. After two hours total reaction time, another 15 ml of acidified 30%  $\rm H_2O_2$  were added. After 5 hours, 25 ml of 3.2 M ammonium acetate in 20% (v/v) nitric acid were added, and the sample was allowed to cool for 30 minutes. The ammonium acetate complexed the metal in solution, so metal oxides could not form. Over the 5 hours which the sample was heated, it was agitated by hand every 10 minutes; when the

sample was cooling, it was agitated constantly by hand. The cooled solution was centrifuged, and the supernatant was placed in an acid washed, 250 ml volumetric. The sediment was rinsed once with 0.02 N HNO3, and centrifuged. The supernatant was added to the volumetric, and this solution was diluted to 250 ml with 0.02 N HNO3. Metals in the 250 ml of leachate were analyzed for Cr, Mn, Fe, Co, Ni, and Cu by atomic absorption spectrophotometry, and the metal concentration in the sediment was calculated on 250 ml leach per 5 g sediment.

The residual sediment from the oxidizable leach was washed with double distilled water and the supernatant discarded. The washed sediment was place in an acid washed beaker and dried. The residual metal content of the sediment was determined by fusion. In a graphite crucible, 0.1000 g of sediment was mixed with 1.000 g of LiBO<sub>2</sub>, heated at 1,000°C for 15 to 20 minutes, then immediatly disolved in 50 ml of double distilled water and 5 ml of concentrated HCl. The solution was diluted to 100 ml with double distilled water, and analyized by atomic absorption spectrophotometry for the metals studied. Cr, Co, Ni, and Cu concentrations could not be determined due to contaminants in the LiBO<sub>2</sub>. Iron and manganese concentrations of the residual sediment were calculated on 100 ml solution per 0.1000 g of residual sediment, and are reported in Appendix B.

The organic carbon content of the sediment determined titration of K<sub>2</sub>Cr<sub>2</sub>O<sub>7</sub> with back by  $Fe(NH_4)_2(SO_4)_2$  (Gaudette and Flight, 1974). The organic matter in 0.2 to 0.5 grams of the dried subsample, weighed to 4 decimal places, was totally oxidized by 10 ml of 1 N  $\mathrm{K}_{2}\mathrm{Cr}_{2}\mathrm{O}_{7}$  which was heated by the exothermic hydration of 20 ml of concentrated  $\mathrm{H}_2\mathrm{SO}_4$  . After the addition of 15 to 20 drops of diphenyl amine indicator, and about 100 ml of double distilled water, the remaining  $K_2Cr_2O_7$  was titrated with 0.5 N  $Fe(NH_4)_2(SO_4)_2$  to a brilliant green end point. The percent organic carbon in the sediments is reported in Appendix B.

#### CHAPTER 4

#### DISCUSSION I: HYDROLOGY

# 4.1 INTRODUCTION

Madre Flats from the major element chemistry and piezometric potential of the groundwater across the sabkha. On the traverse from site 16 in the east to site 9 in the west, the groundwater was chemically equivalent to evaporated seawater and the hydrology was dominated by flood recharge. The groundwater at sites 17 and 18 was effected by the fresh water lense under Padre Island (also found by Amdurer, 1978). Groundwater in the Basin was chemically and hydrologically different from the groundwater in the flood recharge area.

The alkalinity, pH, temperature, and concentrations of Cl, Na, K, Br, Mn, and Fe in water samples analyzed in this study are presented in Appendix C. The calculated piezometric potentials for the trench, shallow, and deep wells are presented in Appendix E. Bromide concentration along the traverse from the Gulf of Mexico and site 18; west to site 13, the ICWW, and site 3; west to site 7, the canal and site 24; northwest to sites 10, 19, 20, 21, 22, and 23, (see Figure 4) are presented in Figure 8. Along the same

traverse, Na/Br, Cl/Br, and K/Br ratios are presented in Figure 9.

Figure 10 presents piezometric potentials along the same traverse as Figures 8 and 9. Piezometric potentials for trench, shallow and deep wells are presented with the piezometric potential of a hypothetical flood water on the surface of the sabkha with a density of water from the ICWW. If the piezometric potential of the hypothetical flood water is higher than the trench, shallow and deep wells, flooding water will have the potential to sink into the sabkha sediments and recharge the groundwater. If the piezometric potential of the hypothetical flood water is lower than the samples, flooding water will not have the potential to sink and recharge the groundwater.

Due to differences in the major element chemistry and piezometric potentials, the sabkha hydrology is divided into three areas: 1) the area dominated by flood recharge, 2) the area influenced by the fresh water lense under Padre Island, and 3) the basin and marginal slope.

#### 4.2 FLOOD RECHARGE AREA

At sites 16, 15, 14, 11, 12, and 13 on the sand bulge, and sites 4, 5, 6, and 7, the major element chemistry and piezometric potentials of the groundwater are similar to samples analyzed at these sites by Gudramovics (1981). Gudramovics (1981) showed that the groundwater at these sites

Figure 8. Bromide concentrations across the sabkha: August, 1982.

- Trench or surface sample Shallow well (1.9 m depth)
- Deep well (3.8 m depth)

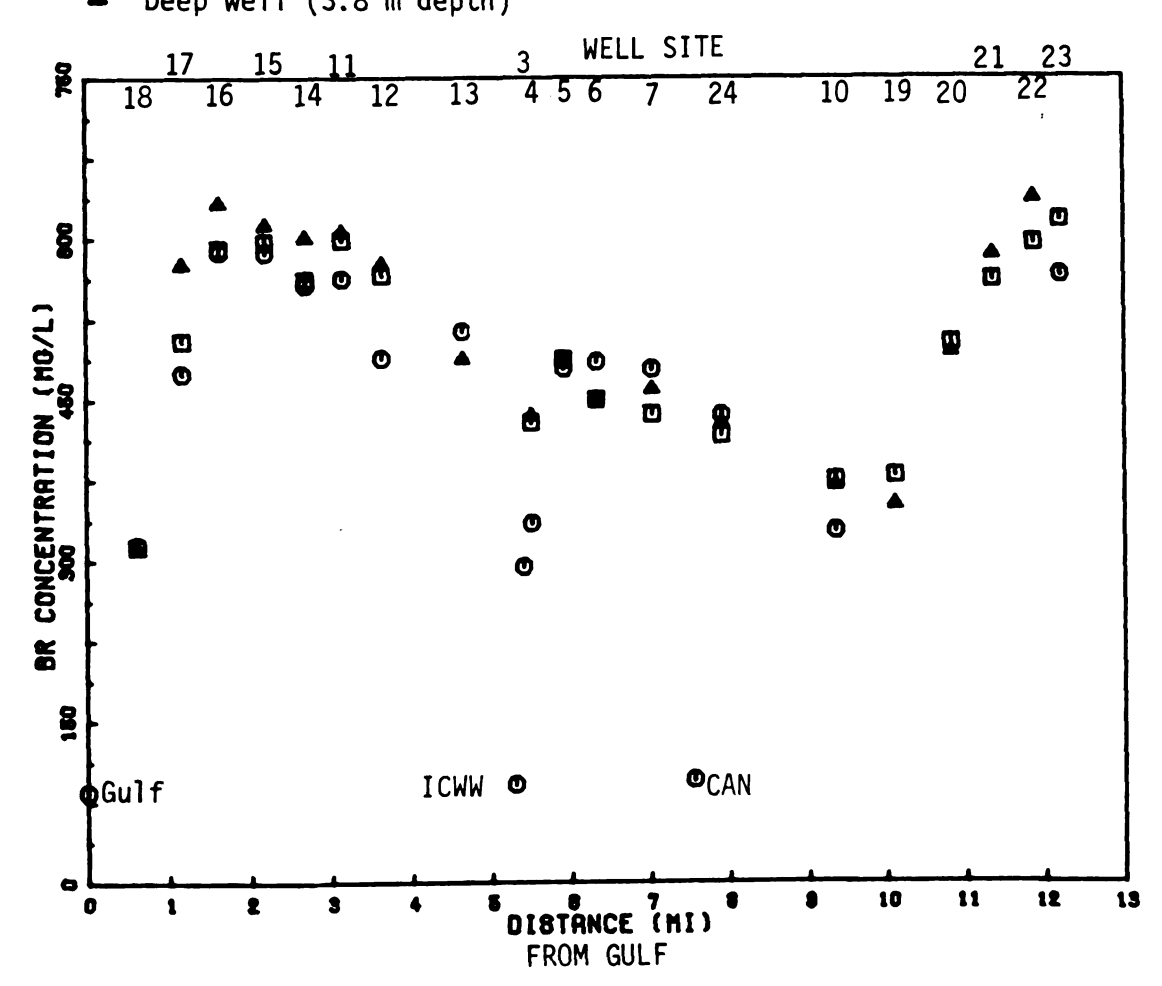


Figure 9. Groundwater Na/Br, Cl/Br, and K/Br ratios across the sabkha.

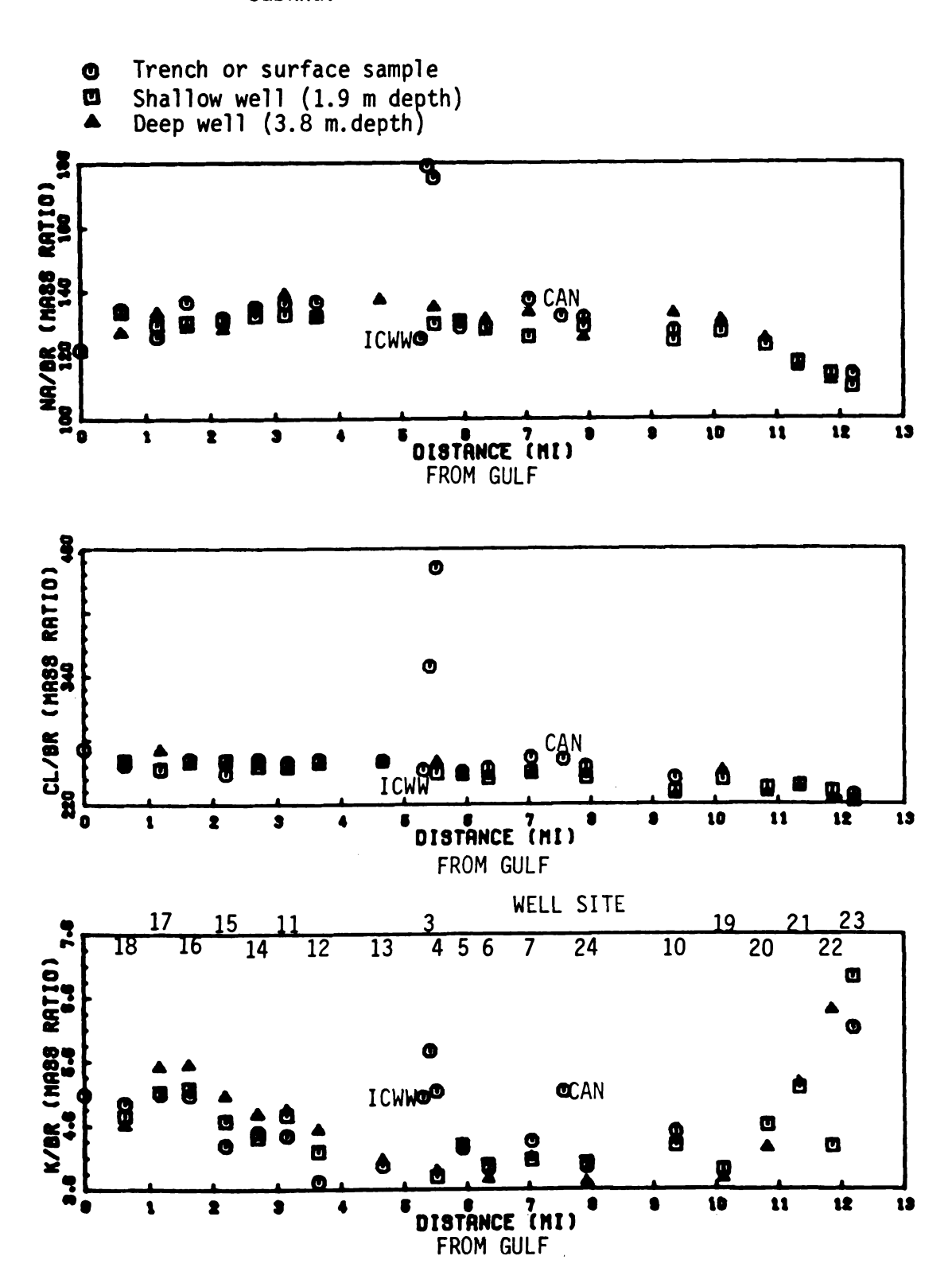
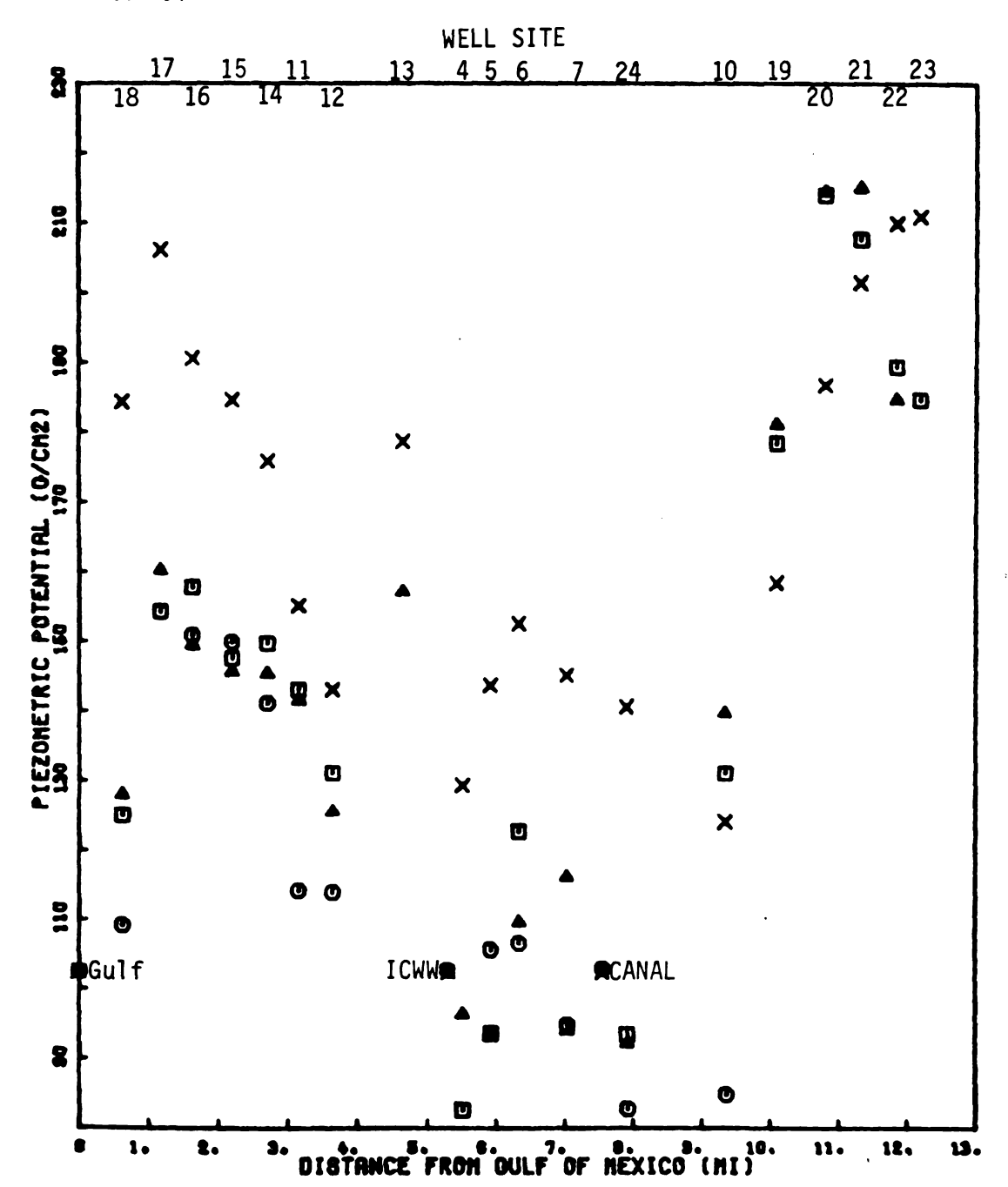


Figure 10. Piezometric potentials across the sabkha.

- Trench or surface sample
  Shallow well (1.9 m depth)
  Deep well (3.8 m depth)
- × Hypothetical flood water



is equivalent to evaporated seawater, and that the hydrology is explained best by the flood recharge model.

In groundwater derived by the evaporation of seawater, bromide concentrations represent the relative amount of evaporation. The bromide concentrations in samples taken from sites in the flood recharge area are similar from August of 1979 to August of 1982: compare Figure 8 with Figure 5. In sample 16D, bromide concentrations during August of 1982 reached 9.4 times the average bromide concentration in seawater (67.3 ppm; Garrels, et al., 1975). Similarly, in August of 1979 bromide concentrations reached 8.6 times the average bromide concentration in sea water, and in March of 1980 bromide concentrations reached 9.4 times the average concentration of bromide in sea water (Gudramovics, 1981). West of site 16, bromide concentrations, or the relative amount of evaporation, decreases (see Figure 8).

In groundwater samples from the flood recharge area, Cl/Br and Na/Br ratios show little variation from the Gulf of Mexico and the ICWW, which supports the evaporation of seawater as the source of groundwater. In all of the samples except 3T and 4T, Cl/Br mass ratios are between 240 and 270, and Na/Br mass ratios are between 125 and 140. This is close to the Cl/Br and Na/Br ratios in the ICWW of 253 and 125, respectively, and in the Gulf of Mexico of 270 and 121, respectively (see Figure 9).

The K/Br ratios at sites 16, 15, 14, 11, and 12 are close to the ratios in the Gulf of Mexico (5.0) and the ICWW (5.1); however, the K/Br ratios on the traverse from site 13 to site 24 are all below 4.5, except for samples 3T and 4T which will be discussed later (see Figure 8). Since the Cl/Br and Na/Br ratios support the conservative behavior of bromide during the evaporation of sea water, the decrease in the K/Br ratio is attributed to nonconservative behavior of K in the sabkha groundwater.

In other environments, a decrease in concentrations in pore fluids has been attrituted to the specific uptake of potassium by clays. Singer and Stoffers (1980) interpret changes in clay mineralogy with depth, from smectite to smectite and illite, as the early diagenetic uptake of potassium by the smectites in two lakes: 1) Lake Albert, Uganda/Zaire, Africa, a fresh water lake with a high K/Na ratio, and 2) Lake Manyara, Tanzania, Africa, a saline,  $Na^{+}-Cl^{-}-HCO_{3}^{-}$  lake. Jones, et al. (1969) attribute an increase in the Na/K ratio in lake bottom pore fluids to the preferential sorption of potassium on sediments in Lake Abert, Oregon, a restricted Na<sup>+</sup>- Cl<sup>-</sup>- HCO<sub>3</sub><sup>-</sup> lake; Jones and Weir (1983) report an inter-stratified illite-smectite in Lake Abert sediments, and interpret an increase in the potassium content of the lake bottom clays to the formation of an interstratified illite-smectite from a smectite.

Samples 3T and 4T have anomalous Na/Br, Cl/Br and K/Br ratios. The variations in these ratios are not caused by the intrusion of distinct waters from below, as samples 4S and 4D are not anomalous. They are not caused by the dissolution of halite, as the Na/Br and Cl/Br ratios do not vary together. They may be due to an input of aerosols from the ICWW: Amdurer (1978) attributed anomalous chemistries in Padre Island groundwater to aerosols from the Gulf of Mexico. However, there is no strong support for this, and the anomaly is left unexplained.

Similar to Gudramovics (1981), piezometric potentials decrease west of site 16, and parallel the decrease in bromide concentrations. In the flood recharge area. piezometric potentials of the groundwater are always below the piezometric potential of the hypothetical flood water (see Figure 10), thus, flood waters would have the potential to pentetrate the sediments and recharge the groundwater. Except for samples 4S, 4D, 5S, 5D, 7T, 7S, 24T, 24S, and 24D, piezometric potentials are higher than potentials in the Gulf, ICWW, or canal. The flood recharge model is consistant with this data (Gudromovics, 1981), with the concentrated brines occuring on topographic highs where flooding will occur the least. At sites 4, 5, 7, and 24, some reflux of groundwater from the man-made ICWW and canal may occur.

## 4.3 AREA INFLUENCED BY PADRE ISLAND

The groundwater at sites 17 and 18 is not as saline as the groundwater at site 16: This is reflected in lower bromide concentrations (see Figure 8). Gudramovics (1981) attributes the lower salinities at sites 17 and 18 to the effect of a fresh water lense under Padre Island. Amdurer (1978) reaches a similar conslusion for wells in the northern portion of the Sand Bulge.

## 4.4 THE BASIN AND MARGINAL SLOPE

The piezometric potentials and major element chemistry of groundwater in the Basin and Marginal Slope are different from the groundwater in the flood recharge area. At sites 10, 19, 20, and 21, piezometric potentials in the shallow and deep wells are above the piezometric potentials for the hypothetical surface flood water. Also, major element ratios change on the traverse through the Basin and up the Marginal Slope.

Brine concentrations increase from site 10 in the Basin, northwest to site 19, 20, 21, and 22 on the Marginal Slope. The increase in bromide concentration is shown in Figure 8, and the increase in Na, Cl, and K can be seen in Appendix C. In the deep well at site 22, bromide concentrations reach 9.5 times their concentration in average seawater (67.3 mg/l; Garrels, et al., 1975).

The Cl/Br and Na/Br ratios decrease from site 10 to 23 (see Figure 9). In the flood recharge area (sites 3 through 7, 11 through 18, 24, the Gulf of Mexico, the ICWW, and the Canal: discarding samples 3T and 4T, and sample 13T for Na/Br) forty-one Cl/Br ratios average 255.92 mg/l with a standard deviation of 6.29 mg/l and forty Na/Br ratios average 130.80 mg/l with a standard deviation of 4.53 mg/l. On the Marginal Slope, some ratios are more than 4 standard deviations below the mean of the Cl/Br and Na/Br ratios in the flood recharge area (below 230.8 mg/l and 112.7 mg/l, respectively).

The decrease in the Cl/Br and Na/Br ratios can be explained by halite precipitation. Though sites 10 through 21 are not highly concentrated, some flood waters may have evaporated past the point of halite saturation before they penetrated the sabkha surface, leaving halite crusts on the sabkha which could be blown away: the sediments at sites 10 and 19 are fine grained (see Appendix A) so infiltration should be slow, and halite crusts were found on the sabkha surface in this area during sampling. Alternatively, the decrease in both ratios can be explained by the mixing of seawater derived groundwater with a continental derived groundwater having lower Cl/Br and Na/Br ratios. To explain the lower ratios at sites 22 and 23, this would predict a greater influx of continental groundwater at sites 22 and 23

then at sites 19 and 20.

The piezometric potentials in the shallow and deep wells at sites 10, 19, 20, and 21 are higher than the piezometric potential of a hypothetical flood water on the surface of the sabkha with a density equivalent to water in the ICWW (see Figure 10). Although flood waters can penetrate into the surface of the sediment at these sites (water did not flow from trenches dug in this area and the piezometric potential of the trench at site 10 is below the hypotheitical surface flood water), they will not recharge the groundwater below 1.9 m. Therefore, flood recharge cannot be the dominant hydrologic process. Piezometric potentials in the shallow and deep wells are higher than in the canal and Gulf, so the influx of canal and Gulf derived groundwater is not feasible. One feasible explanation for the piezometric potentials for sites 10, 19, 20, and 21, is for this area to be in an area of discharge from a regional aquifer. Alternatively, the groundwater at these sites may be in overpressured sand layers confined by clays. Figures 18 and 20 in Appendix A show trenches dug at sites 10 and 19, respectively; at about each site, groundwater can be depth at preferentially draining from a sand layer in the clay sediment, so layers with drastically different permiabilities are present.

The piezometric potentials at sites 22 and 23 are below the piezometric potentials at sites 20 and 21, and below the hypothetical surface flood water. The drop in piezometric potentials could be due to an impermeable layer of sediment blocking the regional head from influencing the groundwater During emplacement of the deep well at site 23, the table. 3.8 m piece of PVC tubing hit a lithified layer and could not be driven all of the way into the sediment; during sampling, not enough water had entered the deep well to sample. impermeable layer may exist below sites 22 and 23. Alternatively, the drop in the piezometric potentials at sites 22 and 23 could be due to the increase in the sand content at these wells, eliminating the confining clay layers which may have been responsible for the high piezometric potentials in the Basin.

Both the major element chemistry and piezometric potentials of the groundwater in the Basin and Marginal Slope can be interpreted to be controlled partly by the influx of continental groundwater. However, major ion ratios predict a greater continental groundwater component at sites 22 and 23 than at sites 10, 19, and 20, while piezometric potentials predict a greater continental groundwater component at sites 10, 19, 20 and 21 than at sites 22 and 23; also, major ion ratios can also be explained by water rock interactions and halite precipitation.

## CHAPTER 5

## DISCUSSION II: TRANSITION METALS

## 5.1 METAL PARTITIONING

In a sediment, transition metals exist in many different states, for instance manganese can be in octahedral sites in the lattice of a clay mineral, coordinated with oxygens and hydroxides in an iron oxide, or substituted for calcium in calcite. On the basis of bond type and strength, metals in different states within a sediment can be grouped into metals in different fractions of a sediment.

One major division of metal in a sediment is between the hydromorphic fraction and the residual fraction. The metal partitioned into the hydromorphic fraction is the metal available for reaction in low temperature, sedimentary environments without altering resistant minerals. The metal partitioned into the residual fraction is the metal bound within resistant minerals, and, over short periods of time, is not available for reaction in sedimentary environments.

In the definitions given above, a resistant mineral is defined as a mineral which does not break down over short periods of time in surface, sedimentary conditions. Quartz, feldspar, and smectite are examples of resistant minerals:

though these minerals are not necessarily thermodynamically stable in a sedimentary environment, they do not weather over short periods of time. Calcite, geothite, and pyrite are not considered resistant minerals, as they may dissolve or precipitate following specific changes in carbonate equilibrium, pH, or pe (Eh).

Metals in the hydromorphic fraction of a sediment can be further divided into more specific fractions: i.e. metals on in exchange sites. metals bound carbonates. incorporated in Fe-Mn oxides, or metals bound with organics and sulfides. Reacting a sediment with sequential chemical leaches in the laboratory has been suggested to leach metals from these specific fractions (Chester and Hughes, 1967; Gupta and Chen, 1975; Tessier, et al., 1979). However, due to differences in sediment composition (such as the type of organics, clay minerals, and oxides in the sediments, and the crystallinity and amount of imperfections in minerals), there is variability and some overlap in the stability of the substrates controlling the different metal fractions. sequential chemical extractions give an estimate of the metals in a specific fraction. Even with this uncertainty, sequential chemical extractions give considerable insight into the distribution of metals in sediments which whole metal contents do not.

To constrain metal paritioning in sediments from the Laguna Madre Flats, sediment samples were washed with double distilled water to remove excess soluble salts, leached with an acidic, reducing solution, and then leached with an acidic, oxidizing solution. It is assumed that the rinse with double distilled water removed a negligible amount of transition metals, and that the acid reducing and acid oxidizing leaches removed all of the metals not bound in resistant minerals and did not remove any metals bound within resistant minerals. Thus, the acid reducing and the acid oxidizing leaches removed the metals in the hydromorphic fraction.

The removal of excess soluble salts by a double rinse with distilled water could remove transition metals (1) in the salts and (2) nonspecifically adsorbed onto cation exchange sites on clays. This is assumed to account for a negligible amount of metal. The clays were in solutions with ionic strengths greater than seawater, so any transition metals adsorbed onto clays must be specifically adsorbed, and would not be rinsed off with a Na-Cl solution. Gypsum dissolution is suggested to be minimal in the short time that the sediments were in contact with the rinsing solutions, as gypsum dissolution was incomplete with repeated rinses during grain size analysis.

The acid-reducing leach is designed to remove Fe-Mn oxides from sediments (Chester and Hughes, 1967). The exposure of the sabkha sediments to the decrease in pe (Eh) and pH during the acid-reducing leach is assumed to (1) dissolve all carbonates, (2) desorb metals specifically adsorbed on clays, (3) dissolve all metal oxides and hydroxides, (4) dissolve iron monosulfides, which form by the reaction of iron and sulfide prior to the formation of pyrite (Berner, 1970 and 1984), (5) partially dissolve gypsum, and (6) dissolve any manganese sulfides (Garrels and Christ, 1965). The metals removed by this leach are referred to as metals in the acid-reducible fraction of a sediment or as acid-reducible metal.

The acid oxidizing leach is designed to remove metals bound with organics and sulfides (Gupta and Chen, 1975). Leaching the sabkha sediments with an acidic, oxidizing solution after the acid reducing leach is assumed to (1) oxidize organic matter and release all of the metals bound to organic matter, (2) oxidize sulfide and release the remaining metals bound as sulfides, and (3) partially or totally dissolve any remaining gypsum. The metals removed by this leach are referred to as metals in the oxidizable fraction of a sediment or as oxidizable metal.

## 5.2 THE HYDROMORPHIC FRACTION

Metals which enter the sabkha sediments will be incorporated into the hydromorphic fraction of the sabkha sediments, unless silicate or other resistant minerals are being formed. Additionally, the metals which undergo reactions in the sabkha sediments will be from the hydromorphic fraction unless silicate or other resistant minerals are being weathered. Thus, to put constraints on the amount of metals available for reaction in the sabkha sediments, metals in the hydromorphic fraction should be analyzed.

The range of Cr, Mn, Fe, Co, Ni, and Cu concentrations in the hydromorphic fraction of the sediments from the Laguna Madre Flats are presented in Table 1. In the sabkha, there are three possible sources of metal to the hydromorphic fraction of the sediments: 1) continental groundwater, 2) flood waters, and 3) the sediments transported to the sabkha.

Changes in groundwater K/Br ratios at sites 22 and 23 and changes in Na/Br and Cl/Br ratios at sites 10 and 19 through 23 may be caused by the mixing of seawater derived groundwater and continental groundwater. However, the changes in these ratios may also be explained by water-rock interactions and halite precipitation. If continental groundwater does enter the sabkha at these sites, it may supply metals to the sediments as well as change the major

Table 1. Metal concentrations in sediments and waters.

SEDIMENT (ppm)		ر د	Ā	Fe	ට	Ë	3
This Study: Hydromorphic fraction	ţ	0.15	8. 67.	241. 3,563.	0.26	0.9 8.4	0.07
Amazon River Sediment: Hydromorphic		30.7	682.	29,700.	23.	.59	54.
Yukon River Sediment: Hydromorphic		30.3	750.	32,700.	19.	93.	40.
Continental Shelf Off the Amazon River: Hydromorphic fraction	ţ	0.34	20.7 836.	1,028. 13,580.	0.4 8.4	1.3	0.7
(relowski, 1963) Grand River, Michigan: Hydromorphic fraction (Gephart, 1982)	to	6.1 93.	87.8 850.	17,000. 99,000.	N.A.	5.5 81.	4.3 204.
Oxic Atlantic Sediments: Hydromorphic fraction (Addy, et al., 1976)		N.A.	265.	17,000.	16.8	23.1	4.2
WATER (ppm)							
Average Seawater		0.0002	0.0019	0.0034	0.00005	0.0066	0.002
Gulf of Mexico (this study)		N.A.	0.01	0.088	0.005	0.005	0.01
N.A. = not analized							

element chemistry of the groundwater.

The fraction of metal in the hydromorphic fraction of the sabkha sediments which is supplied by flood water can be estimated from the rate of metal accumulation in the hydromorphic fraction of the sabkha sediments  $(R_M)$  and the possible rate of metal supplied to the sabkha by flood waters  $(R_{FW})$ . The rate of metal accumulation in the hydromorphic fraction of the sabkha sediments can be estimated as:

$$R_{M} = R_{S} * p_{S} * M_{S}*10^{-6}$$

where  $R_{M}$  = rate of metal accumulation in hydromorphic fraction (mg/mm<sup>2</sup>yr)

R<sub>S</sub> = rate of sedimentation = 7 mm/yr (6.3 to 8.4 mm/yr; Fisk, 1959)

P<sub>S</sub> = estimate of density of unconsolidated clastic sediments

 $= 2.4 \text{ g/cm}^3 = 2.4 \text{ mg/mm}^3 \text{ (Garland, 1979)}$ 

and  $M_S*10^{-6}$  = measured hydromorphic metal concentration  $(ppm*10^{-6} = mg_{metal}/mg_{sediment})$ .

Assuming the complete removal of metals from floodwaters into the sediments, the amount of metal which can be supplied to the hydromorphic fraction of the sabkha sediments by floodwater can be estimated as:

$$R_{FW} = N * D * M_W * 10^{-6}$$
,

where  $R_{FW}$  = the rate of metal supplied to the hydromorphic fraction by floodwater  $(mg/mm^2yr)$ 

N = the rate of flooding on the sabkha
= 12 floods/yr (Fisk, 1959; Amdurer, 1979)

and  $M_W*10^{-6}$  = concentration of the metal in floodwater  $(ppm*10^{-6} = mg_{metal}/mg_{sediment})$ .

The fraction of the hydromorphic metal supplied to the sediments by floodwater (X) is  $R_{FW}/R_{M}$ , or:

$$X = (N * D * M_W)/(R_S * p_S * M_S).$$

Using the range of metal concentrations in the hydromorphic fraction of the sediments  $(M_S)$  and the estimate of metal concentrations in seawater  $(M_W)$  from Table 1, X was calculated for Cr, Mn, Fe, Co, Ni, and Cu, and is listed in Table 2. Iron was also calculated using the measured concentration of iron in the Gulf of Mexico for  $M_W$ . From

Table 2: An estimate of the fraction of metal in the hydromorphic fraction supplied by flood waters.

Cr 0.0027 to >0.14

Mn 0.0030 to 0.025

Fe 0.00010 to 0.0015

Fe\* 0.0037 to 0.054

Co 0.00070 to 0.021

Ni 0.084 to >0.79

Cu 0.12 to >3.1

<sup>\*</sup>  $M_{\widetilde{W}}$  = concentration measured in the Gulf of Mexico (see text for discussion).

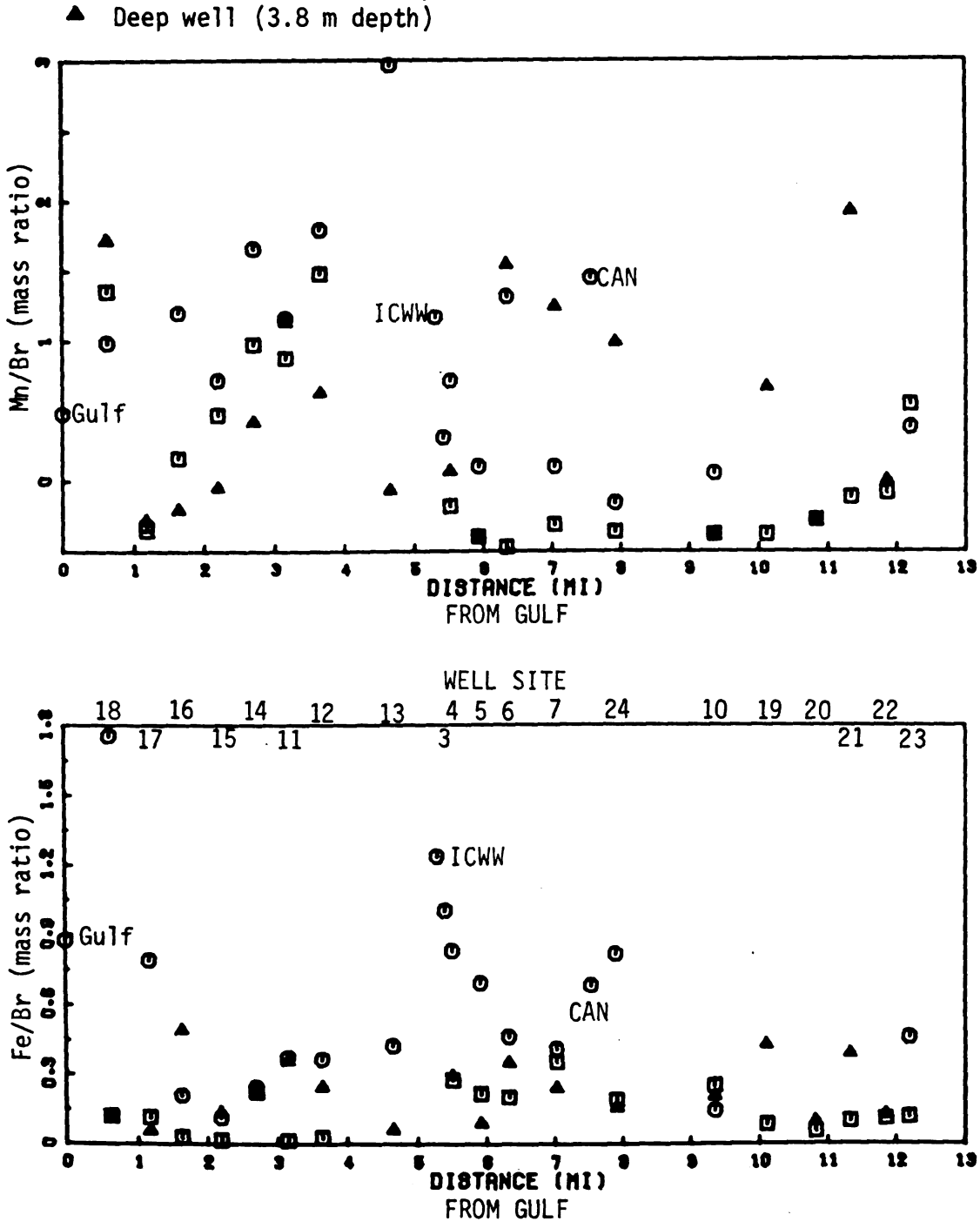
these estimates, in sediments with the lowest metal concentration less than 6% of the hydromorphic Mn, Fe, and Co can be accounted for by the loss of metals from flood waters. The addition of Cr to the hydromorphic fraction of the sediments by flood waters can be significant (>10%) only in sediments with a low hydromorphic Cr concentration. The addition of Ni and Cu to the hydromorphic fraction of the sediments by flood waters can be important in all of the samples.

This estimate of metal supplied to the sabkha by flood waters assumes the complete removal of metals from 12 floods per year with 150 mm (6 inches) average depth per flood, or 180 cm/year of floodwater. If evaporation concentrates the flood waters 6 to 9 fold, this is equivalent to 20 to 30 cm of brine per year. In the Sand Bulge, permeable sands may allow the floodwater to penetrate the surface; however, at sites 10, 19, and 20, impermeable clays may not allow this amount of water to penetrate the sediments and piezometric potentials do not support the infiltration of floodwater into the sediments. Thus, in the Basin this estimate of the amount of metals supplied to the hydromorphic fraction of the sediments may be high.

The assumption that all of the metals in the flood water are added to the hydromorphic fraction of the sediment is also incorrect. Figure 11 shows Mn/Br and Fe/Br ratios

Figure 11. Groundwater Mn/Br and Fe/Br ratios across the sabkha.

- Trench or surface sample Shallow well (1.9 m depth) 0



across the sabkha. Since bromide is conservative during the evaporitive concentration of the groundwater, changes in the metal/Br ratios show depletions or enrichments of the metal in the groundwater: If the metal/Br ratio of a sample is less than the ratio in the Gulf and ICWW, the metal is being removed from the groundwater; if the metal/Br ratio in the groundwater is greater than the ratio in the Gulf and ICWW, the metal is being added to the groundwater from the The Fe/Br ratios in the groundwater are generally sediment. lower than the ratios in the Gulf of Mexico and the ICWW, so iron is being added to the sediments by the groundwater. However, not all of the iron is being removed from the groundwater. The relationship of the Mn/Br ratios in the groundwater to the Mn/Br ratio in the Gulf of Mexico and the ICWW is variable. In some locations Mn is being added to the sediment by evaporation, and in some locations Mn is being removed from the sediments. Thus, the cycling of groundwater through the sabkha sediments may actually remove some Mn from the sabkha.

Metals in the sediments transported to the sabkha are a third source of metals to the hydromorphic fraction of the sabkha sediments. Ideally, to determine if these sediments can be the source for all of the hydromorphic metal in the sabkha, metal concentrations in the hydromorphic fraction of sabkha sediments should be compared to metal concentrations

in the hydromorphic fraction of sediments in the source area for the sabkha sediments, such as the continental shelf, Laguna Madre, and the Rio Grande River. However, this data is unavailable. Instead, the metal concentrations are compared to metal concentrations in the hydromorphic fraction of sediments similar to sediments in the source area.

Presented in Table 1, with the concentration of in the hydromorphic fraction of the sabkha sediments, are metal concentrations in the hydromorphic fraction suspended sediments from the Amazon and Yukon Rivers (Gibbs, 1977), sediments from the continental shelf by the Amazon delta (Pelowski, 1982), and sediments from the Grand River, Michigan (Gephart, 1982), and metal concentrations in the acid-reducible fraction of oxic marine sediments (Addy, et al., 1976). Metal concentrations are not higher in the hydromorphic fraction of the sabkha sediments than in the hydromorphic fraction of the other sediments presented in 1, and the range of Cr, Fe, Co, Ni, and Cu Table concentrations are actually lower than their concentrations in other environments. Thus, the metals in the hydromorphic fraction of the sabkha sediments may be supplied by metals in the hydromorphic fraction of sediments transported to the sabkha.

## 5.3 PARTITIONING WITHIN THE HYDROMORPHIC FRACTION

# 5.3.1 Partitioning in Sediments Transported to the Sabkha

Sediments are transported onto the sabkha by winds and wind tides, which allow open communication between the atmosphere and the sediments; thus, the sediments are in oxidizing conditions during transport and deposition. The partitioning of transition metals in the sediment transported to the sabkha can be estimated by the partitioning of metals in other oxidizing sedimentary environments.

Sequential leaches have been used to determine the metal partitioning in other oxidizing environments: suspended sediments in the Yukon and Amazon Rivers (Gibbs, 1977), ocean shelf sediments by the Amazon River (Pelowski, 1982), bottom sediments in the Grand River, Michigan (Gephart, 1982), lacustrine sediments in Little Traverse Bay, Michigan (Filipek and Owen, 1979), and oxic marine sediments in the NW Atlantic Ocean (Addy, et al., 1976). Data from these studies can be used to constrain the partitioning of hydromorphic metals between four fractions in the sediments: (1) the exchangeable fraction which contains metals on exchange sites, (2) the carbonate fraction which contains metals bound in carbonates, (3) the metal oxides fraction which contains metals bound in Fe-Mn oxides and hydroxides, and (4) the organic fraction which contains metals bound with organics and sulfides.

From the similarities in the partitioning of metals between these different oxidizing sediments, the general partitioning of Cr, Mn, Fe, Co, Ni, and Cu in oxidizing sediments is estimated. Normally, hydromorphic Cr is dominantly in the metal oxide and organic fractions, with minor amounts in the carbonate and exchangeable fractions. Hydromorphic Mn is dominantly in the metal oxide fraction, though the carbonate fraction can be significant; only minor amounts of Mn are in the organic and exchangeable fraction. Hydromorphic Fe, Co, and Ni are usually partitioned into the metal oxide fraction, with sizeable amounts in the organic fraction, and minor amounts in the exchangeable and carbonate fractions. Hydromorphic copper can be evenly partitioned between the four fractions or dominantly partitioned into the metal oxide and/or organic fractions.

Also, in the sediments transported to the sabkha, fine grain sediments should have more metal in the hydromorphic fraction than coarse sediments, as fine grain sediments have a higher surface area per unit mass than coarse grain sediments, and cation exchange reactions and the nucleation of metal oxides and carbonates are surface area dependent. This dependence of metal concentration in sediments has been observed by Filipek and Owen (1979).

The bacterial reduction of organic matter in the sabkha should cause changes in the pe (Eh), total sediments carbonate, and dissolved sulfide concentrations in the pore fluids, and change the stable form of metals in the hydromorphic fraction. In algal mats at Solar Lake, Sinai; Cai and Pekelmeer, Bonaire, the Netherlands Antilles; and Laguna Mormona, Baja California, Mexico, sulfate reducing bacteria accelerate the decay of the algal mat (Lyons, et al., 1984; Horodyski, et al., 1977; Jorgensen and Cohen, 1977). In cyanobacterial mats in Solar Lake, Sinai, Jorgenson and Cohen (1977) showed that the rate of sulfate reduction was highest in the top 1 cm of sediment, and declined untill 20 cm depth where the rate stabilized at 1/1000th of the surface rate.

The approximate stoichiometry of sulfate reduction by organic matter is

$$SO_4^{-} + 2CH_2O = H_2S + 2HCO_3^{-}$$
 (Stumm and Morgan, 1970).

This process reduces the pe (Eh) of the sediments, and increases the sulfide and total carbonate content in the associated pore fluids, which changes the stable form of transition metals in the sediments (Berner, 1964, 1970, 1984; Suess, 1979).

Much of the surface of the Laguna Madre Flats is normally covered with algal mats (Fisk, 1959; Field observations). Field observations support the decay of the organic matter in the sabkha sediments: Trenches dug in the Basin smelled of H<sub>2</sub>S, and the sediments changed in color from orangish at the surface to gray with depth. Thus, when sediment is deposited on the sabkha, chemical changes in the environment cause the forms of metal originally in the sediment to be metastable with respect to other forms of the metal: i.e. iron oxides may become metastable with respect to iron sulfides.

In the remaining discussion, the partitioning of metals in the hydromorphic fraction of the sabkha sediments are discussed. concentration of acid-reducible The and oxidizable metal, amount of fine grained sediment, organic carbon concentration in the sabkha sediment samples are plotted versus depth for sites 23, 22, 19, 10, 24, 6, and 16 in Figure 12. (The amount of fine grain sediment is the silt size fraction plus the clay size fraction.) Metals are discussed seperately, in terms of the range of measured metal concentrations, the general geochemistry of the specific metal, and the probable reactions and forms of the metal in the sabkha

Figure 12. Metal partitioning in the sediments at sites 23, 22, 19, 10, 24, 6, and 16.

KEY:

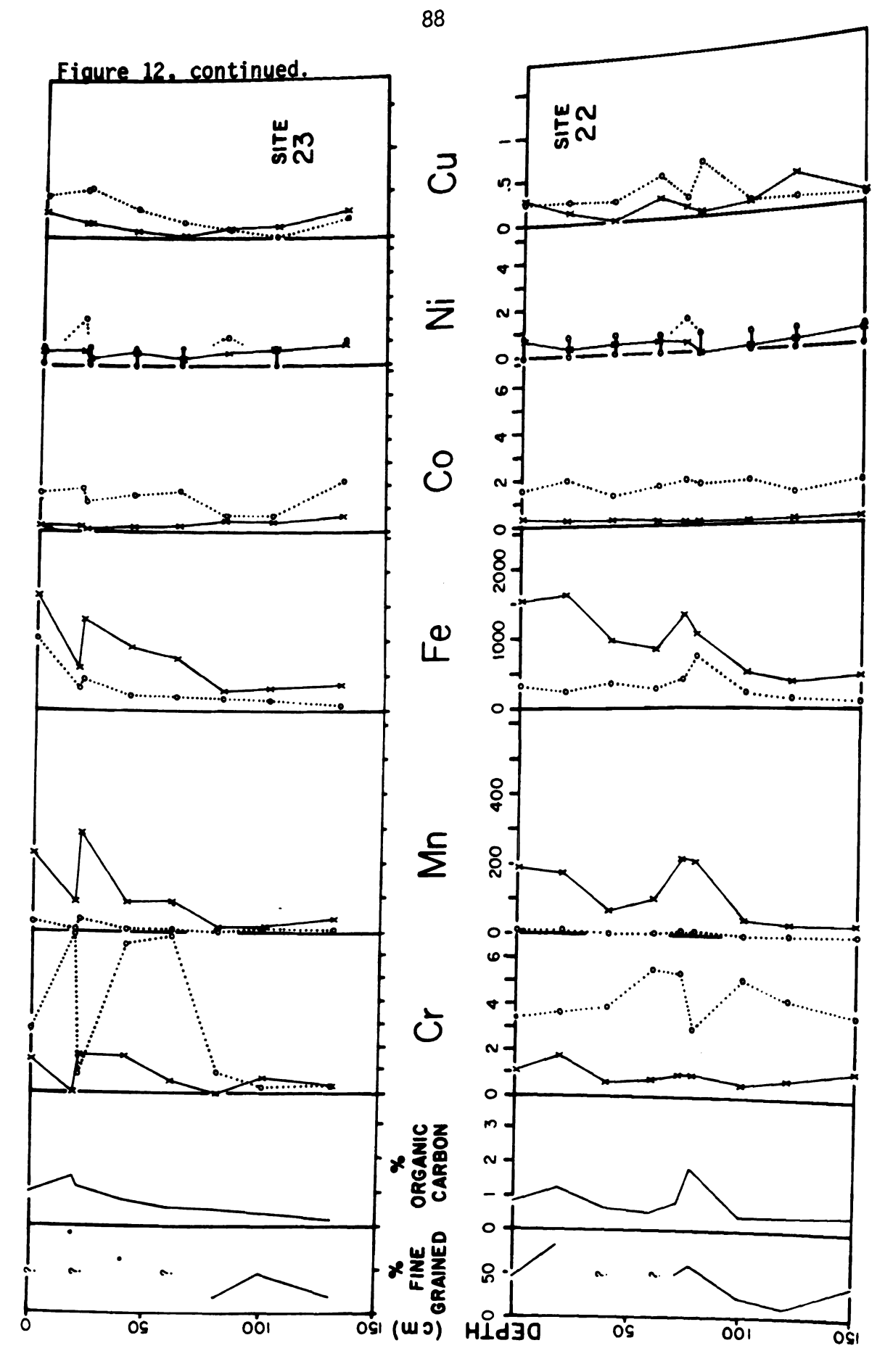
x----x Acid-reducible fraction

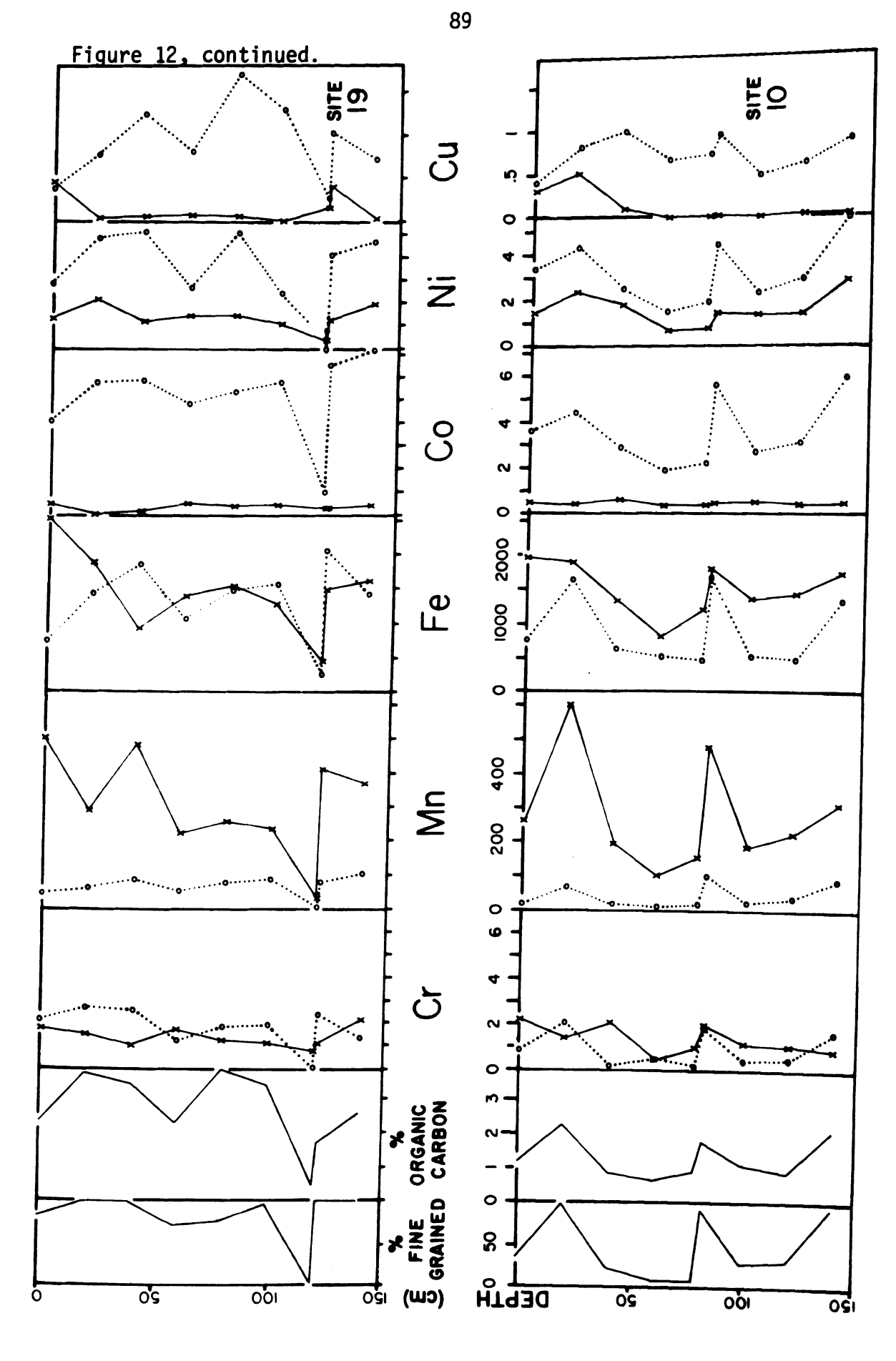
o:....o Oxidizable fraction

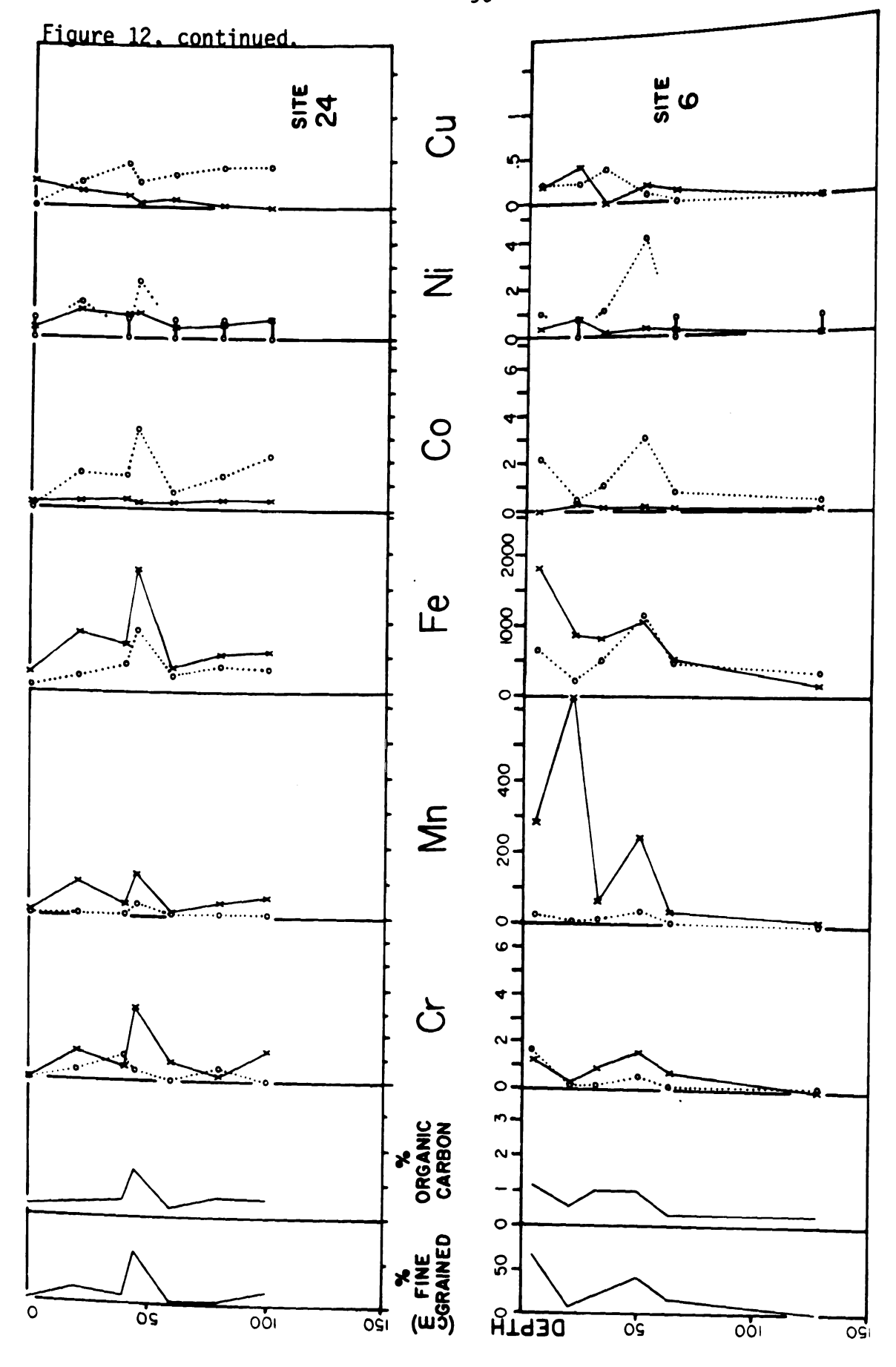
? Missing data point

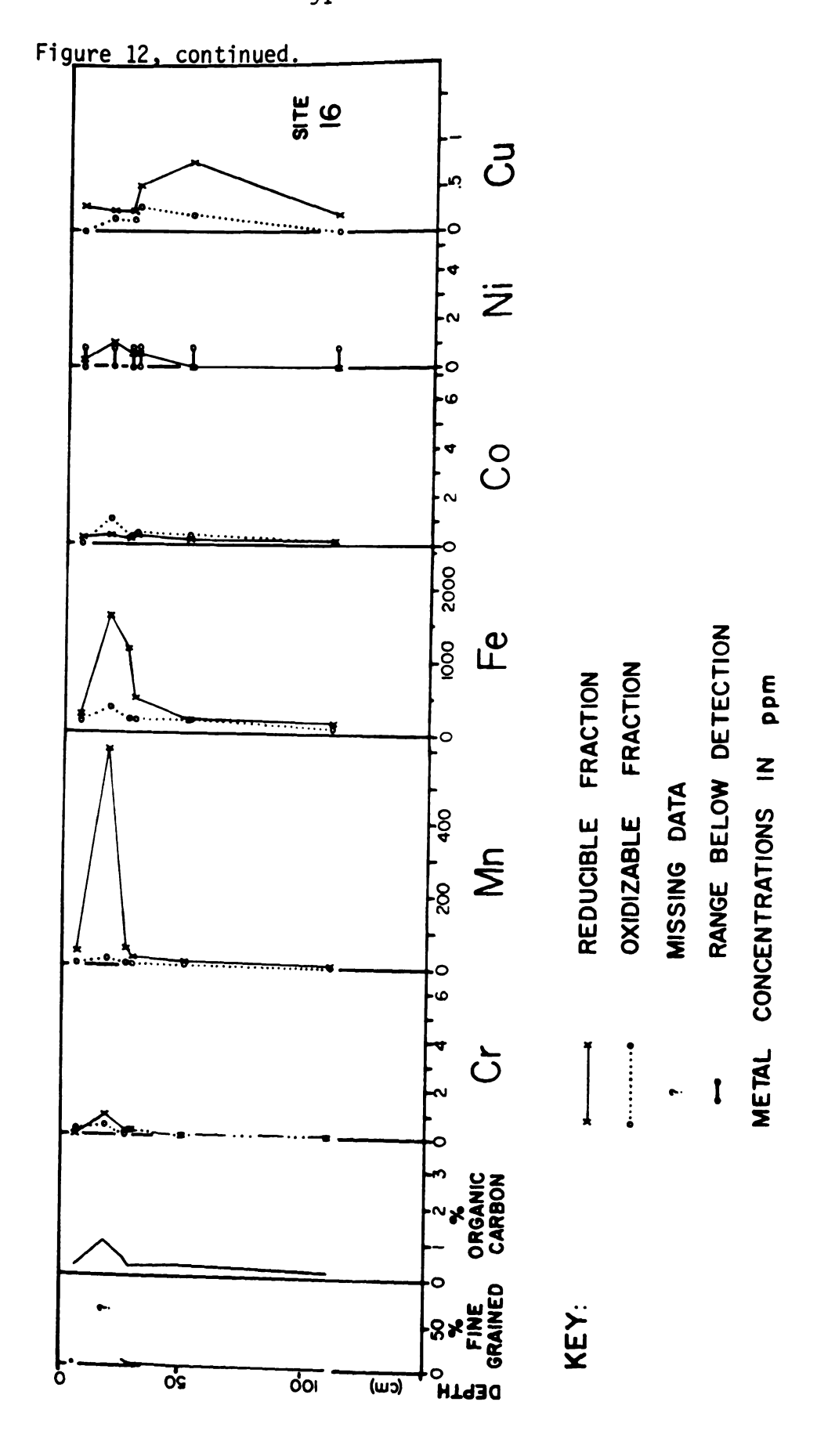
o-o Range below detection for oxidizable Ni

Metal concentrations are in ppm









## 5.3.2 Manganese

In the sediments analyzed from the Laguna Madre Flats, manganese concentrations range from 7 ppm to 638 ppm in the acid-reducible fraction, from 1.1 ppm to 102.5 ppm in the oxidizable fraction, and from 13.6 to 468 ppm in the residual sediment. Hydromorphic manganese is highly partitioned into the acid-reducible fraction: the ratio of manganese in the acid-reducible fraction to manganese in the oxidizable fraction varies from 1.5 to 77. In the water samples analyzed, dissolved Mn varied from <0.01 ppm in the Gulf of Mexico to 1.78 ppm in the trench at site 13.

From the previous discussion on metal partitioning in oxidizable sediments, manganese in the sediments transported to the sabkha is probably dominantly Mn(IV) in Fe-Mn oxides. With the decrease in pe (Eh) in the sabkha sediments from the bacterial decay of organic matter, Mn(IV) is unstable with respect to Mn(II), which does not form a stable oxide below a pH of 8 (Garrels and Christ, 1965; Stumm and Morgan, 1970). In many marine and freshwater sediments which change from oxidizing at the surface to reducing with depth, Mn(II) is mobilized from the reducing sediments into the pore fluids, and the mobilized manganese difuses towards the sediment surface due to a concentration gradient, where it is oxidized to Mn(IV) and precipitated as an oxide. Hydromorphic

manganese is enriched in the surface and depleted with depth in these sediments, and manganese concentrations in the pore waters increase with depth (Eaton, 1979; Trefry and Presley, 1982; Sawlan and Murray, 1983).

However, in the sabkha groundwater samples manganese concentrations do not increase with depth: manganese concentrations in the trenches are not lower than in shallow and deep wells. This apparent anomaly can explained. Trench samples may be taken from below the depth of complete Mn(IV) reduction, as trench samples were taken from pits over 50 cm deep, and water tables are all below 40 cm. Depths of complete manganese reduction are as shallow as 6 cm in some ocean bottom sediments (Bonatti, et Pedersen and Price, 1982) and fresh water sediments (Robbins and Callender, 1975), and the rate of sulfate reduction is highest in the top 20 cm of algal mats in the Solar Lake, Sinai (Jorgenson and Cohen, 1977), so the water table may always lie below the zone of Mn reduction.

In the surface sediment samples at sites 19, 22, and 23, and in the sample from 21 cm depth at site 6, there is an increase in the Mn concentration in the acid reducible fraction, relative to the other sediments at these sites, which does not correspond to an increase in grain size (see Figure 12); this may be attributed to Mn (IV) oxides in the surface sediments. However, Mn concentrations in the

acid-reducible fraction of the sediments generally do not show a decrease with depth which is not paralled by an increase in grain size (wich can effect the original amount of manganese in the hydromorphic fraction of the sediment).

In reducing sediments below the surface of the sabkha, manganese in the acid-reducible fraction is attributed to the incorporation of Mn(II) in the sediments, possibly adsorbed onto CaCO3, or in authogenic MnCO3 (rhodochrosite) or (Ca,Mn)CO3, or in authogenic Mn-sulfides. Manganese in the acid-reducible fraction is not attributed to exchangeable Mn(II), as the major cations in the groundwater, which is more saline then seawater, would displace Mn(II) from nonspecific exchange sites.

In the reducing sabkha sediments, when the Mn(IV) in Fe-Mn oxides is reduced to Mn(II) and released to solution, it may be adsorbed onto CaCO3 surfaces. McBride (1979) reports that Mn(II) in MnCl2 solutions adsorbs onto calcite in the laboratory. Martin and Knauer (1983) report that Mn(II) adsorbs onto CaCO3 in ocean water; Martin and Knauer (1983) add that this process might involve the oxidation of Mn(II) to Mn(IV) and the precipitation of Mn oxides on the CaCO3 surface, which could not occur in the reducing sabkha sediments.

When Mn(II) is released from oxides in the sabkha, it may form rhodochrosite. Increased total carbonate from the decay of organic material may cause rhodochrosite to be saturated in the sabkha groundwater, even at pH<7 (Garrels and Christ, 1965). However, in most reducing sediments, rhodochrosite is not found, instead, if a manganese carbonate is found it is usually a mixed (Mn,Ca) carbonate.

Table 3 lists the stoichiometry of Mn-Ca carbonates found in modern sediments. In cores examined from the Panama Basin, where sediments changed from oxidizing at the surface to reducing with depth, Pederson and Price (1982) found that manganese concentrations in the sediments are depleted within the top 10 to 20 cm. One core had anomalously high manganese concentrations in a bed of volcanic detritus at a depth of 160 cm, and an authogenic Mn-Ca carbonate was found in these sediments. In 3 cores of oceanic sediments, where sediments also change from oxidizing at the surface to reducing with depth, Boyle (1982) reports that the manganese concentrations increased in the pore water, and the Mn/Ca ratio increased in foraminifera at the same depth; surface area calculations show that there is insufficient surface area for the Mn increase in the foraminifera to be caused by adsorption of manganese, so Boyle (1982) suggests the precipitation of thin Mn-Ca carbonate overgrowths. A similar mixed Mn-Ca carbonate may form in the sabkha sediments as Mn(II) is released from

Table 3: Mixed manganese-calcium carbonates reported in the literature (from Pederson and Price, 1982).

Locality

Empirical Formula

Peru Trench MnCO<sub>3</sub> (Zen, 1959)

Baltic Sea (Mn<sub>60-70</sub>Ca<sub>30-32</sub>Mg<sub>0-8</sub>)CO<sub>3</sub>

Baltic Sea (Mn<sub>56.8</sub>Ca<sub>25.5</sub>Mg<sub>9.7</sub>Fe<sub>8.0</sub>)CO<sub>3</sub>

Guatemala Basin (Mn<sub>50-80</sub>Ca<sub>20-50</sub>)CO<sub>3</sub> (Lynn and Bonatti, 1965)

Gulf of Riga (Mn<sub>40</sub>Ca<sub>25</sub>Mg<sub>35</sub>)CO<sub>3</sub> (Shterenberg, et al., 1968)

Oslo Fjord (Mn<sub>50</sub>Ca<sub>50</sub>)CO<sub>3</sub>

Loch Fyne (Mn<sub>47</sub>.7<sup>Ca</sup>45.1<sup>Mg</sup>7.2)<sup>CO</sup>3 (Calvert and Price, 1970).

NW Pacific (Mn<sub>82</sub>Ca<sub>14</sub>Mg<sub>3.7</sub>Fe<sub>0.3</sub>)CO<sub>3</sub> (Logvivenko, et al., 1972)

Baltic Sea (Mn<sub>85</sub>Ca<sub>10</sub>Mg<sub>5</sub>)CO<sub>3</sub> (Suess, 1979)

Panama Basin  $(Mn_{48}Ca_{47}Mg_5)CO_3$  (Pederson and Price, 1982)

Fe-Mn oxides.

Some acid-reducible manganese may exist as acid soluble Mn-sulfide. Suess (1979) found MnS in reducing sediments in the baltic sea. However, for MnS to be stable at a pH of 6.5 to 7 requires unusually high Mn(II) or S<sup>=</sup> concentrations (Garrels and Christ, 1965). Thus, only a minor amount of the acid-reducible manganese, if any, is attributed to Mn-sulfides.

Appreciably all of the manganese in the oxidizable fraction of the sediments is attributed to manganese bound with organic matter. Manganese in the oxidizable fraction does not exist as Mn-sulfides, as Mn-sulfides are acid soluble and would disolve in the acid reducing leach. It is suggested that significant amounts of oxidizable Mn are not from the continued dissolution of gypsum, where Mn may substitute for Ca, as oxidizable Mn correlates strongly with oxidizable Fe, Co, and Ni,  $(r^2=0.86, r^2=0.89, and r^2=0.84, respectively; Appendix D) which will not substitute for calcium, and oxidizable Mn correlates well with organic carbon content <math>(r^2=0.72; Appendix D)$ .

## 5.3.3 Iron

Iron concentrations in the sediment range from 160 ppm to 2550 ppm in the acid-reducible fraction, from 73 ppm to 2060 ppm in the oxidizable fraciton, and from 1200 ppm to 31000 ppm in the residual sediment. The ratio of iron in the

acid-reducible fraction to iron in the oxidizable fraction varies from 0.5 to 6.4, and iron concentrations are higher in the acid reducible fraction then in the oxidizable fraction in all of the samples except 3 samples from site 19 and 2 samples from site 6. Iron concentrations in the sabkha groundwater range from <0.01 ppm to 0.55 ppm.

Similar to Mn, the change in the oxidation potential of the sediments, from oxidizing at the surface to reducing with depth, will cause a change in the stable valance state of Fe. In oxidizing sediments, Fe(III) is stable, and Fe(III) oxides and hydroxides are stable in most oxidizing waters. reducing conditions, Fe(II) is stable, and forms more soluble oxides. Above normal concentrations of dissolved  ${\rm CO}_2$  will cause siderite (FeCO<sub>2</sub>) to be stable, and the presence of small amounts of sulfide will cause pyrite to be more stable siderite (Garrels and Christ, 1965). In modern, than reducing sediments,  $Fe^{2+}$  and  $S^{2-}$  react to form black, fine grained iron monosulfides which are acid soluble. These are unstable with respect to pyrite (FeS2), and, with time, will lose iron or gain sulfur to form pyrite (Berner, 1964, 1970, and 1984).

Observed sediment color changes with depth are consistant with the change in iron from orange iron oxides at the surface to black, fine grained iron-monosulfides in the reducing sediments. Sediments from sites 6, 10, 19, and 24

have definite trends in color, from grayish orange sediments at the surface to gray sediments with depth, site 22 and site 23 have less pronounced trends, and at site 16 a trend in color is not apparent (see Appendix A).

However, the color of a sediment can be caused by a very minor amount of trace elements. The sediments at site 19 are composed predominantly of clays with a few sand lenses. At 120 cm depth, a dark gray sand lense is adjacent to light gray clay, (see figure 21 in Appendix A). The iron content of the hydromorphic fraction in the sand lense is 729 ppm, and in the adjacent light gray clay is 3500 ppm. Thus, the change in color does not imply high iron content.

Some changes in the partitioning of the hydromorphic iron can be explained by the maturation of iron monosulfides. In sediments from Solar Lake, Sinai, Jorgensen and Cohen (1977) report that the acid soluble sulfide decreases below 20 cm, and attribute this to the maturation of iron monosulfides. At sites 6, 10, 19, and 22 in the Laguna Madre Flats, the ratio of iron in the acid-reducible fraction to in the oxidizable fraction increases over the top 20 to 40 cm (see Figure 12). This is attributed to the formation maturation of iron sulfides. Thus, iron in the and oxidizable fraction is attributed to iron bound with organic matter in the surface sediments, and, with depth, to both iron bound with organic matter and iron sulfides.

The form of iron in the acid-reducible fraction is more difficult to constrain. In the oxidizing surface sediments, acid-reducible iron is expected to exist as iron oxides. the reducing sediments below the surface, iron oxides should be metastable with respect to siderite and iron sulfides (Garrels and Christ, 1965). As with manganese, significant amounts of acid-reducible iron should not be bound on exchange sites, as the high ionic strength groundwater would displace nonspecifically adsorbed iron with other cations. In the reducing sediments, some iron in the acid-reducible fraction may be from siderite. Though siderite is unstable with respect to pyrite in the presence of appreciable dissolved sulfide (Garrels and Christ, 1965), siderite may be saturated in the pore waters due to the increased total carbonate, and may precipitate. Also, iron-monosulfides are soluble, and may contribute significantly to the acid acid-reducible fraction, even below 40 cm where some iron sulfides appear to become acid insoluble.

# 5.3.4 Cobalt and Nickel

Cobalt concentrations range from <0.1 ppm to 0.70 ppm in the acid-reducible fraction and from <0.2 ppm to 7.3 ppm in the oxidizable fraction. Cobalt concentrations are higher in the oxidizable fraction than in the acid-reducible fraction in all of the samples except 2 samples from site 16 and 1

sample from site 24.

Nickel concentrations vary from <0.1 ppm to 2.8 ppm in the acid-reducible fraction, and from <0.8 to 5.6 ppm in the oxidizable fraction. In 28 of the 54 samples analyzed, nickel concentrations in the acid oxidizing leach were below the detection limit, equevalent to 0.8 ppm nickel in the oxidizable fraction of the sediment. When above the detection limit, the concentration of nickel is always greater in the oxidizable fraction than in the acid-reducible fraction.

In oxidizing sediments from other environments, cobalt and nickel are usually partitioned dominantly into Fe-Mn oxides, though appreciable quantities may be bound with organic matter or carbonates (Gephart, 1982; Gibbs, 1977; Hem, 1978). The dissolution of Fe-Mn oxides in reducing sediments releases cobalt and nickel to the system. In solutions with a high total dissolved carbonate, cobalt will form a stable carbonate at pH<7.5 and nickel will not. In the presence of dissolved sulfide, the metal sulfide will be the stable form for both metals (Garrels and Christ, 1965).

When appreciable amounts of cobalt and nickel are present in the sabkha sediments studied, the metals are dominantly in the oxidizable fraction. If the metals are bound with sulfides, there should be a decrease in the metal content in the oxidizing, surface sediments. Though there is

a decrease in the oxidizable cobalt and nickel in the surface samples at all sites except site 6 (where the surface sample is actually 5 cm below the sabkha surface), there is also a decrease in organic carbon content and/or amount of fine grained sediment (see Figure 12) which can account for the decrease in the metal content (less organics to bind with, or less metal supplied to the sabkha). Thus cobalt and nickel are bound dominantly as sulfides and/or organics.

# 5.3.5 Copper

Copper concentrations vary from <0.02 ppm to .76 ppm the acid-reducible fraction, and from <0.05 ppm to 1.8 ppm in the oxidizable fraction. The relative partitioning hydromorphic copper between the acid-reducible and oxidizable fractions varies (see Figure 12). At site 16 in the sand bulge, the hydromorphic copper is predominantly in the acid-reducible fraction; at site 6, the partitioning varies randomly with depth; at sites 10 and 19, in the surface samples hydromorphic copper is equally partitioned into the acid-reducible and oxidizable fractions, and below 20 cm hydromorphic copper is partitioned into the oxidizable fraction; at site 24, the copper in the surface sample is all in the acid-reducible fraction, and, with increasing depth, the oxidizable fraction becomes dominant; at site 22 and site 23, there is a similar decrease in the acid-reducible to oxidizable copper below the surface, with a second reversal below 100 and 80 cm, respectively, back to predominantly acid-reducible copper (see Figure 12).

In previously studied oxidizing sediments, the partitioning of hydromorphic copper is variable: though it is usually bound dominantly with oxides and/or organics, significant amounts can be bound on exchange sites or in carbonates (Gephart, 1982; Gibbs, 1977). In the sabkha sediments, the partitioning of hydromorphic copper is expected to be controlled by copper's affinity for organic matter and sulfides (Nissenbaum and Swaine, 1976; Garrels and Christ, 1965).

Due to the increased partitioning of hydromorphic copper into the oxidizable fraction over the first 40 cm at sites 10, 19, 22, and 24, much of the copper in the oxidizable fraction is attributed to copper sulfides. Some of the oxidizable copper is probably bound with organics, as oxidizing surface sediments contain copper in the oxidizable fraction. Acid-reducible copper may be copper bound in carbonates or acid soluble sulfides.

The increase in acid-reducible copper in the sandy sediments from 28.5 cm and 50 cm depth at site 16 does not correspond to an increase in any other metal concentration. This anomalous copper concentration may be caused by the insitu weathering or leaching of copper from the residual fraction. The groundwater at site 16 is a Na-Cl brine

equivalant to seawater concentrated 8 times by evaporation, and may cause some resistant silicate minerals to weather: Though Herber (1981) documented the replacement of feldspar by calcite in wind-tidal flat sediments south of Redfish Bay, Texas calcite is undersaturated in the groundwater at site 16 due to gypsum precipitation (Gudramovics, 1981). Alternatively, the increased copper concentration may be due to an input of copper from flood waters in these porous, sandy sediments.

## 5.3.6 Chromium

Chromium concentrations range from <0.1 ppm to 3.1 ppm in the acid-reducible fraction, and from <0.05 ppm to 6.9 ppm in the oxidizable fraction. The ratio of chromium in the acid-reducible fraction to chromium in the oxidizable fraction varies from 0.07 (dominantly oxidizable chromium) to 26 (dominantly acid-reducible chromium). The dominant fraction of chromium varies between samples at all sites except site 22, where chromium is dominantly in the oxidizable fraction.

Oxidizable chromium does show a trend with oxidizable manganese and percent organic carbon at sites 6, 10, 16, 19 and 24. In the 37 samples from sites 6, 10, 16, 19 and 24, oxidizable chromium correlates with oxidizable manganese  $(r^2=.77)$ , iron  $(r^2=.88)$ , cobalt  $(r^2=.73)$  and nickel  $(r^2=.66)$ , and with percent organic carbon  $(r^2=.70)$ . At sites 6, 10,

16, 19, and 24 the oxidizable chromium is attributed to the bonding of chromium with organic matter.

The anomalously high Cr concentrations in the oxidizable fractions of sites 22 and 23 are attributed to either the insitu weathering of residual minerals, or the input of Cr from continental groundwater. The groundwater at site 22 and 23 is an Na-Cl brine, with chloride concentrations over 6 times the concentration in seawater. These brines may weather or leach Cr from the residual fraction of the sediment (similar to copper at site 16). Alternatively, continental groundwater may flow into the sabkha from the landward side (as discussed in the hydrology section) and transport Cr into the back of the sabkha.

#### CHAPTER 6

## CONCLUSIONS

The goal of this research was to place constraints on the sources, pathways, and sinks of Cr, Mn, Fe, Co, Ni, and Cu in the near surface (<2 m deep) sediments of the Laguna Madre Flats, Texas. To accomplish this goal, five questions were addressed:

- 1. What controls the hydrology of the sabkha?
- 2. How much Cr, Mn, Fe, Co, Ni, and Cu are in the sabkha sediments?
- 3. What are the sources of these metals to the sabkha sediments?
- 4. What are the forms of these metals in the sabkha sediments?
- 5. What reactions do these metals undergo in the sabkha?

Similar to the results of Gudramovics (1981), the hydrology of the sabkha is dominated by flood recharge. In the Basin and Marginal Slope, piezometric potentials and groundwater major element chemistries are inconsistant with the flood recharge model. In this area, the hydrology of the sabkha may be controlled by confining clay layers or the

input of continental groundwater.

Abundances of the transition metals in the hydromorphic fraction of the sabkha sediments decreased in the order of Fe>Mn>Ni=Co=Cr>Cu. Metals in the sabkha sediments were not enriched relative to other recent sediments.

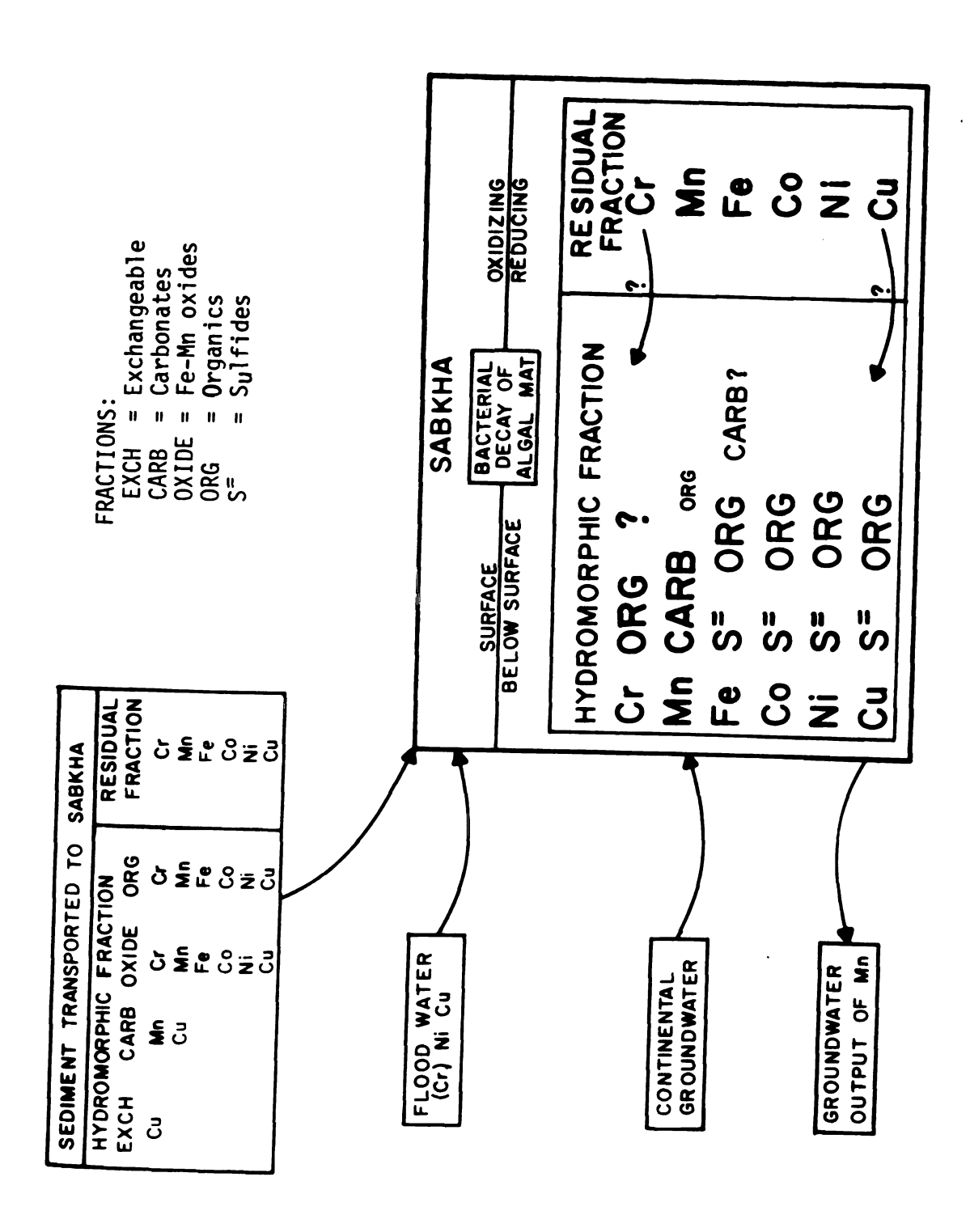
of Figure 13 shows four sources metal to the hydromorphic fraction of the sakbha sediments. The major source of metals to the hydromorphic fraction of the sabkha sediments is the metal in the hydromorphic fraciton of the the sediments transported to sabkha. Continental groundwater, marine derived flood water, and the weathering of metals from the residual fraction are three other possible sources of metal.

The major forms of metals in the sakbha sediments are also shown in Figure 13. Fe, Co, Ni, and Cu are dominantly bound with sulfides and/or organics. Mn is dominantly bound as a carbonate. The partitioning of Cr is difficult to interpret.

The major control on the partitioning of metals in the sabkha sediments appears to be the bacterial decay of algal mats. The major control on the amount of metals in the sediments is the grain size of the sediment.

Figure 13 also shows one output of metal from the sabkha. In areas where the hydrology is dominated by flood recharge, the constant cycle of groundwater through the

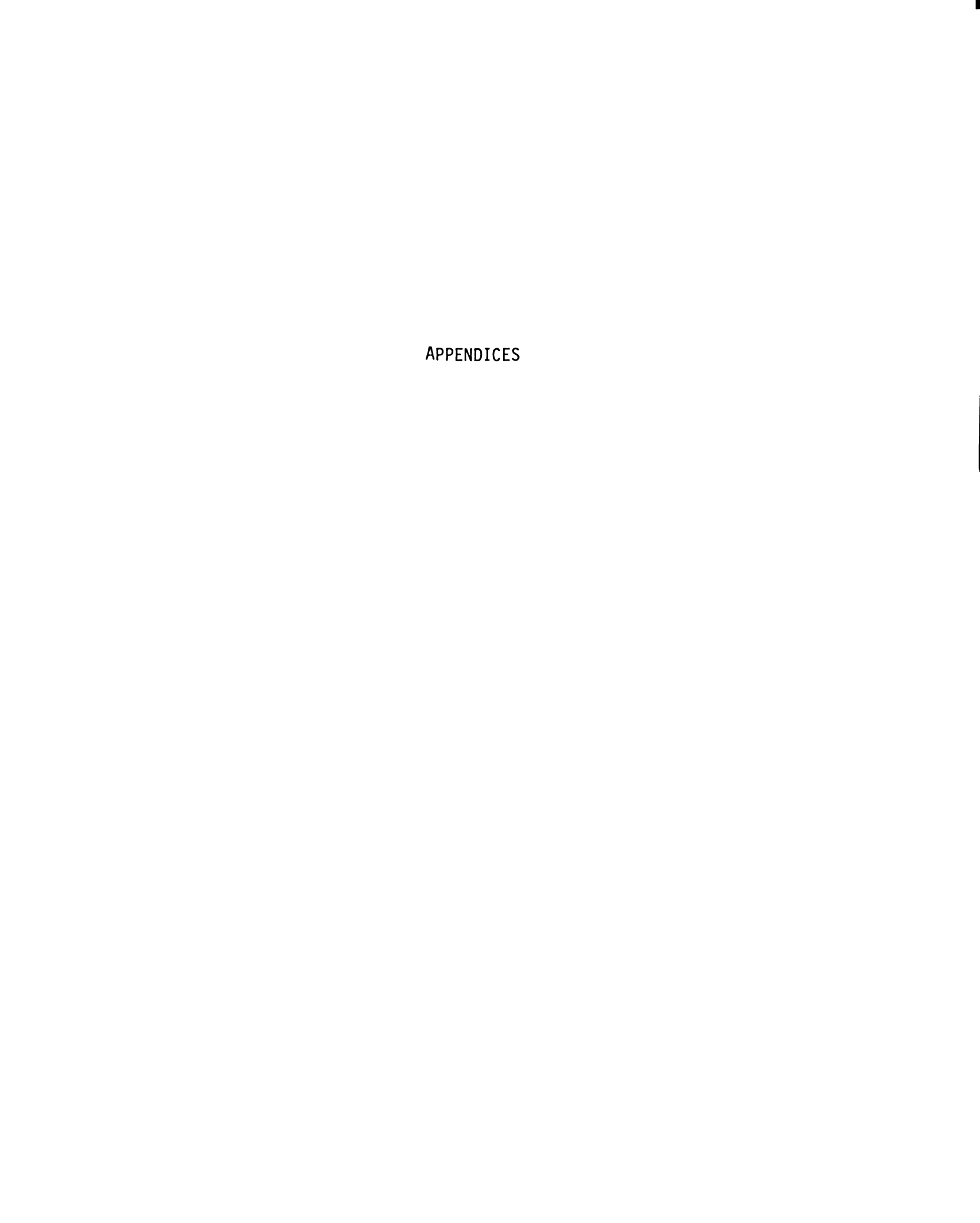
Figure 13. Model of the sources, pathways, and sinks of metals in the sabkha sediments.



1		

sabkha maybe a pathway for some metals out of the sabkha. In many groundwater samples, Mn is enriched relative to equivalently evaporated water from the Gulf of Mexico or the ICWW. When these Mn enriched brines flow out of the sabkha, they will remove Mn from the sabkha. This will not remove Fe, Co, Ni, or Cu from the sabkha, as these metals are not soluble in the presence of sulfide.

The conclusions summarized above form a framework for the interpretation of trace metals in near surface sabkha sediments. Noticeably missing from this framework is a detailed discussion on the effects of continental groundwater on the distribution of trace metals in the sabkha, as the inflow of continental groundwater into the back of the sabkha could not be conclusively shown in this study. Therefore, this study can not be a test of the Renfro (1974) model for the emplacement of stratiform ores, but a framework for the behavior of metals in the marine dominated portion of a sabkha.



#### APPENDIX A

# Description of the sediments

### SITE 16

Sediments from site 16 were sampled in a 5 cm diameter PVC core, in March of 1980. The core from site 16 is shown in Figure 14, just after opening and just prior to sampling. The color reproduction of the wet sediments is not true. The top 17 cm of the core is a dark yellowish brown (10 YR 4/2) fine sand. At 18 cm depth there is a clay rich light gray layer (sampled). From 19 cm to 31 cm the sediment is fine, dark yellowish brown sand with thin dark gray layers. From 32 cm to the bottom of the core at 122 cm, the sediment is a moderate yellowish brown (10 YR 5/2) fine sand with clear gypsum rossettes up to 1 cm in diameter, similar to those described by Masson (1955) and Herber (198).

The clay layer at 18 cm had 0.9 percent organic carbon. The fine sands varied from 0.1 to 0.5 percent organic carbon, and from 1 to 7 percent silt and clay.

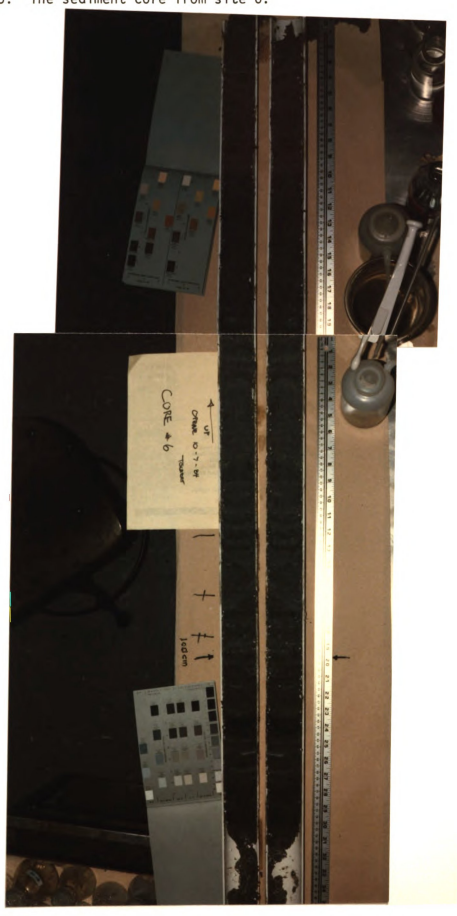
Figure 14. The sediment core from site 16.



Sediments from site 6 were sampled in a 5 cm diameter PVC core, in March of 1980. The core from site 6 is shown in Figure 15, just after opening, and just prior to sampling. The top 26 cm of the core are a pale yellowish brown (10 YR 6/2) to a grayish orange (10 YR 7/4), and consist of fine sands from 1 cm to 4 cm, clay from 4 cm to 9 cm and fine sand from 9 cm to 26 cm. Below 26 cm the color changes to a light to a medium gray (N5 to N7). The sediments are predominantly sands from 26 cm to 49 cm, and sands with minor clay layers from 49 cm to the bottom of the core at 130 cm.

Sediment samples range from 68 to 2 percent silt plus clay, and from 1.1 to .3 percent organic carbon, with finer grained samples having a higher percent organic carbon.

Figure 15. The sediment core from site 6.



4 3

Sediments from site 24 were sampled from a trench in August of 1982. The trench is shown in Figure 16, where the marks on the stick are 20 cm apart, and mark 5 would be on the surface of the sabkha. The sediments are moderate orange brown sands at the top, changing at 25 to 35 cm to medium gray sands. The sands are predominantly fine grained and well sorted, with the silt plus clay fraction varying from 16% to 2%, and the percent organic carbon varying from 0.5% to 0.2%.

The sample from 45 cm is of a poorly sorted clay layer in the sand, with 59% silt plus clay, and 1.3 percent organic carbon. Small evaporitic layers are present, up to 3 mm thick. Figure 17 shows the sediment from 1 m deep, note the old algal mat in the middle of the picture (8 lines in the notebook = 5 cm). The sample analised from 1 m deep is of the sand in the bottom half of Figure 17.

Figure 16. The trench at site 24.



Figure 17. Sediment from 100 cm depth at site 24.



Sediments from site 10 were sampled from a trench in August of 1982. The trench is shown in Figure 18, where the marks on the stick are 20 cm apart, and mark 7 would be at the surface of the sabkha. At around 30 cm, the sediments change from a pale orange to a medium to dark gray. The sediments consist of interbedded sands and clays. Percent silt plus clay ranged from 8% to 96%; and percent organic carbon ranged from 0.6% in the sample with 8% silt plus clay to 2.3% in the sample with 96% silt plus clay. Fine, white, evaporitic layers are present, and are usually discontinuous, and less then 2 mm thick.

Samples taken at 78 cm and 82 cm are adjacent sand and clay layers respectively. The sample from 140 cm contained a fish fossil on a bedding plane; a top view of the fish fossil, and a side view of the bedding in this sample are shown in Figure 19.

In the bottom of the trench shown in Figure 18, moderately rapid drainage can be seen from a sand layer at a depth of 95 cm, with relatively no drainage from adjacent clay layers.

Figure 18. The trench at site 10.



Figure 19. Plain and side view of the sediment from 140 cm depth at site 10.



Sediments from site 19 were sampled from a trench in August of 1982. The trench is shown in Figure 20, where the marks on the stick are 20 cm apart, and mark 7 would be at the surface of the sabkha. The sediments were predominantly gray clays, varying from a massive medium clay with 1.7% organic carbon (shown in Figure 21) to an algal laminated, greenish gray clay with 3.8% organic carbon (shown in Figure 22). Percent silt plus clay in the clay samples varied from 70% to 99%. These sediments are similar to those at SITE 10 with a smaller proportion of sand layers.

Figure 21 shows the clay and sand sampled from  $121\ cm$  and  $120\ cm$  respectively. The sand has 0.5 percent organic carbon, and 3% silt plus clay.

In the bottom of Figure 20, moderately rapid drainage from a sand layer can be seen at a depth of 100 cm, with relatively no drainage from adjacent clay layers.

The sediments in a trench dug down to 140 cm at site 20 was similar, being dominantly gray clay with a few sand layers. At site 20, clear gypsum rossettes up to 10 cm in diameter were found below about 1 m deep

Figure 20. The trench at site 19.

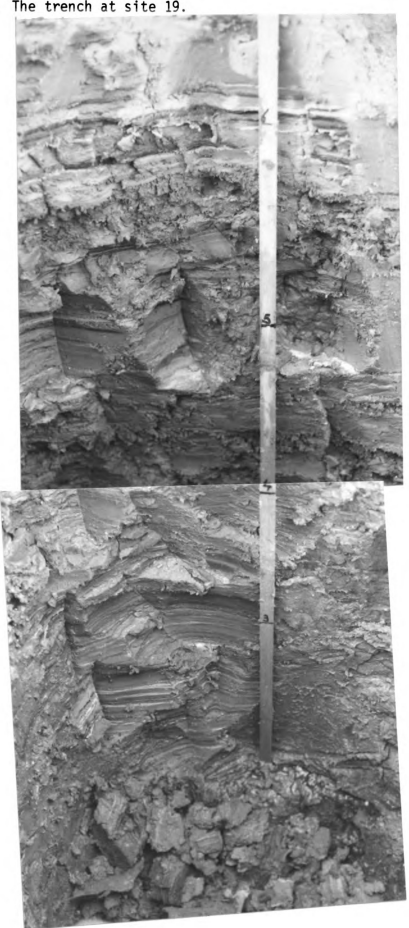
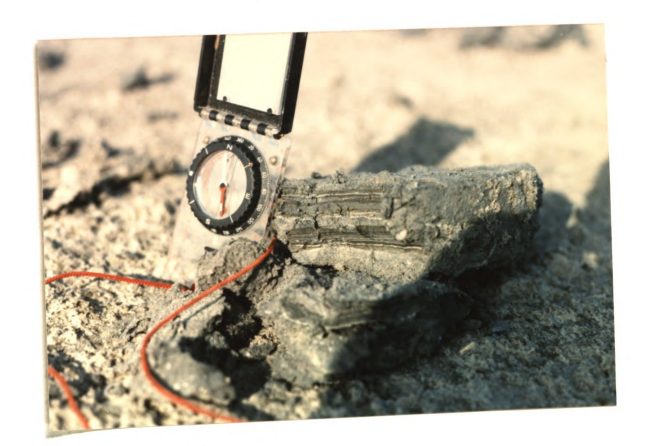


Figure 21. Adjacent clay and sand from 120 cm depth at site 19.



Figure 22. Algal mat from 80 cm depth at site 19.





Sediments from site 22 were sampled from a trench in August of 1982. The trench is shown in Figure 23, where the marks on the stick are 20 cm apart, and mark 7 would be at the surface of the sabkha. The sediments are interlayered clays, fine sands and fine grained evaporites. Layers vary from a few millimeters to a few centimeters. Amount clay plus silt size varied from 12% to 82% where analized. Samples from 60 cm and 40 cm contained a considerable amount of gypsum which would not totally disolve with repeated rinses during the grain size pretreatment, and sand size gypsum crystals were identified in other samples. Percent organic carbon varied from 0.4% to 1.8%.

Figure 24 shows a moderate reddish brown spot at 72 cm and a dark reddish brown spot at 78 cm. Both were sampled. The moderate reddish brown spot at 72 cm was small, and is unidentified. The sample containing this spot has 0.8% organic carbon. The dark reddish brown spot at 78 cm was more extensive and appered to be a twig from a tree. The sediment sample containing this sample has 1.8% organic carbon, the highest at this site.

The sediments in a trench dug down to a depth of 140 cm at site 21 appeared similar to these. Clear gypsum rossettes, 1 cm to 4 cm in diameter, were found at site 21 around 1 m deep.

Figure 23. The trench at site 22.



Figure 24. Colored spots from 72 and 78 cm depth at site 22.



Sediments from site 23 were sampled from a trench in August of 1982. The trench is shown in Figure 25, where the marks on the stick are 20 cm apart, and mark 7 would be at the surface of the sabkha. Above 60 cm the sediments are interlayered clays, fine sands and fine grained evaporites, varying from a few milimeters to a few centimeters thick. Percent organic carbon varied from 0.8% to 1.4%. These top sediments are very similar to the sediments at site 22. From 60 cm to 130 cm deep the sediment is a homogenous, fine, well sorted, olive gray sand. Percent organic carbon decreases with depth from 0.5% at 60 cm to 0.2% at 130 cm.

Samples taken at 18 cm and 20 cm are of the interbedded gypsiferous silt and clay above mark 6 in Figure 25, and the pure clay seen at mark 6 in Figure 25, respectively.

Figure 25. The trench at site 23.



# APPENDIX B

			SI	EDIMEN'	r Data	
column	ns rep	resent	samples			
6	6		6	6	6	SITE number
5	21	32	50	63		DEPTh (cm)
.449	.044	.055	.234	.041		CLAY size fraction
.227	.045	.047	.182	.042		SILT size fraction
.296	.853	.833	.523	.809		Fine Size fraction
.029	.058	.065	.061	.109		Coarse Size fract.
1.142	.529	.991	.985	.337		% ORganic carbon
1.2	.323	.9	1.6	.7	<.1	
284.	638			37.2		MN Reducible fract
1800.				540.		FE Reducible fract
	880				.13	CO Reducible fract
<.1	.28	.12				NI Reducible fract
.36	.78	.13			· 02	CU Reducible fract
.18			.18	.12		
		.20				CR Oxidizable fra. MN Oxidizable fra.
26.3	8.3	14.5	39.0	5.3	270	
	218	. 512.	1166.	500.		FE Oxidizable fra.
2.2			3.1		.5	CO Oxidizable fra.
1.0	<.8	1.1	4.1	< . 8	<.8	NI Oxidizable fra.
.21	.22	.38	.09	<.05	<.05	CU Oxidizable fra.
	27.5	38.4	88.3	32.2		MN Crystalline#
18050.	. 3170	4590.	15900.	5690.	1340.	FE Crystalline#
					00	22 22 CIME
23	23	23	23		23	23 23 SITE
0	18.		40		80	
-	.576	-	.320			.155 .089 CLAY
-	.359	-	.287			.088 .095 SILT
-	.055	-	.388			.734 .788 F S
-	.009	-	.004			.022 .028 C S
.981	1.426	1.154	-	_		.358 .192 OR
1.4	<.1			• -	<.1	.7 .3 CR R*
224.	83.					13.6 38. MN R*
1680.	618.	1320.		780.		312. 385. FE R*
.28	.21	.12	.22			.43 .70 CO R*
.57	.61	.28	.54	. 28		.64 .82 NI R*
.30	.17	.17				.13 .30 CU R*
2.73	6.87	.79	6.48 6.		-	.27 .29 CR O*
22.3	6.3	30.0		7.7		9.3 7.5 MN O*
1055.	315.	465.				151. 96. FE O*
1.7	1.9	1.4		1.8	-	.75 1.2 CO O*
<.8	2.0	<.8		<.8		<.8 1.1 NI O*
.51	.55	.57			.07 <	.05 .22 CU O*
60.9	24.8	93.6			9.7 7	4.3 80.5 MN C#
7410.	3590.	1240.				100. 6970. FE C#
/ 4TO.	3330.	7540.				

<sup>\*</sup> metal concentrations in ppm dried sediment
# metal concentrations in ppm dried residual sediment

# APPENDIX B, continued: SEDIMENT DATA.

257. .20 .36 .28 <.05 1.1 .73. <.2 <.8 <.05 13.6	20 .088 .072 .762 .078 .356 1.2 96. 1340. .33 1.16 .17 .40 7.7 217. 1.5 1.5 .27 37.9	.034 .790 .119 .461 .6 36.8 .40 .97 .12 1.1 6.5 392. 1.4 <.8 .49	3.1 120. 1740. .26 1.01 .04 .43 37.5 860. 3.4 2.4 .28 119.	.022 .009 .843 .126 .220 .8 14.7 318. .25 .41 .09 <.05 3.4 223. .7 <.8 .37 13.7	80 .021 .019 .797 .163 .519 .39.4 .518. .33 .52 .02 .54 8.6 355 1.4 <.8 .44 17.2	.054 .029 .792 .125 .503 1.3 .55. .81 <.02 <.05 9.7 333. 2.8	0 .258 .200 .459 .083 .825 1.1 192. 1560 .38 .70 .30 3.47 10.0 341. 1.6 <.8 .26 63.7	FE R* CO R* NI R* CU R* CR O* MN O* FE O* CO O* NI O* CU O* MN C#
22 20 .524 .301 .163 .012 1.210 1.8 176. 1660. .24 .35 .12 3.67 14.5 259. 2.0 <.8 .26	22 40 - - .656 .70. 980. .24 .47 .02 3.92 7.8 385. 1.3 <.24 41.6	22 60 - - .626 .8 102. 890. .20 .47 .24 5.53 9.1 310. 1.7 <.8 .50 63.1	.806 1.0 222. 1320. .18 .39 .11 5.39 14.3 428. 1.9	22 78 .391 .208 .382 .019 1.818 1.0 212 1080 .20 <.1 .06 2.95 16.5 750 1.8 <.8 .61 85.4	22 100 .083 .150 .737 .030 .417 .6 46.6 .16 .16 .13 5.7 227. 1.9 <.8 .14	22 120 .058 .061 .848 .032 .441 .8 37.2 .384 .22 .31 .39 4.30 5.2 159. 1.3 <.8 .14	22 150 .240 .155 .586 .018 .504 1.2 37.2 493 .29 .61 .14 3.61 7.8 122 1.7 <.8 .12	SITE DEPT CLAY SILT F S C OR CR R* MN R* CO R* CU O* CU O* CU O*

<sup>\*</sup> metal concentrations in ppm dried sediment # metal concentrations in ppm dried residual sediment

# APPENDIX B, continued: SEDIMENT DATA.

```
16
                                                10
                                                       SITE
          16
                 16
                         16
                                16
                                        16
  6
                 26
                        28.5
                                        110
                                                 0
                                                       DEPT
          18
                                50
.009
                               .004
                                      .002
                                               .197
                                                       CLAY
                .036
                        .010
.012
                .043
                        .020
                               .010
                                      .009
                                               .143
                                                       SILT
                        .853
                                                       F S
                                               .595
.743
                .858
                               .869
                                      .803
                                                       C\tilde{S}
.236
                                      .186
                                               .065
                .063
                        .117
                               .117
                                                        OR
         .922
                .453
                        .254
                               .261
                                      .148
                                               1.192
.265
                          . 2
                                <.1
                                                       CR R*
           .8
                                        <.1
                                                2.2
 <.1
                   . 2
                                                       MN R*
                       22.8
                               14.2
                                        7.0
                                                260.
          594.
                44.0
39.6
                                                       FE R*
                                               1980.
 218.
        1600.
                1140.
                         460.
                                188.
                                       160.
                                                       CO R*
                                                .49
                                        .16
                         .30
                                .16
 .25
          .29
                 .20
                                                       NI R*
                                       <.1
                                               1.46
                 .49
                         .51
                                <.1
 .28
          .95
                                                       CU R*
                                                .31
 .27
          .22
                 .21
                         .50
                                .76
                                        .18
                                                .86
                                                       CR O*
                                      <.05
                         .20
                               <.05
 .20
          .39
                <.05
                                               20.8
                                2.9
                                       1.4
                                                       MN 0*
                         4.7
 3.2
        19.8
                 5.8
                                                       FE O*
                                                780.
                         173.
                                         81.
                                175.
 152.
          334.
                 185.
                                                       CO 0*
                          . 4
                                 . 3
                                                3.6
                                         .1
 <.2
                  . 3
          1.0
                                                       NI O*
                                                3.4
                                <.8
                         <.8
                                       <.8
                 <.8
 <.8
          <.8
                                                       CU O*
                         .26
                                .17
                                      <.05
                                                .41
                 .12
<.05
          .13
                         167. 68.3
                                      77.6
                                               78.4
                                                       MN C#
69.9
          468.
                 185.
                                                       FE C#
                       5840. 2460.
                                               7960.
                                      2640.
       18600.
                6180.
2740.
                                                        10.
                                                                SITE
                                         10
                                                10
                         10
                                 10
                 10
  10
          10
                                                        140
                                                                DEPT
                                                120
                                         100
                                 82
                         78
  20
          40
                 60
                                                       .601
                                                                CLAY
                                        .130
                                               .175
                                .399
                .050
                        .009
 .587
         .136
                                                                SILT
                                        .149
                                               .125
                                                       .332
                                .517
        .083
                .033
                        .068
 .383
                                                       .065
                                                                F S
                                               .615
                                .081
                                        .666
                        .769
         .757
                .806
 .026
                                                                C S
                                                       .001
                                               .085
                                        .055
                                .002
                        .154
        .024
                .111
 .004
                                                      2.108
                                                                % OR
                               1.734
                                      1.095
                                               .848
                .627
                        .875
2.267
         .879
                                                          .9
                                                                CR R*
                                         1.2
                                                1.1
                                 2.0
                        1.0
  1.4
          2.1
                 0.5
                                                         312.
                                                                MN R*
                                                226.
                                         187.
                                 480.
  604.
                 102.
                        154.
          194.
                                                                FE R*
                                               1440.
                                                       1720.
                                       1370.
                                1800.
                       1220.
                 820.
 1870.
        1320.
                                                          . 5
                                                                CO R*
                                         .52
                                                .44
                                 .45
                         .40
          .63
                 .34
  .46
                                                                NI R*
                                                       2.84
                                       1.33
                                               1.42
                                1.41
                         .79
                 .66
 2.36
        1.79
                                                                CU R*
                                                .03
                                                         .05
                                       <.02
                                <.02
                       <.02
  .50
          .09
                <.02
                                                                CR O*
                                                       1.67
                                         .40
                                                .49
                                1.82
                         .19
 2.09
          .17
                 .47
                                                                MN O*
                                                       89.3
                                        25.3
                                               39.1
                               102.5
                13.5
                       19.0
        20.5
 71.0
                                                                FE O*
                                                500.
                                                       1328.
                                         533.
                                1685.
                         495.
                 527.
 1658.
          636.
                                                                CO 0*
                                                         5.9
                                         2.7
                                                3.1
                                 5.6
                         2.2
          2.9
                 1.9
  4.4
                                                         5.6
                                                                NI O*
                                                2.9
                                         2.3
                                 4.4
                 1.5
                         1.9
  4.3
          2.5
                                                                CU O*
                                                         .88
                                                .62
                                         .49
                                  .93
                         .71
          .98
                 .66
  .81
                                                                MN C#
                                                         246.
                                               96.6
                                       71.7
                                 191.
                       39.7
  226. 84.5
                39.3
                              21400. 5200. 7248.
                                                      27300.
                       3320.
                2450.
26600. 6650.
```

<sup>\*</sup> metal concentrations in ppm dried sediment

<sup>#</sup> metal concentrations in ppm dried residual sediment

### APPENDIX B, continued: SEDIMENT DATA.

```
19
           19
                   19
                                   19
                           19
                                           19
                                               SITE
   0
           20
                   40
                           60
                                   80
                                          100
                                               DEPT
 .420
                 .595
                                 .450
                                         .493
                                               CLAY
         .615
                         .439
 .388
         .377
                 .374
                         .258
                                 .299
                                         .458
                                                SILT
                                         .046
                 .028
                         .294
                                 .236
                                               F S
 .172
         .008
                                 .014
                                               C S
                 .003
                         .009
                                         .003
 .019
         .000
        3.714
                        2.281
2.310
                3.433
                                3.838
                                        3.341
                                                 OR
                                          1.1
                                                CR R*
  1.8
          1.5
                  1.0
                          1.7
                                  1.2
                  489.
                          222.
                                  258.
                                          236. MN R*
  502.
          292.
                                 1540.
                                         1280. FE R*
                  930.
                         1400.
 2550.
         1900.
                                               CO R*
                  .17
                          .45
                                  .38
                                          .36
  .46
          <.1
                                               NI R*
                                 1.42
                                         1.08
 1.30
         2.16
                 1.19
                         1.40
                          .07
                                  .06
                                         <.02
                                               CU R*
          .04
  .45
                  .06
                                 1.86
                                         1.94
                                                CR 0*
                         1.22
 1.13
         1.70
                 2.55
                                               MN O*
                                 75.8
                                         90.0
                         56.5
                 89.5
 46.0
         61.8
                                         1570. FE O*
                                 1490.
  765.
         1435.
                 1871.
                         1085.
                                               CO 0*
                                          5.8
                                  5.4
                          4.9
  4.1
          5.8
                  5.9
                                               NI O*
                          2.7
                                  5.1
                                          4.4
          4.9
  2.8
                  5.1
                                                CU O*
                                         1.31
                                 1.72
          .79
                          .81
                 1.25
  .38
                                          249. MN C#
                                  155.
                          154.
  222.
          244.
                  231.
       31000. 30000. 17450. 18500. 23900. FE C#
26300.
                        SITE number
                  19
  19
          19
                        DEPTh of sample (cm)
                 140
 120
         121.
                        CLAY size fraction
        .472
                .628
.019
                        SILT size fraction
.009
                .365
        .514
                        Fine Sand size fraction
        .014
                .005
.799
                        Coarse Sand size fraction
                .002
.173
        .000
                        % ORganic carbon
.449
      1.677
               2.565
                        CR Reducible fraction*
  .8
                 2.2
         1.1
                        MN Reducible fraction*
                 372.
35.7
         414.
                        FE Reducible fraction*
 461.
        1500.
                1620.
                        CO Reducible fraction*
                 .40
 .23
         .29
                        NI Reducible fraction*
        1.21
                1.94
 .38
                        CU Reducible fraction*
         .41
                 .04
 .08
                        CR Oxidizable fraction*
                1.37
        2.38
<.05
                        MN Oxidizable fraction*
               105.8
 9.1
        79.5
                        FE Oxidizable fraction*
 268.
        2063.
                1405.
                        CO Oxidizable fraction*
                 7.3
 1.0
         6.6
                        NI Oxidizable fraction*
                 4.7
 <.8
         4.1
                        CU Oxidizable fraction*
 .27
        1.03
                 .72
                        MN Crystalline or resicual fract.#
                 286.
20.3
         190.
                        FE Crystalline or resicual fract.#
1410. 25400. 30100.
```

<sup>\*</sup> metal concentrations in ppm dried sediment

<sup>#</sup> metal concentrations in ppm dried residual sediment

## APPENDIX C

#### WATER CHEMISTRY

I.D.	Cl mg/l	Na mg/l	K mg/l	Br mg/l	ALK. \$	рН	temp. degress cent.
33.0	23000.	10300.	430.	85.	125.	8.50	29.25
18.1	81000.	42300.	1560.	315.	-	6.70	31.50
18.2	82000.	41900.	1490.	314.	-	7.10	32.00
18.3	80000.	39500.	1430.	311.	158.	6.90	31.50
17.1	120000.	59700.	2420.	475.	138.	6.80	32.00
17.2	128000.	65400.	2590.	505.	145.	7.20	32.00
17.3	156000.	76800.	3180.	576.	127.	6.60	31.50
16.1	154000.	80300.	2980.	588.	85.	6.50	32.00
16.2	154000.	77000.	3060.	591.	89.	6.80	32.50
16.3	163000.	81300.	3510.	633.	89.	6.30	32.00
15.1	146000.	77200.	2520.	587.	107.	6.80	32.50
15.2	156000.	78100.	2790.	597.	210.	6.90	32.00
15.3	158000.	78400.	3100.	613.	265.	6.75	32.00
14.1	146000.	75200.	2500.	557.	103.	6.50	33.00
14.2	144000.	74300.	2480.	562.	98.	6.90	32.00
14.3	155000.	80300.	2870.	601.	100.	6.50	32.00
11.1	146000.	76700.	2500.	563.	116.	6.80	32.75
11.2	153000.	79400.	2850.	599.	214.	6.90	31.50
11.3	153000.	84300.	2940.	606.	165.	6.90	31.50
12.1	128000.	66800.	1820.	489.	165.	6.80	31.00
12.2	147000.	74700.	2370.	566.	272.	6.65	31.00
12.3	148000.	75800.	2610.	576.	366.	6.50	31.00 31.25
13.1	134000.	133000.	2040.	514.	205.	6.50	30.50
13.3	126000.	67000.	1980.	488.	212.	6.40	31.00
32.0	23000.	11400.	460.	91.	135.	8.00	31.00
3.1	103000.	52800.	1700.	295.	218.	6.40	<del>-</del>
4.1	148000.	58700.	1720.	335.	195.	6.45 6.20	_
4.2	107000.	55600.	1630.	429.	260.	6.20	_
4.3	113000.	58700.	1690.	435.	356.	6.40	_
5.1	120000.	61500.	2030.	479.	187. 223.	6.45	_
5.2	121000.	63500.	2090.	487.	281.	6.30	_
5.3	122000.	63300.	2100.	487.		6.10	_
6.1	123000.	62300.	1900.	485.	210. 244.	6.30	_
6.2	110000.	57600.	1790.	450.	2 <b>44.</b> 326.	6.10	_
6.3	111000.	59000.	1690.	450.	320.	0.10	

<sup>\*</sup> well identification: XX.Y where XX is the site number,
 and Y=1: trench or surface sample
 Y=2: shallow well sample
 Y=3: deep well sample
 Y=4: bottom of canal sample
\$ reported as mg/l of CaCO3

APPENDIX C, continued: WATER CHEMISTRY.

I.D.	Cl	Na	K	Br	ALK.	рН	temp.
*	mg/1	mg/1	mg/l	mg/l	\$		degress cent.
7.1	126000.	65600.	2080.	478.	165.	6.40	-
7.2	109000.	54700.	1770.	436.	261.	7.00	-
7.3	114000.	61100.	1880.	459.	294.	6.20	-
8.2	92000.	51200.	1590.	401.	294.	6.35	31.75
8.3	90000.	52200.	1520.	400.	319.	6.20	31.25
9.1	86000.	48800.	1650.	365.	405.	-	33.00
9.2	90000.	49800.	1660.	375.	336.	6.38	32.00
9.3	93000.	51400.	1650.	391.	308.	-	33.00
24.1	111000.	57200.	1720.	435.	281.	6.50	32.00
24.2	102000.	53600.	1670.	416.	410.	6.25	32.00
24.3	106000.	53500.	1580.	427.	397.	6.35	32.00
31.0	25000.	12600.	490.	96.	126.	8.15	33.50
31.4	23000.	10600.	460.	91.	80.	8.30	-
52.1	74000.	40700.	1300.	330.	559.	6.40	33.00
52.3	53000.	27600.	900.	187.	443.	7.00	33.00
53.1	63000.	33400.	1080.	259.	969.	6.68	32.00
53.2	57000.	32000.	950.	223.	380.	6.60	34.75
53.3	53000.	27000.	720.	176.	382.	6.55	31.75
54.1	79000.	43000.	1340.	300.	545.	6.50	32.00
54.2	54000.	32400.	1010.	218.	396.	6.50	35.50
54.3	52000.	27300.	810.	203.	471.	6.50	32.50 33.00
55.1	69000.	37400.	1240.	292.	760.	6.50 6.60	34.75
55.2	63000.	34900.	1140.	272.	336. 475.	6.50	32.75
55.3	57000.	31500.	1060.	254.	475.	6.50	30.50
10.1	80000.	41700.	1470.	327. 375.	434.	6.25	32.75
10.2	87000.	46600.	1610.	369.	338.	6.20	31.50
10.3	84000.	49000.	1610.	379.	432.	6.33	33.00
19.2	92000.	48100.	1480.	351.	343.	6.30	31.75
19.3	88000.	45800.	1320. 2310.	502.	259.	6.20	33.50
20.2	118000.	61600.	2090.	493.	250.	6.25	33.25
20.3	113000.	61500. 65800.	2910.	561.	259.	6.20	34.00
21.2	133000.	67500.	3070.	584.	272.	6.15	33.50
21.3	137000.	67700.	2540.	595.	417.	6.25	32.00
22.2	138000.	70900.	4070.	636.	401.	6.10	31.00
22.3	143000.	64200.	3460.	565.	343.	6.70	32.00
23.1	129000.	67600.	4260.	616.	379.	6.45	32.75
23.2	137000.	07000.	12001				

<sup>\*</sup> well identification: XX.Y where XX is the site number,
 and Y=1: trench or surface sample
 Y=2: shallow well sample
 Y=3: deep well sample
 Y=4: bottom of canal sample
\$ reported as mg/l of CaCO3

APPENDIX C, continued: WATER CHEMISTRY.

I.D.	Mn mg/l	Fe mg/l	I.D.	Mn mg/l	Fe mg/l
33.0 18.1 18.2 18.3 17.1 17.2 17.3 16.1 16.2 16.3 15.1 14.2 14.3 11.1 11.2 11.3 12.1 12.2 12.3 13.1 13.3 32.0	.040 .469 .583 .690 .091 .077 .128 1.000 .392 .188 .715 .580 .278 1.201 .829 .553 .932 .825 .987 1.120 1.120 .650 1.780 .211 .050	.044 .553 .038 .036 .376 .059 .033 .123 .019 .311 .067 .011 .083 .136 .127 .136 .210 .010 .217 .179 .017 .142 .218 .030 .122	3.1 4.1 4.2 4.3 5.1 5.2 5.3 6.1 6.2 6.3 7.1 7.2 7.3 31.0 24.1 24.2 24.3 10.1 10.2 10.3 19.2 19.3 20.2 20.3 21.2 21.3 22.2 22.3 23.1 23.2	.238 .406 .137 .246 .287 .050 .050 .880 .013 .919 .286 .082 .799 .010 .149 .057 .635 .180 .045 .045 .045 .408 .111 .110 .214 1.410 .214 1.410 .245 .315 .495 .640	.296 .278 .119 .128 .331 .106 .044 .224 .091 .157 .196 .154 .111 .046 .355 .079 .067 .047 .075 .032 .049 .028 .047 .026 .049 .026 .049 .026 .049 .027 .026 .027 .027 .027 .028

<sup>\*</sup> well identification: XX.Y where XX is the site number,

and Y=1: trench or surface sample
Y=2: shallow well sample
Y=3: deep well sample
Y=4: bottom of canal sample

# APPENDIX D COEFFICIENTS OF DETERMINATION FOR METAL PARTITIONING DATA 54 samples

	*	<b>&amp;</b>	REDUC	CIBLE				
	ORG.	FINES\$	Cr	Mn	Fe	Co	Ni	Cu
% FINES\$	.704							
REDUCI BLE								
Cr	.216	.295						
Mn	.359	.462	.180					
Fe	.391	.496	.546	.511				
Co	.010	.009	.065	.036	.071	263		
Ni	.402	.358	.233	.327	.403.	.361	007+	
Cu	.036*	.005*	.039*	.026	.001*	.000*	.007*	
OXIDI ZABLE		250	000	000	000	.059*	.023*	.004*
Cr	.017	.252	.002	.000	.008	.059	.526	.026*
<b>M</b> n	.716	.656	.265	.445	.376 .368	.027	.420	.011*
Fe	.699	.621	.252	.425	.436	.027	.591	.042*
Co	.740	.711	.364	.360	.336	.103	.638	.020*
Ni	.696	.572	.226 .134	.341	.216	.095	.392	.058*
Cu	.656	.572	.134	. 214	.210	.075		.000
RESIDUAL	204	.596	.009	.461	.332	.024	.328	.006
Mn Fig.	.394	.774	.235	.508	.454	.028	.484	.000*
Fe	. / 0 /	. / / 4	. 233	. 500				• • • •
	חוצט	IZABLE	FRACT	ON			RESII	DUAL
	Cr	Mn	Fe	Со	Ni	Cu	Mn	
OXIDI ZABLE	٠.	••••						
<b>M</b> n	.000*							
Fe	.000	.861						
Co	.014	.889	.824					
Ni	.001*		.789	.852				
Cu	.004	.598	.618	.621	.575			
RESIDUAL								
<b>M</b> n	.004*		.338	.356	.345	.161	672	
Fe	.006	.778	.716	.785	.686	.336	.672	

<sup>\*</sup> negative slope on correlation

<sup>\$</sup> samples without grain size data were deleted for correlations with % FINE, so 48 samples were used. # a coefficient of determination between two populations

of .xyz indicates that xy.z of the variability in one population can be explained by a linear relationship with the other population. Coefficients vary from 0 for unrelated populations to 1.00 for a perfect linear relationship (Netter & Wasserman, 1974).

APPENDIX E PIEZOMETRIC POTENTIALS

well I.D.	piezometric potential	density	site elevation	water level
*	g/cm2	g/cm3 \$	cm	cm #
4.1	82.613	1.142	26.152	-52.39
4.3	96.372	1.127	26.152	-40.64
5.1	105.576	1.133	40.173	-46.99
5.2	93.587	1.136	40.173	-57.79
5.3	93.669	1.137	40.173	-57.79
6.1	106.506	1.135	48.768	-54.93
6.2	122.604	1.124	48.768	-39.69
6.3	109.591	1.126	48.768	-51.44
7.1	94.810	1.141	41.514	-58.42
7.2	94.487	1.120	41.514	-57.15
7.3	116.134	1.130	41.514	-38.74
8.2	80.113	1.108	23.104	-50.80
8.3	68.146	1.108	23.104	-61.60
9.1	80.093	1.102	40.630	-67.95
9.2	110.489	1.105	40.630	-40.64
9.3	116.522	1.109	40.630	-35.56
10.1	84.858	1.090	21.031	-43.18
10.2	131.033	1.100	21.031	-1.91
10.3	139.680	1.102	21.031	5.72
11.1	114.165	1.164	51.420	-53.34
11.2	143.108	1.171	51.420	-29.21
11.3	141.593	1.177	51.420	-31.12
12.1	113.958	1.144	39.624	-40.01
12.2	131.136	1.162	39.624	-26.77
12.3	125.565	1.164	39.624	-31.75
13.3	157.210	1.143	74.371	-36.83
14.1	141.134	1.162	71.628	-50.17
14.2	149.730	1.160	71.628	-42.55
14.3	145.450	1.173	71.628	-47.63
15.1	149.962	1.165	80.162	-51.44
15.2	147.633	1.170	80.162	-53.98
15.3	145.659	1.172	80.162	-55.88
16.1	150.958	1.172	85.954	-57.15
16.2	157.859	1.168	85.954	-50.80 -59.05
16.3	149.492	1.178	85.954	-53.05

<sup>\*</sup> well identification: XX.Y where XX is the site number, and Y=1: trench or surface sample

Y=2: shallow well sample
Y=3: deep well sample
Y=4: bottom of canal sample
\$ calculated from (Cl) and (Na): see Methods, Chapter 3 + for above ground, - for below ground

APPENDIX E, continued: PIEZOMETRIC POTENTIALS.

well	piezometric		site	water
I.D.	potential	density	elevation	level
*	g/cm2	g/cm3 \$	cm	cm #
17.1	154.295	1.131	101.194	-64.77
17.2	154.345	1.142	101.194	-66.04
17.3	160.216	1.169	101.194	-64.14
18.1	109.197	1.092	79.858	-79.86
18.2	124.977	1.092	79.858	-65.41
18.3	127.979	1.088	79.858	-62.23
19.2	178.350	1.104	54.559	6.99
19.3	181.026	1.099	54.559	10.16
20.2	213.995	1.133	82.205	6.67
20.3	214.502	1.130	82.205	7.62
21.2	207.717	1.145	96.652	-15.24
21.3	215.003	1.149	96.652	-9.53
22.2	189.438	1.149	104.882	-40.01
22.3	184.719	1.156	104.882	-45.09
23.2	184.721	1.149	105.857	-45.09
24.1	82.823	1.124	37.186	-63.50
24.2	93.488	1.115	37.186	-53.34
24.3	92.237	1.117	37.186	-54.61
31.0	102.900	1.029	0.000	0.00
32.0	102.700	1.027	0.000	0.00
33.0	102.700	1.025	0.000	0.00
52.1	92.576	1.087	35.966	-50.80
52.3	29.019	1.060	35.966	-108.59
53.1	86.212	1.072	32.492	-52.07
53.2	90.643	1.068	32.492	-47.62
53.3	151.211	1.060	32.492	10.16
54.1	80.631	1.092	33.528	-59.69
54.2	123.845	1.067	33.528	-17.46
54.3	150.963	1.060	33.528	8.89
55.1	86.120	1.080	34.351	-54.61
55.2	109.506	1.074	34.351	-32.39
55.3	164.362	1.067	34.351	19.69
JJ.J	104.306	2.00.	<b>3</b>	

<sup>\*</sup> well identification: XX.Y where XX is the site number, and Y=1: trench or surface sample

Y=2: shallow well sample

Y=3: deep well sample

Y=4: bottom of canal sample

<sup>\$</sup> calculated from (C1) and (Na): see Methods, Chapter 3 + for above ground, - for below ground

APPENDIX F
LOCATION OF SITES

FROM,	TRAVEL	AT,	FOR,	TO.	
east side o by marke site 13 site 12 site 11 site 14 site 15 site 16 site 17 site 18		96° 63° 71° 75° 45° 16° 78°	3370' 5660' 2610' 2398' 2944' 2973' 3365' 3617' 4060'	site site site site site site Site	12 11 14 15 16
West side o by marke site 2 site 3 site 4 site 5 site 6	f ICWW r 215	243° 262° 261° 279° 294°	143' 442' 517' 2168' 2177' 3704'	site site site site site	3 4 5 6
bend in canaby site Am2 site Am3 site Am4 site Am5 site 10 site 19 site 20 site 21 site 22		2590 2590 2590 2590 2550 3330 3270 3210 313	408' 165' 513' 513' 1198' 3994' 3735' 2696' 2763' 1793'	site site site site site site site site	Am3 Am4 Am5 10 19 20 21
bend in can by site		279 <sup>0</sup>	2565'	site	24
end of canaby site Aml site 8		263° 238° 270°	1283' 1580' 2015'	site site site	

#### BIBLIOGRAPHY

- Adams, J.E. and Rhodes, M.L., 1960. Dolomitization by seepage refluxation. Bull. Am. Assoc. Petro. Geol., 44: 1912-1920.
- Addy, S.K., Presley, B.J. and Ewing, M., 1976. Distribution of manganese, iron and other trace elements in a core from the northwest Atlantic. J. Sediment. Petrol., 46: 813-818.
- Amdurer, M., 1978. Geochemistry, Hydrology and Mineralogy of the Laguna Madre Flats, South Texas. M.S. Thesis, Univ. of Texas at Austin (unpublished).
- Amdurer, M., Munson, M.G. and Valastro, S.Jr., 1979. Depositional history and rate of deposition of a flood-tidal delta, Central Texas Coast. Contributions in Marine Sci., 22: 205-214.
- Amdurer, M. and Land, L.S., 1982. Geochemistry, hydrology and mineralogy of the Sand Bulge area, Laguna Madre Flats, south Texas. J. Sediment. Petrol., 52: 703-716.
- Armstrong, A.K., 1975. Mississippian tidal deposits, north-central New Mexico. In: R.N. Ginsburg (Editor), Tidal Deposits. Springer-Verlag, New York, N.Y., pp. 325-331.
- Beales, F.W. and Lozej, G.P., 1975. Ordivician tidalites in the unmetamorphosed sedimentary fill of the Brent meteorite crater, Ontario. In: R.N. Ginsburg (Editor), Tidal Deposits. Springer-Veralag, New York, N.Y., pp. 315-323.
- Behrens, E.W. and Land, L.S., 1972. Subtidal Holocene dolomite, Baffin Bay, Texas. J. Sediment. Petrol., 42: 151-161.
- Berner, R.A., 1964. Iron sulfides formed at low temperatures and atmospheric preasure. J. Geol., 72: 293-306.
- Berner, R.A., 1970. Sedimentary pyrite. Am. J. Sci., 268: 1-23.
- Berner, R.A., 1984. Sedimentary pyrite formation: An update. Geochim. Cosmochim. Acta, 48: 605-615.

- Bonatti, E., Fisher, D.E., Joensuu, O. and Rydell, H.S., 1971. Postdepositional mobility of some transition elements, phosphorus, uranium and thorium in deepsea sediments. Geochim. Cosmochim. Acta, 35: 189-201.
- Bosellini, A. and Hardie, L.A., 1973. Depositional theme of a marginal marine evaporite. Sedimentology, 20:5-27.
- Boyle, E.A., 1982. Manganese carbonate overgrowths on Foraminifera tests. Geochim. Cosmochim. Acta, 47: 1815-1819.
- Brown, L.F. Jr., McGowen, J.H., Evans, T.J., Groat, C.G. and Fisher, W.L., 1977. Environmental Geologic Atlas of the Texas Coastal Zone--Kingsville Area. Bureau of Economic Geology, University of Texas at Austin.
- Bush, P.R., 1970. Chloride-rich brines from sabkha sediments and their possible role in ore formation. Trans. Sec. B. Applied Earth Science Institution of Mining and Metallurgy, 79B, pp. 137-144.
- Butler, G.D., 1969. Modern evaporite deposition and geochemistry of coexisting brines, the sabkha, Turcial Coast, Arabian Gulf. J. Sediment. Petrol., 39: 70-89.
- Calvert, S.E. and Price, N.B., 1970. Composition of manganese nodules and manganese carbonates from Loch Fyne, Scotland. Cotr. Mineral. and Petrol., 29: 215-233.
- Carpenter, A.B., 1978. Origin and chemical evolution of brines in sedimentary basins. Oklahoma Geol. Circ., 79: 60-77.
- Chester, R. and Hughes, M.J., 1967. A chemical technique for the seperation of ferromanganese minerals, carbonate minerals and adsorbed trace metals from pelagic sediments. Chem. Geol., 2: 249-262.
- Davis, J.H., 1977. Genesis of the Southeast Missouri lead district. Econ. Geol., 72: 443-450.
- Deffeyes, K.S., Lucia, F.J. and Weyl, P.K., 1965. Dolomitization of Recent and Plio-Pleistocene sediments by marine evaporite waters on Bonaire, Netherlands Antilles. In: Dolomitization and Limestone Diagenesis. Soc. of Economic Paleontologists and Mineralogists Spec. Pub., 13: 71-88.

- DeGroot, K., 1973. Geochemistry of tidal flat brines at Um Said, SE Qatar, Persian Gulf. In: B.H. Purser (Editor), The Persian Gulf. Springer-Verlag, New York, N.Y., pp. 377-394.
- Demina, L.L., Gordeyev, V.V. and Formina, L.S., 1978. Forms of occurance of Fe, Mn, Zn and Cu in river water and suspended matter, and their variation in the zone of mixing of river and seawater (as exemplified by rivers of the Black Sea, Sea of Azov, and Caspian Sea basins). Geochem. Intl., 15: 146-163.
- Dissanayake, C.B., 1984. Metals in algal mats -- A geochemical study from Sri Lanka. Chem. Geol., 47: 303-320.
- Doff, D.H., 1969. The Geochemistry of Recent Oxic and Anoxic Sediments of Oslo Fjord, Norway. Ph.D. Dissert., University of Edinburgh (unpublished).
- Eaton, A., 1979. The impact of anoxia on Mn fluxes in the Chesapeake Bay. Geochim. Cosmochim. Acta, 43: 429-432.
- Eugster, H.P. and Jones, B.F., 1979. Behavior of major solutes during closed-basin brine evolution. Am. J. Sci., 279: 609-631.
- Evans, G., Schmidt, V., Bush, P. and Nelson, H., 1969. Stratigraphic and geologic history of the sabkha, Abu Dhabi, Persian Gulf. Sedimentology, 12: 145-159.
- Fan, P., 1984. Geologic setting of selected copper deposits of China. Econ. Geol., 79: 1785-1795.
- Ferguson, J. and Burne, R.V., 1981. Interactions between saline redbed groundwaters and peritidal carbonates, Spencer Gulf, South Australia: significance for models of stratiform copper ore genesis. J. Australian Geol. Geophysics, 6: 319-325.
- Filipek, L.H. and Owen, R.M., 1979. Geochemical associations and grain size partitioning of heavy metals in lacustrine sediments. Chem. Geol., 26: 105-117.
- Filipek, L.H., Chao, T.T. and Carpenter, R.H., 1981. Factors effecting the partitioning of Cu, Zn and Pb in boulder coatings and stream sediments in the vacinity of a polymetallic sulfide deposit. Chem. Geol., 33: 45-64.

- Fisk, H.N. and McFarlin, E.Jr., 1955. Late Quaternary deltaic deposits of the Mississippi River. In: A. Poldervaart (Editor), Crust of the Earth. Geol. Soc. Am. Secial Paper, 62: 279-302.
- Fisk, H.N., 1959. Padre Island and the Laguna Madre Flats, coastal south Texas. Louisiana St. Univ. Coastal Studies, Second Coastal Geography Conference, pp. 103-151.
- Folk, R.L. and Pittman, J.S., 1971. Length-slow chalcedony: a new testament for vanished evaporites. J. Sediment. Petrol., 41: 1045-1058.
- Friedman, G.M. and Sanders, J.E., 1967. Origin and occurance of dolostone. In: G.V. Chilingar, H.J. Bissel, and R.W. Fairbridge (Editors), Carbonate Rocks: Origin, Occurance and Classification. Developments in Sedimentology 9A, Elsevier, Amsterdam, The Netherlands, pp. 267-348.
- Fryberger, S.G., Al-Sari, A.M. and Clisham, T.J., 1983. Eolian dune, interdune, sand sheet and siliciclastic sabkha sediments of an offshore prograding sand sea, Dharan area, Saudi Arabia. Am. Ass. Petro. Geol. Bull., 67: 280-312.
- Fuller, J.G.C.M. and Porter, J.W., 1969. Evaporite formations with petroleum resources in Devonian and Mississippian of Alberta, Saskatchewan and North Dakota. Bull. Am. Ass. Petro. Geol., 53: 909-926.
- Garland, G.D., 1979. Introduction to Geophysics. W.B. Saunders Co., Philladelphia, PA.
- Garlick, W.G., 1981. Sabkhas, slumping, and compaction at Mufulira, Zambia. Econ. Geol., 76: 1817-1847.
- Garlick, W.G., 1982. Erosion of the folded copper-rich arenite filling of a rolled-up algal mat, Mufulira, Zambia. Econ. Geol., 77: 1934-1939.
- Garrels, R.M. and Christ, C.L., 1965. Solutions, Minerals, and Equilibrium. Freeman, Cooper & Co., San Fransisco, CA.
- Garrels, R.M., Mackenxie, F.T. and Hunt, C., 1975. Chemical Cycles and the Global Environment; Assessing Human Influences. William Kaufmann, Inc., Los Altos, CA.

- Gaudette, H.E. and Flight, W.R., 1974. An inexpensive titration method for the determination of organic carbon in Recent sediments. J. Sediment. Petrol., 44: 249-252.
- Gaudette, H.E. and Lyons, W.B., 1984. Trace metal concentrations in modern marine sabkha sediments. In: Microbial Mats: Stromatolites. Alan R. Liss, Inc., New York, N.Y., pp. 425-434.
- Gephart, C.J., 1982. Relative Importance of Iron-oxide, Manganese-oxide and Organic Material on the Adsorption of Chromium in Natural Water Sediment Systems. M.S. Thesis, Michigan State Univ. (unpublished).
- Gibbs, W., 1977. Transport phases of transition metals in the Amazon and Yukon Rivers. Geol. Soc. Am. Bull., 88: 829-843.
- Goldberg, M., 1967. Supratidal dolomitization and dedolomitization in Jurassic rocks of Hamakhtesh Haqatan, Isreal. J. Sediment. Petrol., 37: 760-773.
- Gudramovics, R., 1981. A Geochemical and Hydrological Investigation of a Modern Coastal Marine Sabkha. M.S. Thesis, Michigan State Univ. (unpublished).
- Gupta, S.K. and Chen, K.Y., 1975. Partitioning of trace metals in selective chemical fractions of nearshore sediments. Environ. Lett., 10: 129-158.
- Handford, C.R., 1981. Coastal sabkha and salt pan deposition of the lower Clear Fork formation (Permian), Texas. J. Sediment. Petrol., 51: 761-778.
- Hartman, M., 1964. Zur Geochemie von Mangan und Eisen in der Ostse. Meyniana, 14: 3-20.
- Hayes, M.O., 1967. Hurricanes as Geologic Agents: Carla, 1961, and Cindy, 1963. Report of Investigations 61, Univ. Texas Bureau of Econ. Geology.
- Hem, J.D., 1978. Redox processes at surfaces of manganese oxide and their effects on aqueous metal ions. Chem. Geol., 21: 199-218.
- Herber, J.B., 1981. Holocene Sediments Under Laguna Madre, Cameron County, Texas. M.A. Thesis, Univ. of Texas at Austin (unpublished).

- Horodyski, R.J., Bloeser, B. and Vonder Haar, S., 1977. Laminated algal mats from a coastal lagoon, Laguna Mormona, Baja California, Mexico. J. Sedimet. Petrol., 47: 680-696.
- Hsu, K.J. and Siegenthaler, C., 1969. Preliminary experiments on hydrodynamic movement induced by evaporation and their bearing on the dolomite problem. Sedimentology, 12: 11-26.
- Illings, L.V., Wells, A.J. and Taylor, J.M.C., 1965. Penecontemporary dolomite in the Persian Gulf. In: Dolomitization and Limestone Diagenesis. Soc. of Economic Paleontologists and Mineralogists Spec. Pub., 13: 89-111.
- Jackson, M.L., 1979. Soil Chemical Analysis Advanced Course. 2nd edition, 11th printing, published by the author, Madison, Wisconsin.
- Jorgensen, B.B. and Cohen, Y., 1977. Solar Lake (Sinai). 5. The sulfur cycle of the benthic cyanobacterial mats. Limnol. Oceangr., 22: 657-666.
- Jones, B.F., Vandenburgh, A.S., Truesdell, A.H. and Rettig, S.L, 1969. Interstitial brines in playa sediments. Chem. Geol., 4: 253-262.
- Jones, B.F. and Weir, A.H., 1983. Clay minerals of Lake Albert, an alkaline, saline lake. Clays and Clay Minerals, 31: 161-172.
- Kendall, C.G.St.C. and Skipwith, Sir P.A.D'E., 1968. Recent algal mats of a Persian Gulf lagoon. J. Sediment. Petrol., 38: 1040-1058.
- Kinsman, D.J.J., 1969. Modes of formation, sedimentary associations, and diagnostic features of shallow-water and supratidal evaporites. Am. Assoc. Petro. Geol. Bull., 53: 830-840.
- Kinsman, D.J.J. and Park, R.K., 1976. Algal belt and coastal sabkha evolution, Turcial Coast, Persian Gulf. In: M.R. Walter (Editor), Stromatolites. Developments in Sedimentology 20, Elsevier, Amsterdam, The Netherlands, pp. 421-433.

- Lambert, I.B., Donnelly, T.H. and Etminan, H., 1984. Genesis of Late Proterozoic copper mineralization, Copper Clain, South Australia. Econ. Geol., 79: 461-475.
- Lange, I.M. and Murray, C.M., 1977. Evaporite brine reflux as a mechanism for moving deep water brines upward in the formation of Mississippi Valley-type base metal deposits. Econ. Geol., 72: 107-109.
- Lange, I.M. and Eby, D.E., 1981. Stratabound copper-silver-bearing oolitic deposits in the Belt Supergroup of Montana. Econ. Geol., 76: 933-937.
- LeBlanc, R.J. and Hodgson, W.D., 1959. Origin and development of the Texas shoreline. Coastal Studies Inst., Second Coastal Geography Conf., Louisiana State Univ., pp. 57-101.
- Levy, Y., 1977 a. The origin and evolution of brines in coastal sabkhas, Norhtern Sinai. J. Sediment. Petrol., 47: 451-462.
- Levy, Y., 1977 b. Description and mode of formation of the supratidal evaporite facies in northern Sinai coastal plain. J. Sediment. Petrol., 47: 463-474.
- Lind, W.B. and Ratzlaff, K.W., 1979. Chemical and physical characteristics of water in estuaries of Texas, October 1973--September 1974. Texas Department of Water Resources, Report 231.
- Logan, B.W., Davies, G.R., Read, J.F. and Cebulski, D.E., 1970. Carbonate Sedimentation and Environments, Shark Bay, Western Australia. Am. Ass. Petro. Geol., Tulsa, Oklahoma.
- Logvinenko, N.V., Volkov, I.I. and Sokolova, Ye.G., 1972. Rhodochrosite in deep sea sediments of the pacific ocean. Dokl. Akad. Navk., SSSR, 203: 204-207.
- Lohse, E.A., 1956. Dynamic geology of the modern coastal region, Northeast Gulf of Mexico. In: J.L. Hough (Editor), Finding Ancient Shorelines. Soc. Econ. Paleontologists and Min. Spec. Pub., 3, pp. 99-104.
- Long, D.T. and Angino, E.E., 1976. Occurance of copper sulfides in the (Permian age) Milan Dolomite, south-central Kansas. Econ. Geol., 71: 656-661.

- Long, D.T. and Gudramovics, R., 1983. Major-element geochemistry of brines from the Wind Tidal Flat area, Laguna Madre, Texas. J. Sediment. Petrol., 53: 797-810.
- Long, D.T., Lyons, W.B. and Gaudette, H.E., 1985. Trace metal concentrations in modern marine sabkhas. Chem. Geol., in press.
- Lyons, W.B., Hines, M.E. and Gaudette, H.E., 1984. Major and minor element pore water geochemistry of modern marine sabkha: The influence of cyanobacterial mats. In: Microbial Mats: Stromatolites. A.R. Liss (Editor), New York, N.Y., p. 411-423.
- Lynn, D.C. and Bonatti, E., 1965. Mobility of manganese in diagenesis of deep-sea sediments. Mar. Geol., 3: 457-474.
- Manheim, F.T., 1961. A geochemical profile in the Baltic Sea. Geochim. Cosmochim. Acta, 25: 52-71.
- Martin, E.A. and Miller, R.J., 1982. A simple diver-operated coring device for collecting undisturbed shallow cores. J. Sediment. Petrol., 52: 641-642
- Martin, J.H. and Knauer, G.A., 1983. VERTEX: Manganese transport with CaCO<sub>3</sub>. Deep Sea Research, 30: 411-425.
- Mason, P.H., 1955. An occurance of gypsum in south west Texas. J. Sediment. Petrol., 25: 72-77.
- McBride, M.B., 1979. Chemistries and precipitation of Mn<sup>2+</sup> at CaCO<sub>3</sub> surfaces. Soil Sci. Soc. Am. J., 43: 693-698.
- McGowen, J.H., Groat, C.G., Brown, L.F., Fisher, W.L. and Scott, A.J., 1970. Effects of Hurricane Celia--A Focus on Environmental Geologic Problems of the Texas Coastal Zone. Bureau of Economic Geology, Geologic Circular 70-3, University of Texas at Austin.
- McKenzie, J.A., Hsu, K.J. and Schneider, J.F., 1980. Movement of subsurface waters under the sabkha, Abu Dhabi, U.A.E., and its relation to evaporitive dolomite genesis. Soc. Econ. Paleontologists and Min. Spec. Pub., 28, pp. 11-30.

- Miller, J.A., 1975. Facies characteristics of Laguna Madre Wind Tidal Flats. In: R.N. Ginsburg (Editor), Tidal Deposits. Springer-Verlag, New York, N.Y., pp. 67-73.
- Mortland, M., 1984. (Personal communications) Department of Geological Sciences, Michigan State University, East Lansing, MI.
- National Oceanic and Atmospheric Administration, 1982. Climatological Data, Annual Summary, Texas, 1982. Volume 87, number 13, Department of Commerce, Asheville, N.C..
- Netter, J. and Wasserman, W., 1974. Applied Linear Statistical Models. R.D. Irwin, Inc., Homewood, IL.
- Nichols, K.M., 1974. Coextensive supratidal dolomite and underlying secondary dolomite in the Triassic of north-central Nevada. J. Sediment. Petrol., 44: 783-789.
- Nissenbaum, A. and Swaine, D.J., 1976. Organic matter-metal interactions in recent sediments: the role of humic substances. Geochim. Cosmochim. Acta, 40: 809-816.
- Parker, C.R., 1972. Water Analysis by Atomic Absorption. Varian Techtron, Springervale, Vic., Australia.
- Patterson, R.J. and Kinsman, D.J.J., 1977. Marine and continental groundwater sources in a Persian Gulf coastal sabkha. In: Reefs and Related Carbonates Ecology and Sedimentology. Am. Ass. Petro. Geol. Studies in Geology, 4: 381-397.
- Patterson, R.J. and Kinsman, D.J.J., 1981. Hydrologic framework of a sabkha along Arabian Gulf. Am. Ass. Petro. Geol., 65: 1457-1475.
- Pederson, T.F. and Price, N.B., 1982. The geochemistry of manganese carbonate in Panama Basin sediments. Geochim. Cosmochim. Acta, 46: 59-68.
- Pelowski, S.M., 1983. Behavior of Selected Trace Metals in Sediments from the Continental Shelf of the Amazon River. M.S. Thesis, Michigan State Univ. (unpublished).
- Piper, D.Z., 1971. The distribution of Co, Cr, Cu, Fe, Mn, Ni and Zn in Framvaren, a Norwegian anoxic fjord. Geochim. Cosmochim. Acta, 35: 531-550.

- Presley, B.J., 1971. Part I: Determination of selected minor and major inorganic constituents. In: J.I. Eving and others (Editors), Initial Reports of the Deep Sea Drilling Project, Vol. VII. U.S. Govt. Print. Off., Wash., D.C., pp. 1749-1755.
- Price, W.A., 1933. Role of diastrophism in topography of Corpus Christi area, South Texas. Bull. Am. Assoc. Petro. Geol., 17: 907-962.
- Purser, B.H., 1973. The Persian Gulf. Springer-Verlag, New York, N.Y..
- Ratzlaff, K.W., 1976. Chemical and Physical Characteristics of Water in Estuaries of Texas, October 1971--September 1973. Texas Department of Water Resources, Report 208.
- Renfro, A.R., 1974. Genesis of evaporite-associated metaliferous deposits --A sabkha process. Econ. Geol., 69: 33-45.
- Robbins, J.A. and Callender, E., 1975. Diagenesis of manganese in Lake Michigan sediments. Am. J. Sci., 275: 512-533.
- Rusnak, G.A., 1960. Sediments of Laguna Madre, Texas. In: F.P. Shepard and others (Editors), Recent Sediments, Northwestern Gulf of Mexico. Am. Ass. Petro. Geol., Tulsa, OK, pp. 153-196.
- Russel, R.J., 1940. Quaternary history of Louisiana. Bull. Geol. Soc. Am., 51: 1199-1233.
- Sawlan, J.J. and Murray, J.W., 1983. Trace metal remobilization in the interstitial waters of red clay and hemipelagic marine sediments. Earth Planet. Sci. Lett., 64: 213-230.
- Schenk, P.E., 1967. The Macumber Formation of the Maritime Provinces, Canada -- A Mississippian analog to recent strand-line carbonates of the Persian Gulf. J. Sediment. Petrol., 37: 365-376.
- Schenk, P.E., 1969. Carbonate-sulfate-redbed facies and cyclic sedimentation of the Windsorian Stage (Middle Carboniferous), Maritime Provinces. Can. J. Earth Sci., 6: 1037-1066.

- Schneider, J.F., 1975. Recent tidal deposits, Abu Dhabi, U.A.E., Arabian Gulf. In: R.N. Ginsburg (Editor), Tidal Deposits. Springer-Verlag, New York, N.Y., pp. 209-214.
- Shinn, E.A., 1973. Sedimentary accretion along the leeward, SE coast of Qatar Peninsula, Persian Gulf. In: B.H. Purser (Editor), The Persian Gulf. Springer-Verlag, New York, N.Y., pp. 199-209.
- Shterenberg, L.E., Gorshkova, T.I. and Naktinas, E.M., 1968. Manganese carbonates in ferromanganese nodules in the Gulf of Riga. Lithol. Miner. Resour., 4: 438-443.
- Siedlecka, A., 1972. Length-slow chalcedony and relects of sulphate--Evidences of evaporitic environments in the Upper Carboniferous and Permian beds of Bear Island, Svalbard. J. Sediment. Petrol., 42: 812-816.
- Siedlecka, A., 1976. Silicified Precambrian evaporite nodules from northern Norway: a preliminary report. Sediment. Geol., 16: 161-175.
- Singer, A. and Stoffers, P., 1980. Clay mineral diagenesis in two East African lake sediments. Clay Minerals, 15: 391-307.
- Skougstad, M.W., Fishman, M.J., Friedman, L.C., Erdmann, D.E. and Duncan, S.S., 1979. Techniques of Water-Resources Investigations of the United States Geological Survey, Chapter Al, Methods for Determination of Inorganic Substances in Water and Fluvial Sediments. U.S. Govt. Print. Off., Wash., D.C..
- Smith, G.E., 1976. Sabkha and tidal flat facies control of stratiform copper deposits in north Texas. In: K.H. Wolf (Editor), Handbook of Strata-bound and Stratiform Ore Deposits, Volume 6. Elsevier, Amsterdam, The Netherlands, pp. 407-446.
- Stein, H., 1980. Evidence for intertidal-supratidal facies control of stratiform ore at Magmont Mine, Viburnum Trend, southeast Missouri. In: J.D. Ridge (Editor), Proceedings of the Fifth IAGOD Symposium, volume 1, Stuttgard, Germany, pp. 767-784.
- Stumm, W. and Morgan, J.J., 1970. Aquatic Chemistry. Wiley-Interscience, New York, N.Y..

- Suess, E., 1979. Mineral phases formed in anoxic sediments by microbial decomposition of organic matter. Geochim. Cosmochim. Acta, 43: 339-352.
- Tessier, A.P., Campbel, G.C. and Bisson, M., 1979. Sequential extraction procedure for the speciation of particulate trace metals. Analytical Chem., 51: 844-850.
- Tessier, A.P., Rapin, F. and Carignan, R., 1985. Trace metals in oxic lake sediments: Possible adsorption onto iron hydroxides. Geochim. Cosmochim. Acta, 49: 183-194.
- Thompson, R.W., 1968. Tidal Flat Sedimentation on the Colorado River Delta, Northwestern Gulf of California. Geol. Soc. Am. Memoir 107.
- Tolbert, J.N., Long, D.T. and Gudramovics, R., in preparation. The effect of hurricane Allen on the hydrology of the sabkha, Laguna Madre Flats, Texas.
- Trefry, J.H. and Presley, B.J., 1982. Manganese fluxes from Mississippi delta sediments. Geochim. Cosmochim. Acta, 46: 1715-1726.
- Tucker, M.E., 1976. Quartz-replaced anhydrite nodules (Bristol diamonds) from the Triassic of the Bristol District. Geol. Magazine, 113: 569-574.
- Van Andel, T.H. and Poole, D.M., 1960. Sources of Recent sediments in the northern Gulf of Mexico. J. Sediment. Petrol., 30: 91-122.
- Van Edan, J.G., 1978. Stratiform copper and zinc mineralization in the Cretaceous of Angola. Econ. Geol., 73: 1154-1161.
- West, I.M., Brandon, A. and Smith, M., 1968. A tidal flat evaporitic facies in the Visean of Ireland. J. Sediment. Petrol., 38: 1079-1093.
- Woods, P.J. and Brown, R.G., 1975. Carbonate sedimentation in an arid zone tidal flat, Nilemah embayment, Sharks Bay, western Australia. In R.N. Ginsburg (Editor), Tidal Deposits. Springer-Verlag, New York, N.Y., pp. 223-232.
- Zen, E.A., 1959. Mineralogy and petrology of marine bottom sediment samples off the coast of Peru and Chile. J. Sed. Petrol., 29: 513-539.

Zupan, A.J.W., 1972. Surficial Sediments and Sedimentary
Structures: Middle Ground, Padre Island, Texas. M.S.
Thesis, University of Texas at Austin (unpublished).

,			_
1			
•			
.1			
,			
ï			
,			
·			
7			
.•			
,			
•			
•			
,			
•			
٠			
1			
1			
:			
,			
1			
•			
;			
.1			
1			

